LUND UNIVERSITY

A General Formalism for Continuous Feedback Control in Quantum Systems

Annby-Andersson, Björn

2022

A General Formalism for Continuous Feedback Control in Quantum Systems

BJÖRN ANNBY-ANDERSSON
DEPARTMENT OF PHYSICS | FACULTY OF SCIENCE | LUND UNIVERSITY

A General Formalism for Continuous Feedback Control in
Quantum Systems

A General Formalism for Continuous Feedback Control in Quantum Systems

by Björn Annby-Andersson

Organization	Document name	
LUND UNIVERSITY	**LICENTIATE DISSERTATION**	
Department of Physics Box 118 SE–221 00 LUND Sweden	Date of disputation	
	2022-10-21	
	Sponsoring organization	
Author(s) Björn Annby-Andersson		

Title and subtitle
A General Formalism for Continuous Feedback Control in Quantum Systems

Abstract

This thesis devolops a general formalism for continuous feedback control in quantum systems. The main result is a quantum Fokker-Planck master equation describing the joint dynamics of a quantum system and a detector with finite bandwidth. For a fast detector, this equation can be reduced to a Markovian master equation for the system dynamics. In particular, the formalism is amenable to analytical treatments of feedback protocols that depend nonlinearly on the measured signal. Previously, only numerical methods were available for this. We apply the formalism on two toy models to highlight its usefulness. We find that the formalism provides insight into the connection between thermodynamics and information theory.

Key words
quantum measurements, quantum control, stochastic thermodynamics, information thermodynamics, full counting statistics, open quantum systems

Classification system and/or index terms (if any)

Supplementary bibliographical information	Language
	English

ISSN and key title	ISBN
	978-91-8039-372-0 (print) 978-91-8039-371-3 (pdf)

Recipient's notes	Number of pages	Price
	146	
	Security classification	

Signature _Björn Annby-Andersson_   Date ___2022-8-29___

A General Formalism for Continuous Feedback Control in Quantum Systems

by Björn Annby-Andersson

A licentiate thesis at a university in Sweden takes either the form of a single, cohesive research study (monograph) or a summary of research papers (compilation thesis), which the doctoral student has written alone or together with one or several other author(s).

In the latter case the thesis consists of two parts. An introductory text puts the research work into context and summarizes the main points of the papers. Then, the research publications themselves are reproduced, together with a description of the individual contributions of the authors. The research papers may either have been already published or are manuscripts at various stages (in press, submitted, or in draft).

Faculty of Science, Department of Physics

Contents

List of publications

This thesis is based on the following publications, referred to by their Roman numerals:

I **Quantum Fokker-Planck Master Equation for Continuous Feedback Control**

Björn Annby-Andersson, Faraj Bakhshinezhad, Debankur Bhattacharyya, Guilherme De Sousa, Christopher Jarzynski, Peter Samuelsson, and Patrick P. Potts
Physical Review Letters **129**, 050401 (2022)

All papers are reproduced with permission of their respective publishers.

Publications not included in this thesis:

Maxwell's demon in a double quantum dot with continuous charge detection

Björn Annby-Andersson, Peter Samuelsson, Ville F. Maisi, and Patrick P. Potts
Physical Review B **101**, 165404 (2020)

Acknowledgements

First, I would like to thank my supervisor, Peter, for giving me the opportunity to become a PhD student in his group. I am especially thankful for all the guidance, support, and encouragement during these years. You have given me a lot of freedom in my work, and the opportunity to supervise bachelor and master students. This has been very rewarding.

I would also like to thank my assistant supervisor, Patrick, for providing exciting tasks to work with, and for always helping out when I cannot solve my problems. I have learnt a lot of physics from you.

Next, I would like to acknowledge all the people from the Info-as-fuel collaboration, in which the work of this thesis was made. In particular, I would like to thank Faraj, Debankur, Guilherme and Chris for all discussions and joint work.

I would like to thank Katarina for all the help with everything at the office. I am also grateful for all the fun moments with people from the division, especially my office mates. In particular, I would like to thank Asimina and Axel for making the last couple of months hilarious. Finally, I would also like to thank my family for all the support.

Populärvetenskaplig sammanfattning

Återkopplade reglersystem har spelat en viktig roll inom naturvetenskap, medicin och teknik sedan den industriella revolutionen. Den grundläggande idén är att mäta en observabel hos ett system och använda den erhållna informationen för att styra systemet mot ett visst tillstånd. Detta är en av hörnstenarna i all modern teknik. Ett viktigt exempel är pacemakern, som genom att mäta hjärtrytmen kan hjälpa hjärtat att slå när det avviker från den normala rytmen.

Gemensamt för dagens reglersystem är att dom kan beskrivas väl av den klassiska fysiken, det vill säga termodynamik, elektromagnetism och klassisk mekanik. Då modern teknik börjar närma sig storleksordningar av 100 nanometer eller mindre, blir kvantmekaniska effekter, såsom tunnling och kvantkoherens, påtagliga. Det blir därför viktigt att ta hänsyn till detta. Av stort intresse är att utnyttja dessa effekter i ett användbart syfte. Detta är idén med kvantdatorer, där målet är att använda kvantmekaniska egenskaper för att uföra vissa beräkningar mer effektivt än en vanlig dator. Det är därför av intresse att studera och implementera återkopplade reglersystem under kvantmekaniska förhållanden – förhoppningsvis kan detta leda till nya teknologier som kan utveckla vårt samhälle eller förbättra vårt välbefinnande.

Vi står dock inför en rad utmaningar. Att mäta ett kvantmekaniskt system medför att dess kvantkoherens påverkas. Om mätproceduren interagerar för starkt med systemet förstörs koherensen, och egenskaperna som vi vill utnyttja går förlorade. Det är därför viktigt att interagera svagt för att bevara systemets kvantegenskaper. Under dom senaste årtiondena har metoder för att utföra sådana mätningar utvecklats. Samtidigt är det viktigt att kunna återkoppla mätinformationen för att styra systemet på ett användbart sätt. Det har till exempel utförts experiment där återkoppling har utnyttjats för att stabilisera kvantkoherens – ett viktigt steg för att kunna utveckla kvantteknologier.

För att förstå vad som är möjligt att uppnå med återkopplade kvantsystem krävs teoretiska verktyg. Dessa bör beskriva befintliga experiment med hög precision, men ska också kunna förutspå vad som är möjligt att implementera. Idag finns det en rad sådana verktyg, men dessa ger vanligtvis endast kvantitativa resultat. För att få en bredare och mer kvalitativ inblick har vi i denna licentiatuppsatsen utvecklat en generell formalism för återkopplade kvantsystem. Vårt huvudresultat är en masterekvation som beskriver dynamiken hos ett allmänt system under tidskontinuerlig mätning och återkoppling, samt dynamiken hos detektorn som mäter systemet. Detta ger oss möjligheten att kvalitativt beskriva återkopplade kvantsystem. Vi använder den härledda formalismen för att studera två enklare modeller. Vi finner att formalismen ger en inblick i hur energi och information kan manipuleras på mikroskopisk skala, och lägger grunden för fortsatta studier av återkopplade kvantsystem.

Chapter 1

Introduction and main result

Feedback control of dynamical systems has been of great scientific and technological importance over the last centuries [1]. The basic idea is to measure a system observable and use the obtained information to apply forces that drive the system towards a desired state. Almost all modern technology is based on this concept. A few examples are cruise control in cars, indoor climate control, pacemakers, and robotic systems. All of these examples are macroscopic systems, well described by classical physics. As modern technology is approaching the microscopic scale, quantum effects, such as tunneling and entanglement, must be accounted for. In particular, it is crucial to find ways of controlling and exploiting these effects. This is the central idea of quantum computers, where the aim is to use quantum effects to outperform classical computers on certain tasks [2].

With the fast development of modern technology, it is believed that quantum technologies, such as quantum computers, will become reality during the upcoming century. For this to happen, the development of accurate measurement and control procedures is of utmost importance. As measurements unavoidably dephase a quantum system, it is central to minimize backaction to preserve quantum coherence. Simultaneously, it is desired to apply highly controllable feedback forces that can steer the system towards a target state with long coherence times. During the last decades, several steps in this direction have been taken, including, for instance, deterministic entanglement generation [3], quantum state stabilization [4–6], and reversing quantum jumps [7].

From a fundamental perspective, it is crucial to understand what is physically possible to realize with quantum measurements and feedback control. Such questions are raised in the field of quantum thermodynamics [8], where Maxwell's demon [9–11] is a central concept. The idea of the demon is to use measurement and feedback to realize processes that seemingly violate the second law of thermodynamics. In fact, this seemingly paradoxical concept

has propelled several generalizations of the second law [12–22], where the thermodynamics of information [23–25] is taken into account in the thermodynamic book-keeping. These generalizations show that feedback controlled systems, such as Maxwell's demon, are not violating the second law. Simulateneously, a substantial number of experimental implementations of the demon have been realized in various classical [26–33] as well as quantum systems [34–37]. This provides promising platforms for further fundamental investigations of feedback control on the microscopic scale. Of special interest are solid state electronic circuits [38] equipped with quantum dots [39] and superconducting qubits [40]. These platforms allow for experiments with large statistical samples, and can be measured as well as controlled with high precision [41–47].

To properly understand quantum feedback control, it is essential to develop theroteical tools that can describe experimental results with high accuracy. Existing tools are typically based on stochastic differential equations [48–59]. These provide a powerful framework that can describe any type of feedback control, discrete as well as continuous in time. Typically, stochastic equations need to be solved numerically, limiting the possibility to draw general qualitative conclusions. A special case where analytical methods are available is the Wiseman-Milburn equation [52] – a Markovian master equation for time-continuous feedback protocols that depend linearly on the measured signal. It is, however, common that optimal control protocols involve a nonlinear depependence on the measured signal. An important example is bang-bang control [60, 61], where the feedback controller instantaneously switches between two different control forces depending if the measured signal is above or below a threshold value. A corresponding master equation description for such nonlinear feedback does not exist.

In this thesis, we fill this gap by deriving a general formlism for continuous measurement and feedback control in quantum systems, able to describe linear as well as nonlinear protocols. The main contribution is a quantum Fokker-Planck master equation describing the joint dynamics of a quantum system and a detector with finite bandwidth. For a fast detector, this can be reduced to a Markovian master equation for the system dynamics, independent of the detector. This Markovian description can be applied for arbitrary feedback protocols, linear as well as nonlinear. As such, this equation extends the work by Wiseman and Milburn beyond linear feedback, and provides a general analytical tool for investigating feedback in quantum systems.

We now briefly present the main result of this thesis and the underlying assumptions of its derivation. Finally, we discuss the major highlights and implications of this result. Detailed derivations and discussions follow in the upcoming chapters. Figure 1.1 is an illustration of a general setup for continuous measurement and feedback control. We consider an open quantum system whose dynamics, in the absence of measurement and feedback, is described by a Liouvillian superoperator $\mathcal{L}$. This superoperator is assumed to be on Lindblad form, and the system dynamics are assumed to be Markovian. The detector is continuously

measuring the (Hermitian) system observable $\hat{A}$, and the measurement strength is parameterized by λ. In the weak measurement limit $\lambda \to 0$, quantum coherence is preserved, but at the cost of introducing a large measurement uncertainty. The limit $\lambda \to \infty$ corresponds to a strong, projective measurement with small measurement uncertainty, but with the cost of destroying quantum coherence. To describe a realistic detector, we assume that the circuitry and electronic components of the detector collectively introduce a bandwidth γ, acting as a low-pass frequency filter eliminating high frequency noise. This introduces a detector delay time $1/\gamma$. In the final step of Fig. 1.1, feedback is continuously applied on the system by using the measurement outcome D to control the system Liouvillian via $\mathcal{L}(D)$.
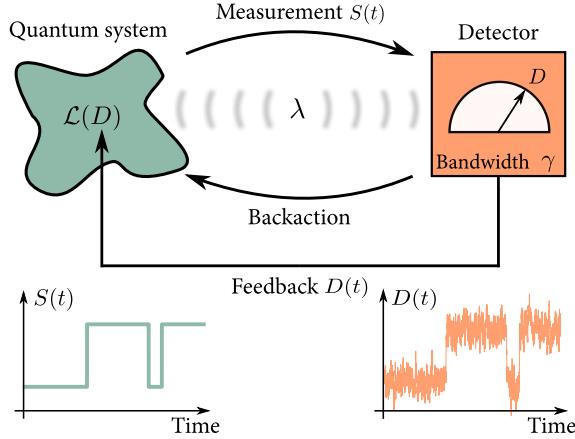
Figure 1.1: A general setup for continuous feedback control. An open quantum system is continuously measured by a detector with bandwidth γ. The measurement strength λ quantifies the backaction and uncertainty of the measurement. Based on the measurement outcome D, feedback is continuously applied on the system, controlling the system Liouvillian $\mathcal{L}(D)$. In the bottom, two typical trajectories of the system state and the corresponding measurement outcome are visualized. Figure taken from Paper I.

The main result of this thesis is the following Quantum Fokker-Planck Master Equation (QFPME),

$$\partial_t \hat{\rho}_t(D) = \mathcal{L}(D)\hat{\rho}_t(D) + \lambda \mathcal{D}[\hat{A}]\hat{\rho}_t(D) - \gamma \partial_D \mathcal{A}(D)\hat{\rho}_t(D) + \frac{\gamma^2}{8\lambda}\partial_D^2\hat{\rho}_t(D), \qquad (1.1)$$

describing the joint system-detector dynamics in Fig. 1.1 under continuous measurement and feedback control. The joint state of system and detector is represented by the density operator $\hat{\rho}_t(D)$. The system state, independent of the measurement outcome D, is given by $\hat{\rho}_t \equiv \int dD \hat{\rho}_t(D)$. Our state of knowledge of the detector is represented by the probability distribution $P_t(D) \equiv \mathrm{tr}\{\hat{\rho}_t(D)\}$. The first term on the RHS of Eq. (1.1) describes the feedback controlled time evolution of the system. We stress that the dependence of D in $\mathcal{L}(D)$ is not specified, and this term can therefore describe feedback protocols that are linear as well as nonlinear in D. The second term on the RHS represents the effect of measurement

3

backaction, with $\mathcal{D}[\hat{A}]\hat{\rho} = \hat{A}\hat{\rho}\hat{A} - \frac{1}{2}\{\hat{A}^2, \hat{\rho}\}$. In the eigenbasis of $\hat{A}$, this term describes how the coherence of the system, for nondegenerate eigenstates, is exponentially damped at a rate proportional to λ. The last two terms on the RHS constitute the Fokker-Planck equation for an Ornstein-Uhlenbeck process, describing the dynamics of the detector. The Ornstein-Uhlenbeck process describes a noisy relaxation towards an equilibrium value, i.e., how the position of the detector needle (see Fig. 1.1) evolves over time. The first of these terms, with superoperator drift coefficient $\mathcal{A}(D)\hat{\rho} \equiv \frac{1}{2}\{\hat{A} - D, \hat{\rho}\}$, describes the coupling between system and detector, determining the average position of the detector for a given system state. This position is set by one of the eigenvalues of $\hat{A}$. The second term, with diffusion constant $\gamma/8\lambda$, defines the magnitude of the detector noise. In the time traces at the bottom of Fig. 1.1, we visualize how the detector signal (right time trace) changes when the system state follows the trajectory in the left time trace.

The main implications and highlights of Eq. (1.1) are now briefly discussed. First, by assuming that the detector timescale $1/\gamma$ is much larger than the dominating timescale of the system, we can separate timescales and derive a Markovian master equation for the system state $\hat{\rho}_t$. This is discussed in detail in Chapter 6. In particular, this equation can handle feedback protocols that are nonlinear in D, going beyond the master equation for linear feedback derived by Wiseman and Milburn [52]. A major highlight is that this equation can provide analytical insight into the problem at hand. This is in contrast to Eq. (1.1) that, in general, must be solved numerically. Second, by separating the system and detector timescales for a linear feedback Liouvillian $\mathcal{L}(D)$, we can re-derive the master equation by Wiseman and Milburn. This highlights the generality of Eq. (1.1) and connects it to previous results in the field of quantum feedback control. Third, the Markovian description of the system implies fluctuation theorems, providing insight into the relationship between information theory and thermodynamics. Equation (1.1) is thus a promising tool for future studies in quantum thermodynamics. This is further discussed in Chapter 7. Finally, we note that a similar result to Eq. (1.1), but without feedback, was derived by Warszawski and Wiseman in Refs. [62, 63], and is also discussed in Ref. [57].

Before presenting these results in more detail, we will provide the necessary theoretical background of this thesis. Chapter 2 introduces stochastic processes and stochastic calculus. As these subjects are reoccurring throughout the thesis, this chapter acts as an important reference for the proceeding chapters. In Chapter 3, we discuss the basics of open quantum systems – the first main pillar of this thesis. We introduce the density operator, an indispensable tool for describing such systems, and review the Lindblad master equation, which describes the dynamics of open systems that are weakly coupled to their environment. We also introduce full counting statistics, a tool for determining transport statistics in nanosized systems. Chapter 4 is devoted to quantum measurements – the second main pillar of this thesis. We begin by discussing von Neumann and generalized quantum measurements. Building on this, we introduce Gaussian measurements and discuss weak continuous meas-

urements. Finally, we shortly review two of the central results in the field of continuous feedback control. Chapter 5 reviews stochastic and information thermodynamics – two fields of research where measurement and feedback are central. The idea of this chapter is to provide background to the results presented in Chapter 7. In Chapter 6, we derive Eq. (1.1) by using two approaches, one based on conventional calculus, and one based on stochastic calculus. We also give the details of the separation of timescales expansion that reduces the QFPME to a Markovian master equation for the system. In Chapter 7, we apply Eq. (1.1) on two toy models to highlight its usefulness. At last, in Chapter 8, we discuss possible directions of future research.

Chapter 2

Stochastic processes and stochastic calculus

The dynamics of physical systems can be described by differential equations. Two important examples are Maxwell's equations and the Schrödinger equation. These descriptions are deterministic, such that if we (with precision) know the initial conditions of a system, we can with certainty predict its future. If a system is subjected to randomly fluctuating forces, its dynamics are no longer deterministic, but rather stochastic, and it is difficult to predict its exact future. A prime example of this is Brownian motion [64], where the spatial trajectory of a pollen grain becomes random when suspended in a liquid. Due to the thermal motion of the liquid molecules, the pollen grain is kicked in random directions when colliding with them. Another example is noise in electronic circuits. Here we discuss two such noise sources, Johnson-Nyquist (thermal) noise [65, 66] and shot noise [67]. At finite temperature, the velocities of electrons in any conductor follow a thermal distribution. This means that at any instance in time, there is a thermally fluctuating current in the conductor, even in the absence of an external voltage source. The magnitude of these fluctuations scales with the square root of the temperature of the conductor. By lowering the temperature, we may thus reduce such fluctuations. This is known as Johnson-Nyquist noise. Shot noise, on the other hand, is due to the intrinsic properties of a conductor. For instance, consider a solid state device with a tunnel barrier. With a train of electrons approaching the barrier, only a fraction tunnel through it – the others are reflected. The arrival times of tunneling electrons are random, leading to a fluctuating tunnel current with an average determined by the height and width of the barrier. As a final example, we discuss measurements, which are central for this thesis. In classical physics, the stochasticity of a measurement can be due to imperfections in the detector, such as thermal noise and disturbances from adjacent electronics. In quantum physics, we know from the postulates of quantum mechanics that

a measurement yields random outcomes [2]. In addition, the coupling strength between the measured system and the detector determines the level of uncertainty in the outcome [68], i.e., with weaker coupling, we observe more fluctuations in the outcome statistics.

All of the above examples describe stochastic processes. To model such processes, it is common to employ stochastic differential equations (SDE). In the physical sciences, SDEs are commonly written as Langevin equations – first order differential equations describing the deterministic and stochastic contributions to the dynamics of a system. The stochastic contribution is commonly driven by white noise. As white noise is an idealization (as we will see later in this chapter), the Langevin equation must be handled with care. With too naive mathematical manipulations, one reaches erroneous results. To resolve this issue, one can introduce the concept of Itô calculus, and rewrite the Langevin equation on Itô form. This provides a sound framework for calculations. Both the Itô and Langevin equations describe the dynamics of some stochastic variable. Instead of studying the dynamics of this variable, one can study the dynamics of its probability distribution. These dynamics are governed by a Fokker-Planck equation – typically formulated as a second order partial differential equation. We note here that every Itô (or Langevin) equation has a corresponding Fokker-Planck equation. That is, we can always describe the stochastic dynamics from two points of view – via the stochastic variable or its probability distribution.

We begin this chapter by briefly discussing stochastic processes in Sec. 2.1. We introduce the concepts of stochastic trajectories, trajectory averages, and correlation functions. Towards the end of the section, we define Markovian processes. Section 2.2 introduces Langevin, Itô, and Fokker-Planck equations on a general level. We also provide two important examples of stochastic processes, Brownian motion (Wiener process) and the Ornstein-Uhlenbeck process. In Sec. 2.3, we motivate why it is necessary to introduce Itô calculus.

2.1 Stochastic processes

Above we introduced a few examples of stochastic processes in physical systems – it could be the position of a particle, the current in an electronic circuit, or the outcome of a measurement. In this thesis, we typically denote the value of a random process at time t by a capital letter $X(t)$. The process can be continuous or discrete in time. Any observation of $X(t)$ over time results in a trajectory $\boldsymbol{X} = \{x_0, x_1, \ldots, x_{n-1}\}$, where $x_j = X(t_j)$ is the value of the process at time $t_0 \leq t_j \leq t_{n-1}$, with t_0 and t_{n-1} being the initial and final times of the trajectory, respectively. By observing a very large number of trajectories, we can determine the probability $P[\boldsymbol{X}] = P[x_0, \ldots, x_{n-1}]$ of observing a specific trajectory $\boldsymbol{X}$. Integrating $P[\boldsymbol{X}]$ over all possible values except x_j, we get

$$P[x_j] = \int dx_0 \cdots dx_{j-1} dx_{j+1} \cdots dx_{n-1} P[x_0, \ldots, x_{n-1}], \qquad (2.1)$$

where $P[x_j]$ is the probability distribution of observing x_j at time t_j. Note that we will use the notations $P[x_j] = P[X(t_j)] = p_{t_j}(x)$ interchangeably. With Bayes' theorem, the probability of observing trajectory $\boldsymbol{X}$ can be written as

$$P[x_0, \ldots, x_{n-1}] = \left[\prod_{j=1}^{n-1} P[x_{n-j}|x_0, x_1, \ldots, x_{n-j-1}]\right] P[x_0], \qquad (2.2)$$

where $P[x_{n-j}|x_0, x_1, \ldots, x_{n-j-1}]$ is the transition probability to observe x_{n-j} given that the random process followed trajectory $x_0, x_1, \ldots, x_{n-j-1}$ up till time t_{n-j-1}. With the trajectory probability, we may calculate trajectory averages over functionals $f[\boldsymbol{X}]$. The functional could, for instance, be the work performed on a system along a trajectory $\boldsymbol{X}$ – this will be the case in Chapter 5, where we define work, heat and entropy along stochastic trajectories of microscopic systems. A trajectory average can be computed with a path integral according to

$$\langle f[\boldsymbol{X}] \rangle = \int \mathcal{D}[\boldsymbol{X}] f[\boldsymbol{X}] P[\boldsymbol{X}], \qquad (2.3)$$

where $\mathcal{D}[\boldsymbol{X}] = dx_0 \cdots dx_{n-1}$. For functions $f[X(t_j)]$, depending only on the value of $X(t_j)$ at any arbitrary time $t_0 \leq t_j \leq t_{n-1}$, we get the trajectory average

$$\langle f[X(t_j)] \rangle = \int dx_j f[x_j] P[x_j] = \int d[X(t_j)] f[X(t_j)] P[X(t_j)]. \qquad (2.4)$$

We will use this in Sec. 2.3, as well as in Chapters 4 and 6. Trajectory averages are also important when computing correlation functions, such as

$$\mathcal{C}_X(t, t') = \langle X(t)X(t') \rangle - \langle X(t) \rangle \langle X(t') \rangle. \qquad (2.5)$$

Compared to the average $\langle X(t) \rangle$ and the variance $\langle X^2(t) \rangle - \langle X(t) \rangle^2$, the correlation function $\mathcal{C}_X(t, t')$ provides additional information about the dynamics of a stochastic process. In particular, it measures how the value of the process at time t, $X(t)$, influences the value $X(t')$ at a later time $t' > t$. Typically, we are interested in the stationary state of the correlation function, where it only depends on the difference in time $\tau = t' - t$, i.e., when $\mathcal{C}_X(t, t') = \mathcal{C}_X(\tau)$. It is useful to define the power spectrum of the stationary correlator $\mathcal{C}_X(\tau)$ as

$$S_X(\omega) = \int_{-\infty}^{\infty} d\tau\, e^{i\omega\tau} \mathcal{C}_X(\tau). \qquad (2.6)$$

This provides a spectrum of the underlying frequencies present in the noise of the stochastic process. An important example is delta correlated noise, with stationary correlation function $\mathcal{C}_X(\tau) = \delta(\tau)$, where $\delta(\cdot)$ is the Dirac delta function. Its power spectrum reads $S_X(\omega) = 1$. That is, the spectrum is flat, and contains an equal weight of all frequencies. This is important when, for example, studying Johnson-Nyquist noise [69]. The concept

of correlation functions and power spectra will be especially useful in Chapters 3 and 6, where we discuss Full counting statistics and detector bandwidths.

Up to this point, the theory is completely general, and we have not made any assumptions, except introducing the concept of having a stationary state. However, it is often required to make assumptions in order to derive analytical results. A common assumption, that is relevant for this thesis, is the one of Markovian dynamics. In this case, we assume that the transition probabilities only are conditioned on the previous value of the process, rather than the entire history of values, i.e., $P[x_j|x_0, \ldots, x_{j-1}] = P[x_j|x_{j-1}]$. This is referred to as a Markov process, and the trajectory probability [Eq. (2.2)] can be written as

$$P[x_0, \ldots, x_{n-1}] = \left[\prod_{j=1}^{n-1} P[x_{n-j}|x_{n-j-1}] \right] P[x_0]. \qquad (2.7)$$

This will be important in Chapter 5 when we derive fluctuation theorems. The probability of observing three consecutive events x_{j-2}, x_{j-1}, and x_j in any Markov process can be written as $P[x_{j-2}, x_{j-1}, x_j] = P[x_j|x_{j-1}]P[x_{j-1}|x_{j-2}]P[x_{j-2}]$. With Bayes' theorem, we find the Chapman-Kolmogorov equation [69]

$$P[x_j|x_{j-2}] = \int dx_{j-1} P[x_j|x_{j-1}]P[x_{j-1}|x_{j-2}], \qquad (2.8)$$

stating that if the transition probabilities $P[x_j|x_{j-1}]$ and $P[x_{j-1}|x_{j-2}]$ are known, we can always find the transition probability $P[x_j|x_{j-2}]$. This will be an important reference when discussing Markovian dynamics of quantum systems in Chapter 3.

2.2 Langevin, Itô, and Fokker-Planck equations

In the previous section, we studied trajectory probabilities of stochastic processes. Now we change focus to stochastic differential equations, and study the dynamics of the random process $X(t)$. In the physical sciences, it is common to write the equation of motion of $X(t)$ as a Langevin equation [69]

$$\dot{X}(t) = \alpha[X(t)] + \beta[X(t)]\xi(t), \qquad (2.9)$$

where α and β are real functions, and $\xi(t)$ is a time-continuous, rapidly varying random process (noise term) with mean $\langle \xi(t) \rangle = 0$. Here $\langle \cdot \rangle$ denotes a trajectory average as defined in Eq. (2.3). We may assume that the mean is zero as any non-zero mean can be baked into the function α. The first term on the RHS of the Langevin equation describes the deterministic dynamics of the process, and is commonly referred to as a drift term as it describes the overall direction in which $X(t)$ is moving. The second term describes how randomly

fluctuating forces influence the dynamics of $X(t)$, and adds noise on top of the deterministic behavior. The noise term is assumed to be stationary, such that its correlation function $\langle\xi(t)\xi(t+\tau)\rangle$ is invariant under translations in t, and thus only depend on the distance τ between two points in time. We require that the correlation function is normalized according to

$$\int_{-\infty}^{\infty} d\tau\langle\xi(t)\xi(t+\tau)\rangle = 1. \tag{2.10}$$

In this way, we assure that $\langle\xi(t)\xi(t+\tau)\rangle$ decays to zero for large τ, such that the present state of $\xi(t)$ is uncorrelated with itself in the distant past. In fact, we will concentrate on Markovian processes, where the characteristic correlation time is so short that for any $\epsilon > 0$, we have

$$\int_{-\epsilon}^{\epsilon} d\tau\langle\xi(t)\xi(t+\tau)\rangle = 1. \tag{2.11}$$

This implies that the noise term is delta correlated, with $\langle\xi(t)\xi(s)\rangle = \delta(t-s)$. The power spectrum [see Eq. (2.6)] is thus flat (as discussed above), and we refer to $\xi(t)$ as a white noise process, as it similarly to white light contain the same weight of all frequencies. In particular, we note that the variance of $\xi(t)$ diverges, $\text{Var}[\xi(t)] = \delta(0)$. This is unphysical, and therefore, somewhat problematic, but the noise term still has physical meaning. For example, it can serve as a good approximation, or be used to derive other stochastic processes. Note that white noise should be considered as an idealization, or a limiting case of a random process that is physical. For instance, the singularity of the variance may be derived from another process $\eta(t)$ with correlation function $\langle\eta(t)\eta(t+\tau)\rangle = \tau_c^{-1}e^{-|\tau|/\tau_c}$, where τ_c is a finite characteristic correlation time. When τ_c is small, formally when $\tau_c \to 0$, we get a delta correlation in accordance with the Markov assumption above. That is, if the characteristic correlation time of a process is very small, we approximate the process as delta correlated. It should be noted that this approximation can lead to peculiar results, as indicated with the diverging variance above. Therefore, Langevin equations should be treated with care. In general, one must introduce Itô calculus and rewrite the Langevin equation on Itô form, as will be motivated in Sec. 2.3.

The Itô form of the Langevin equation (2.9) is given by

$$dX(t) = a[X(t)]dt + b[X(t)]dW(t), \tag{2.12}$$

where $dX(t) = X(t+dt) - X(t)$ is an infinitesimal increment of the stochastic process, with dt being an infinitesimal timestep, while a and b are real functions related to α and β via

$$\begin{cases} a(x) & = \alpha(x) + \frac{1}{2}\beta(x)\beta'(x), \\ b(x) & = \beta(x), \end{cases} \tag{2.13}$$

where the prime denotes differentiation with respect to x, and $dW(t)$ is a Wiener increment, which is a Gaussian random variable with mean $\langle dW(t)\rangle = 0$ and variance

Var$[dW(t)] = dt$. The Wiener increment stems from the Wiener process, and is discussed in some more detail below. We assume that $X(t)$ and $dW(t)$ are independent at time t, such that $\langle f[X(t)]dW(t)\rangle = 0$ for any function f. This is proven in Appendix A. Also note that $dW(t)$ at different instances of time are independent. In particular, we note that $[dW(t)]^2 = dt$ – this is the main rule of (Itô) stochastic calculus, and we sometimes refer to it as the Itô rule. Note that the Itô rule implies that $dW(t)$ scales as $\sqrt{dt}$, which is important when expanding functions of $X(t)$ to first order in dt, which corresponds to second order in $dW(t)$. In Sec. 2.3, we motivate the origin of this rule, and why it is necessary for obtaining sensible results. We point out that this is not the only type of stochastic calculus. If the noise term $dW(t)$ is non-Gaussian, other rules of stochastic calculus apply [57, 64]. However, in this thesis, we concentrate solely on Gaussian noise. The Itô equation provides a useful tool for simulating trajectories of $X(t)$ and for calculating statistics of the process. Solving it analytically is, in general, hard, but there exists a few cases where it is possible [64] – its solution specifies the probability distribution of $X(t)$. One can also think of individual trajectories of $X(t)$ as solutions to the Itô equation. As the increment $dW(t)$ can be chosen in an infinite number of ways, the Itô equation has infinitely many solutions – if all of them were known, we could construct the probability distribution of $X(t)$ at all times t. Before proceeding, we note that the Itô rule implies that any function $f[X(t)]$ has an infinitesimal increment

$$df(X) = [a(X)f'(X) + \frac{1}{2}b^2(X)f''(X)]dt + b(X)f'(X)dW, \qquad (2.14)$$

where we omitted the time arguments for brevity. To obtain this equation, we expanded $f(X + dX)$ around X to first order in dt, i.e., to second order in dW.

While the Itô equation is useful for studying the dynamics of $X(t)$ on a trajectory level, it does not, in general, provide the dynamics of the full distribution $p_t(x) = P[X(t) = x]$ of $X(t)$. To find a description of the dynamics of $p_t(x)$, one can work with Fokker-Planck equations. In fact, every Itô (or Langevin) equation has a corresponding Fokker-Planck equation. In the remaining paragraphs of this section, we outline how the Itô equation (2.12) can be transformed into a Fokker-Planck equation for $p_t(x)$.

We begin by noting that the distribution is given by

$$p_t(x) = \langle \delta[X(t) - x]\rangle = \int d[X(t)]\delta[X(t) - x]P[X(t)], \qquad (2.15)$$

where $\langle \cdot \rangle$ again denotes the trajectory average defined in Eq. (2.3). From Eq. (2.14), we find the increment

$$d\delta[X(t) - x] = \left\{ a[X(t)]\delta'[X(t) - x] + \frac{1}{2}b^2[X(t)]\delta''[X(t) - x] \right\} dt + b[X(t)]\delta'[X(t) - x]dW(t),$$
$$(2.16)$$

where primes denote derivatives with respect to $X(t)$. By taking the average $\langle \cdot \rangle$ over this equation, we get

$$dp_t(x) = -\partial_x[a(x)p_t(x)]dt + \frac{1}{2}\partial_x^2[b^2(x)p_t(x)]dt, \tag{2.17}$$

where we used that $\langle b[X(t)]\delta'[X(t) - x]dW(t)\rangle = 0$ as $X(t)$ and $dW(t)$ are independent – see Appendix A. Since this equation is linear in dt, we find the standard form of the Fokker-Planck equation

$$\partial_t p_t(x) = -\partial_x[a(x)p_t(x)] + \frac{1}{2}\partial_x^2[b^2(x)p_t(x)]. \tag{2.18}$$

The drift term $a(x)$ determines the deterministic evolution of the stochastic process, i.e., how the center of $p_t(x)$ evolves over time. The diffusion term $b^2(x)$ determines the magnitude of the noise in the process, in other words how broad $p_t(x)$ is.

The three descriptions above – Langevin, Itô, and Fokker-Planck equations – are equivalent, and can be used to describe the same process. We now briefly study two common processes in terms of these three descriptions.

2.2.1 Brownian motion (Wiener process)

Brownian motion can be defined via the Langevin or Itô equations

$$\dot{X}(t) = \sigma\xi(t) \qquad \text{and} \qquad dX(t) = \sigma dW(t), \tag{2.19}$$

where $\sigma > 0$ is referred to as the diffusion constant. In the case of a particle subjected to thermal fluctuations, σ is proportional to the temperature of its environment. If $\sigma = 1$, we refer to the process as a Wiener process, even though its qualitatively identical to Brownian motion. The Itô equation may be solved by integration,

$$X(t) = \sigma \int_{t_0}^t dW(t) = \sigma \lim_{N\to\infty} \sum_{j=0}^{N-1} \delta W(t_0 + j\delta t), \tag{2.20}$$

where we in the last equality discretized time into N segments of length $\delta t = (t - t_0)/N$, and introduced the finite Wiener increment $\delta W(t)$, which is a Gaussian random variable with mean 0 and variance δt. The integral object in this equation is referred to as a (Itô) stochastic integral [64, 69]. In this thesis, we will not need this type of mathematical tools, and will thus not dig deeper into it than this. Instead, we use the sum representation in Eq. (2.20), together with the central limit theorem, to conclude that $X(t)$ is a Gaussian random variable with mean $\langle X(t)\rangle = 0$ and variance $\text{Var}[X(t)] = \sigma^2(t - t_0)$.
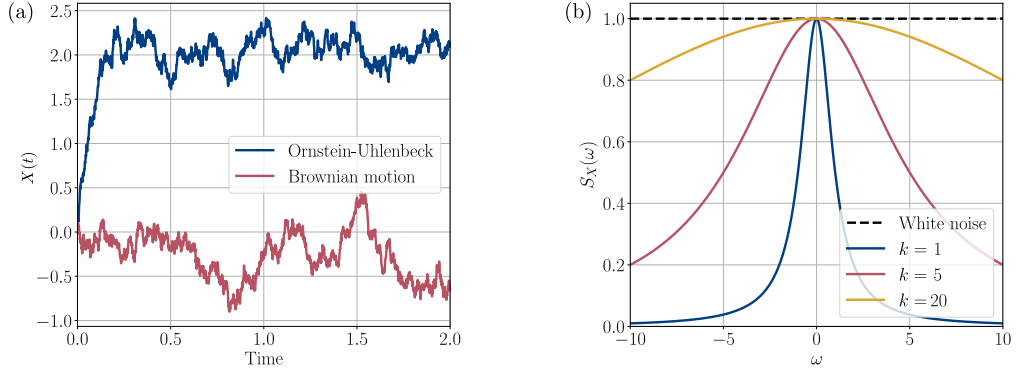
Figure 2.1: (a) Typical trajectories of Brownian motion and the Ornstein-Uhlenbeck process. The Brownian motion stays, on average, around 0, while the Onstein-Uhlenbeck process drifts towards an equilibrium position. To simulate these trajectories, we used the Itô equations (2.19) and (2.23), together with the following parameters, $x_0 = 0$, $\sigma = 30$, $k = 15 \cdot 10^{-3}$, $m = 2$, and $dt = 10^{-3}$. (b) Comparison of the power spectra of a white noise process (black, dashed line) and the Ornstein-Uhlenbeck process [see Eq. (2.28)] for a few choices of k (solid lines). Note that Eq. (2.28) tends to the white noise spectrum as k is increased. Here we use $\sigma = k/\sqrt{2}$.

Equivalently, one can define Brownian motion via the Fokker-Planck equation

$$\begin{cases} \partial_t p_t(x) & = \frac{\sigma^2}{2} \partial_x^2 p_t(x), \\ p_{t_0}(x) & = \delta(x), \end{cases} \tag{2.21}$$

where the second line defines the intial condition. The solution to this initial value problem reads [69]

$$p_t(x) = \frac{e^{-x^2/2\sigma^2(t-t_0)}}{\sqrt{2\pi\sigma^2(t-t_0)}}. \tag{2.22}$$

That is, $X(t)$ is a Gaussian random variable centered at $x = 0$ with variance $\sigma^2(t - t_0)$, just as above. With the initial value used here, the process describes the position of a Brownian particle moving in one dimension, starting at the origin at t_0. As random, unbiased noise is the only force acting on the particle, it stays at the origin on average. The variance of the position grows linearly with time as the particle always has the possibility of moving far from the origin if it is exposed to the random force for a long time. In Fig. 2.1(a), we illustrate a typical trajectory of Brownian motion in one dimension.

As mentioned above, if $\sigma = 1$, we refer to this process as a Wiener process, and denote it by $W(t)$. A special property of this process is that all increments $\Delta W(t) = W(t + \Delta t) - W(t)$ are independent of each other, and of $W(t)$ for any $\Delta t > 0$. Note that the Wiener increment is Gaussian as well, with $\langle \Delta W(t) \rangle = 0$ and $\text{Var}[\Delta W(t)] = \Delta t$ [69].

2.2.2 The Ornstein-Uhlenbeck process

The Ornstein-Uhlenbeck process is a generalization of Brownian motion with an additional drift term that drives the process towards a specific position. Its Langevin and Itô equations are given by

$$\dot{X}(t) = k[m - X(t)] + \sigma\xi(t) \qquad \text{and} \qquad dX(t) = k[m - X(t)]dt + \sigma dW(t). \quad (2.23)$$

Here $k, \sigma > 0$ are constants, with units of inverse time, and m determines the position towards which the system is driven [it has the same unit as $X(t)$]. In practice, the Ornstein-Uhlenbeck process describes the position of a Brownian particle with overdamped dynamics in a harmonic potential, where the friction term proportional to $\dot{X}(t)$ dominates over the acceleration term proportional to $\ddot{X}(t)$, such that the latter can be neglected from the equation of motion. The Ornstein-Uhlenbeck process thus describes a noisy relaxation towards an equilibrium position. As we will see in Chapters 4 and 6, it can be used to model measurement signals. We note that it has applications in a wide range of situations, for instance, in financial mathematics, where it is used to model interest rates [70].

The Itô equation in Eq. (2.23) can be solved analytically, see, e.g., Ref. [64], but to avoid clutter, we present only the solution of the corresponding Fokker-Planck equation. The solutions are equivalent anyway. The Fokker-Planck equation is given by

$$\begin{cases} \partial_t p_t(x) & = k\partial_x[(x - m)p_t(x)] + \sigma^2\partial_x^2 p_t(x), \\ p_0(x) & = \delta(x - x_0), \end{cases} \quad (2.24)$$

where the initial distribution is centered at some arbitrary value x_0. The solution reads

$$p_t(x) = \sqrt{\frac{k}{2\pi\sigma^2(1 - e^{-2kt})}} e^{\frac{k}{2\sigma^2(1-e^{-2kt})}\left[x - m(1-e^{-kt}) - x_0 e^{-kt}\right]^2}. \quad (2.25)$$

The Ornstein-Uhlenbeck process is thus a Gaussian random variable with mean $\langle X(t)\rangle = m(1 - e^{-kt}) + x_0 e^{-kt}$ and variance $\text{Var}[X(t)] = \sigma^2(1 - e^{-2kt})/k$. In the stationary limit, we obtain

$$p_{\text{ss}}(x) = \lim_{t\to\infty} p_t(x) = \sqrt{\frac{k}{2\pi\sigma^2}} e^{-\frac{k}{2\sigma^2}(x-m)^2}. \quad (2.26)$$

The Ornstein-Uhlenbeck process thus reaches a stationary distribution – this was not the case with Brownian motion. In fact, the Ornstein-Uhlenbeck process is the only single-variable stochastic process which is Gaussian, Markovian, and has a stationary distribution [69]. We also see that Eqs. (2.25) and (2.26) provide a nice illustration of the noisy relaxation mentioned above. At $t = 0$, the process starts at the initial position x_0 and makes a random walk towards the equilibrium position $x = m$ that is reached in the stationary limit. The timescale of the relaxation is determined by $1/k$. The variance is 0 at time $t = 0$ (we know

exactly where the particle is), and grows towards σ^2/k at a rate given by $2k$. We illustrate a sample trajectory of the Ornstein-Uhlenbeck process in Fig. 2.1(a).

The stationary correlation function of the Ornstein-Uhlenbeck process is given by [69]

$$C_X(\tau) = \frac{\sigma^2}{k} e^{-k|\tau|}. \tag{2.27}$$

That is, the correlation between two points in time separated by τ decays exponentially on a timescale $1/k$, as expected for a Markovian process. Its power spectrum [see Eq. (2.6)] reads

$$S_X(\omega) = \frac{2\sigma^2}{k^2 + \omega^2}. \tag{2.28}$$

The spectrum thus has a Lorentzian shape with width $2k$ (full width at half maximum). In Fig. 2.1(b), we compare Eq. (2.28) to the spectrum of white noise for different choices of k, where we use $\sigma = k/\sqrt{2}$ such that the maximum of $S_X(\omega)$ remains invariant under changes of k. We observe that the width of the spectrum increases with k, and in the limit $k \to \infty$, we recover the white noise spectrum. This can also be seen from the correlation function, $C_X(\tau) \to \delta(\tau)$ as $k \to \infty$ for $\sigma = k/\sqrt{2}$. This will be important when interpreting the effect of a finite detector bandwidth in Chapter 6.

2.3 Motivation for stochastic calculus

As the final part of this chapter, we provide a motivation for why stochastic calculus and the Itô equation are necessary for obtaining sensible results. In fact, the Langevin equation, or rather the white noise term $\xi(t)$ in Eq. (2.9), is not rigorously defined, such that a too naive mathematical treatment leads to the wrong results. We begin by motivating this, and then show how we can go from the Langevin equation to the Itô equation. Note that the idea of this section is to motivate why stochastic calculus is needed, rather than providing rigorous derivations. We closely follow the discussions in Refs. [57] and [69].

We begin by assuming that $X(t)$ and $\xi(t)$ are statistically independent, and that $\dot{X} = dX/dt$. The latter assumption corresponds to what we would expect from conventional calculus. We now show that these two assumptions cannot be true simultaneously, and that one of them needs to be relaxed. To this end, it is illuminating to calculate the infinitesimal increment $dX(t) = X(t + dt) - X(t)$. The Langevin equation (2.9) provides the following result,

$$dX(t) = \alpha[X(t)]dt + \beta[X(t)]\xi(t)dt. \qquad \text{(wrong)} \tag{2.29}$$

We indicate already here that this result is wrong, and should not be used for calculations – we only work with it in this paragraph to highlight the subtleties of the Langevin equation. It yields the average increment $\langle dX(t) \rangle = \langle \alpha[X(t)] \rangle dt$, which is independent of the
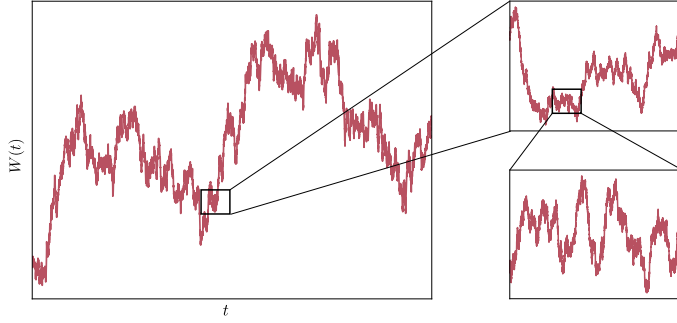
Figure 2.2: Illustration of the fractal structure of a Wiener process $W(t)$. When zooming in, the Wiener process never becomes linear. Therefore, it has no derivative.

noise term, as expected from the assumptions. For the variance of the increment, we get $\text{Var}[dX(t)] = \langle [dX(t)]^2 \rangle = 0$, where we used that all nonlinear terms in dt vanish. This suggests that the increments are deterministic, and that the noise term does not induce any noise to the process – quite contrary to what to expect from a stochastic process. We understand that our two assumptions cannot be true simultaneously. Here we will relax the second assumption. That is, the fluxion $\dot{X}$ will not be interpreted as dX/dt, but we still assume independence between $X(t)$ and $\xi(t)$. Note that we are not required to make this relaxation – one can still assume that $\dot{X} = dX/dt$ holds, but must then relax the other assumption. Equation (2.9) is then referred to as a Stratonovich equation, and requires computational tools that are not discussed here [57].

To further motivate why we relaxed this assumption, we will, in this paragraph, assume that $\dot{X} = dX/dt$ holds, and show that we run into other problems than the one above. Under this assumption, the solution to Eq. (2.9) would read

$$X(t) - X(t_0) = \int_{t_0}^{t} dt' \alpha[X(t')] + \int_{t_0}^{t} dt' \beta[X(t')]\xi(t'). \tag{2.30}$$

For this to hold, the function

$$W(t) = \int_{t_0}^{t} dt' \xi(t') \tag{2.31}$$

must exist. From the central limit theorem, $W(t)$ can be shown to be a Gaussian distributed random variable with mean 0 and variance $t - t_0$. In fact, $W(t)$ is a Wiener process [69]. Because of the fractal structure of $W(t)$, see Fig. 2.2, it is impossible to linearize it as $h \to 0$ in $[W(t + h) - W(t)]/h$. Therefore, the derivative $\dot{W}(t)$, and thereby also $\xi(t)$, does not exist in a rigorous mathematical sense [69]. This provides further support why $\dot{X} \neq dX/dt$. Despite being nonexistent in a mathematical sense, we will continue to use $\xi(t)$ in our discussion as it is commonly used in the physical sciences.

From the discussion in the preceding paragraphs, we understand that analyzing and solving the stochastic differential equation (2.9) raise several warning bells, indicating that the equation must be treated with care. As conventional calculus does not apply as we are used to, one way to proceed is to introduce Itô calculus, and rewrite Eq. (2.9) on Itô form. Itô calculus provides computational rules that allow us to calculate and manipulate the increment dX in a mathematically and physically sensible way.

To introduce the Itô calculus, we begin by studying the Wiener process in Eq. (2.31), and note that for $t > s$

$$W(t) - W(s) = \int_s^t dt' \xi(t'), \tag{2.32}$$

implying that any Wiener increment $\Delta W(t) = W(t + \Delta t) - W(t)$ is independent of $W(t)$, as discussed above. We also note that $\Delta W(t)$ is Gaussian with $\langle \Delta W(t) \rangle = 0$ and $\mathrm{Var}[\Delta W(t)] = \langle \Delta W^2(t) \rangle = \Delta t$, as we expect for the Wiener process, see discussion above. This gives us the infinitesimal increment $dW(t) = \xi(t)dt$, suggesting that $\xi(t)$ is the derivative $dW(t)/dt$. As noted above, mathematically this derivative does not exist, but is still used here (and in the physical sciences) because of the convenient notation. The main result of Itô calculus is that $[dW(t)]^2 = dt$ – a quite surprising result as $dW(t)$ appears to be proportional to dt.

To understand why $[dW(t)]^2 = dt$, we make use of a small Wiener increment $\delta W(t) = W(t + \delta t) - W(t)$ and study it over a time period $\Delta t = t - t_0$. By discretizing Δt into N intervals, $\delta t = \Delta t / N$. We now define a quantity

$$\chi = \sum_{j=0}^{N-1} [\delta W(t_j)]^2, \tag{2.33}$$

where $t_j = t_0 + j\delta t$. The mean and variance of χ are given by

$$\begin{cases} \langle \chi \rangle & = \Delta t, \\ \langle \chi^2 \rangle - \langle \chi \rangle^2 & = \frac{\Delta t}{N/2}. \end{cases} \tag{2.34}$$

In the continuous limit, $N \to \infty$, the variance vanishes and χ becomes deterministic – more specifically, $\chi \to \Delta t$. In this limit, we may interpret the sum in Eq. (2.33) as an integral, and we get

$$\Delta t = \int_t^{t+\Delta t} dt = \int_t^{t+\Delta t} dW^2, \tag{2.35}$$

where we omitted the time argument for brevity. This implies the Itô rule $dW^2 = dt$. When we analyzed Eq. (2.9) above, we thought that $dW = \xi(t)dt$ was scaling as dt. The Itô rule teaches us that dW actually scales as $\sqrt{dt}$, and partly explains why our analysis of Eq. (2.9) went wrong. At this point, it is tempting to replace $\xi(t)dt$ with dW in Eq. (2.29), but a little more care is needed to find the correct form for the infinitesimal increment $dX(t)$.

To find the increment $dX(t)$ corresponding to Eq. (2.9), we Taylor expand $X(t + dt)$ as

$$X(t + dt) = e^{dt\partial_s}X(s)\Big|_{s=t}, \tag{2.36}$$

where we write the expansion as an exponential function for brevity. In fact, all terms in the expansion are not needed, only the ones scaling as dt. To calculate the derivatives $\partial_s^n X(s)$ ($n > 1$), we assume that

$$\partial_s X(s)\Big|_{s=t} = \Big(\alpha[X(s)] + \beta[X(s)]\xi(t)\Big)\Big|_{s=t}. \tag{2.37}$$

This assumption is based on the fact that $\xi(t)$ in reality must have a small, but finite correlation time τ_c over which it remains constant. That is, during an infinitesimal time increment $dt \ll \tau_c$, $\xi(t)$ is constant, and is not affected by time derivatives of Eq. (2.37). Using this, as well as the first and second order terms in the Taylor expansion (2.36), alternatively to first order in dt, i.e., second order in $dW(t) = \xi(t)dt$ due to the Itô rule, we get the correct increment

$$dX(t) = a[X(t)]dt + b[X(t)]dW(t), \tag{2.38}$$

where the coefficients $a[X(t)] = \alpha[X(t)] + \frac{1}{2}\beta[X(t)]\beta'[X(t)]$ and $b[X(t)] = \beta[X(t)]$ show the relation to Eq. (2.9). The prime in $a[X(t)]$ denotes the derivative with respect to X. Equation (2.38) is known as an Itô stochastic differential equation. It implies that the variance of dX reads

$$\langle (dX)^2 \rangle = \langle b^2(X) \rangle dt, \tag{2.39}$$

where we used that $\langle dX \rangle = \langle a(X) \rangle dt$, and that $X(t)$ and $dW(t)$ are independent. That is, the variance of the increment is nonzero, indicating that the noise term induces noise in the process as desired. This motivates why Itô calculus is required to obtain reasonable results, and the increment in Eq. (2.29) should be avoided. We note that Itô calculus will be used in Chapter 6 when we derive Eq. (1.1).

Chapter 3

Open quantum systems

The textbook description of basic quantum mechanics is based on closed systems that are completely isolated from their environment and described by pure states, i.e., we are certain what state the system is in. Such a description can teach us a great deal about the foundations of quantum physics, but it is inevitable that quantum systems never are isolated in reality. They always interact with their environment by exchanging energy and/or particles, and are thereby open. A typical example of this is the light-matter interaction between an atom (system) and an electromagnetic field (environment) [71, 72]. Another relevant example is solid state quantum dots (system) [39] defined in semiconductor materials (environment), where the quantum dots may exchange electrons and phonons with its environment. A complete description of the physics of these examples requires a full theoretical treatment of both the system and the environment. For instance, to understand all processes in the example of light-matter interactions, we must quantize the electromagnetic field, and keep track of all possible photon states of the field. As there, theoretically, are an infinite number of photon states, it is, in general, a formidable task to theoretically model such a problem. To this end, it is necessary to develop a manageable theory for open quantum systems [2, 68, 73]. The joint unit of system and environment can be treated as a closed system, and by tracing out the environment, we obtain a description of the system alone. By performing such a trace operation, we lose information about the correlations between the system and the environment, and introduce uncertainty about which state the system is in. The state of an open quantum system is thus, typically, mixed. Often, we are interested in the dynamics of these systems. By assuming a weak coupling between the system and the environment, it is possible to find a general Markovian master equation for open systems – the Lindblad equation. This equation effectively describes how the environment influences the system, without having to keep track of the environmental degrees of freedom. The Lindblad equation is an important tool for modeling open quantum systems, and plays a significant role in this thesis, especially in Chapters 4, 6, and 7, where we

study continuous measurements and feedback control of open quantum systems.

In this chapter, we discuss the basic theoretical tools required to describe open quantum systems. We begin by reviewing the dynamics of pure states in closed systems in Sec. 3.1. This acts as a reference for the proceeding sections. Section 3.2 introduces mixed states and the density operator. The latter is a valuable tool in the theory of open quantum systems. In particular, we motivate the origin of mixed states. Section 3.3 is devoted to the dynamical description of open systems. Most importantly, we introduce the Lindblad master equation. Before concluding this chapter, we introduce full counting statistics in Sec. 3.4 – a tool for gaining full statistical knowledge of particle transport in nanoscale systems described by Markovian master equations. This will be a useful tool in Chapter 7, where we study the statistics of energy exchanges between a thermal environment and an open system.

3.1 Pure states

The state of a quantum system is said to be pure if it can be described by one single, normalized state vector $|\psi(t)\rangle$, for which $\langle\psi(t)|\psi(t)\rangle = 1$. For a closed system, the time evolution of this state is described by the Schrödinger equation

$$\partial_t |\psi(t)\rangle = -i\hat{H}(t) |\psi(t)\rangle, \tag{3.1}$$

where $\hat{H}(t)$ is the (possibly time dependent) Hamiltonian of the system. The time dependence may be due to the interaction with an external driving field, such as in the semi-classical description light-matter interactions. Note that we have absorbed the factor of $\hbar^{-1}$ into the Hamiltonian in Eq. (3.1) such that all energy units are given in inverse units of time (alternatively known as the convention $\hbar = 1$). The solution to the Schrödinger equation is given by

$$|\psi(t)\rangle = \hat{U}(t, t_0) |\psi(t_0)\rangle, \tag{3.2}$$

where $|\psi(t_0)\rangle$ is the initial state vector of the system at time t_0, with $\langle\psi(t_0)|\psi(t_0)\rangle = 1$, and $\hat{U}(t, t_0)$ is the time evolution operator given by

$$\hat{U}(t, t_0) = \mathcal{T} e^{-i \int_{t_0}^{t} ds \hat{H}(s)}, \tag{3.3}$$

where $\mathcal{T}$ is the time ordering operator. The time evolution operator is unitary, i.e., $\hat{U}(t, t_0)\hat{U}^\dagger(t, t_0) = \hat{U}^\dagger(t, t_0)\hat{U}(t, t_0) = 1$, such that the normalization of the state vector is preserved; $\langle\psi(t)|\psi(t)\rangle = \langle\psi(t_0)|\hat{U}^\dagger(t, t_0)\hat{U}(t, t_0)|\psi(t_0)\rangle = \langle\psi(t_0)|\psi(t_0)\rangle = 1$. With the state vector, we may calculate all moments of any observable $\hat{A}$ at time t as $\langle\hat{A}^k\rangle = \langle\psi(t)|\hat{A}^k|\psi(t)\rangle$.

3.2 Mixed states

The preceding discussion was concerned with pure states of closed quantum systems. We now proceed with mixed states which cannot be described by a single state vector. Suppose that we are dealing with a quantum system (closed or open), where we are uncertain about the exact system state. This uncertainty can be expressed by a probability distribution p_j, normalized with $\sum_j p_j = 1$, specifying the probability that the system is in some state $|\psi_j\rangle$. The possible system states $|\psi_j\rangle$ are not necessarily mutually orthogonal. Under these conditions, the system state is said to be mixed, and is represented by the density operator

$$\hat{\rho} = \sum_j p_j |\psi_j\rangle\langle\psi_j| . \tag{3.4}$$

The density operator is positive (and thereby Hermitian, $\hat{\rho}^\dagger = \hat{\rho}$), i.e., $\langle\Phi|\hat{\rho}|\Phi\rangle \geq 0$ for any state vector $|\Phi\rangle$, and has trace $\mathrm{tr}\{\hat{\rho}\} = 1$. The latter property follows from the normalization of the distribution p_j, stating that the system must be in one of the states $|\psi_j\rangle$. Note that if $p_{j=k} = 1$ for some $j = k$, and 0 for all $j \neq k$, the state is pure and has density operator $\hat{\rho} = |\psi_k\rangle\langle\psi_k|$ – in this case, the system is equally well described by the state vector $|\psi_k\rangle$. Regardless of being pure or mixed, the density operator can always be written as a matrix in any orthonormal basis $\{|n\rangle\}_n$, where the diagonal elements $\rho_{nn} = \langle n|\hat{\rho}|n\rangle$ are referred to as populations and give us the probability to be in state $|n\rangle$, while the off-diagonal elements $\rho_{nm} = \langle n|\hat{\rho}|m\rangle$ are referred to as coherences and originates from superpositions of basis states. We note that if all coherences vanish, there exist no superpositions of basis states. We will return to this point when discussing quantum measurements in Chapter 4, where we will see that the coherences are exponentially damped when measuring continuously on a quantum system. Before continuing, we note that all moments of an observable $\hat{A}$ can be calculated with the density matrix as $\langle\hat{A}^k\rangle = \mathrm{tr}\{\hat{A}^k\hat{\rho}\}$.

Above we pointed out that we need to describe a system with a density matrix when there is an uncertainty about which state the system is in. This uncertainty can arise in various situations – here we discuss two cases. First, imagine that we are preparing a state vector for an experiment. Due to imprecisions in the lab equipment, it is not possible to know with certainty which state the system is in. If this is the case, the system state is mixed, and needs to be described by a density matrix.

As a second case, we consider an open quantum systems S coupled to an environment E, as visualized in Fig. 3.1. The state of the combined unit $S + E$ is pure and can be written as

$$|\psi\rangle = \sum_{jk} c_{jk} |s_j\rangle \otimes |e_k\rangle , \qquad\qquad \sum_{jk} |c_{jk}|^2 = 1, \tag{3.5}$$

where $|s_j\rangle \otimes |e_k\rangle$ are orthonormal basis vectors for the composite state space of $S + E$, while $|s_j\rangle$ and $|e_j\rangle$ are orthonormal basis vectors for S and E, respectively, and $c_{jk} = (\langle s_j| \otimes$
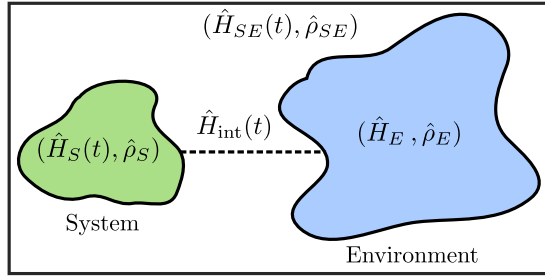
Figure 3.1: Illustration of an open quantum system that interacts with its environment. The system, referred to as S in the text, has a bare Hamiltonian $\hat{H}_S(t)$ and density operator $\hat{\rho}_S$. The environment (E) has a bare Hamiltonian $\hat{H}_E$ and density operator $\hat{\rho}_E$. The system and the environment interacts by exchanging energy and particles – this is described by the interaction Hamiltonian $\hat{H}_{\text{int}}(t)$. By the rectangular box we highlight that the combined unit of system and environment constitutes a closed system which is described by Hamiltonian $\hat{H}_{SE}(t)$ and density operator $\hat{\rho}_{SE}$.

$\langle e_k|)\,|\psi\rangle$ are complex coefficients for which $|c_{jk}|^2$ is the probability to obtain outcome ξ_{jk} when measuring the observable $\hat{A} = \sum_{jk} \xi_{jk}\,|s_j\rangle\langle s_j| \otimes |e_k\rangle\langle e_k|$. The corresponding density operator of $S + E$ is given by $\hat{\rho}_{SE} = |\psi\rangle\langle\psi|$. To find a description of system S alone, we trace $\hat{\rho}_{SE}$ over the environment, and find the system density matrix

$$\hat{\rho}_S = \text{tr}_E\{\hat{\rho}_{SE}\} = \sum_k \langle e_k|\psi\rangle\,\langle\psi|e_k\rangle = \sum_k |\tilde{\psi}_k\rangle\langle\tilde{\psi}_k|\,, \tag{3.6}$$

where $\text{tr}_E\{\cdot\}$ denotes the partial trace over the environment (here computed in the basis $|e_k\rangle$), and $|\tilde{\psi}_k\rangle = \sum_j c_{jk}\,|s_j\rangle$ is a vector in the state space of S. Note that $|\tilde{\psi}_k\rangle$ is not normalized as

$$\langle\tilde{\psi}_k|\tilde{\psi}_k\rangle = \sum_j |c_{jk}|^2 < 1. \tag{3.7}$$

We therefore introduce $|\tilde{\psi}_k\rangle = \sqrt{p}_k\,|\psi_k\rangle$, for which $\langle\psi_k|\psi_k\rangle = 1$, where $p_k = \langle\tilde{\psi}_k|\tilde{\psi}_k\rangle$ is interpreted as the probability to be in state $|\psi_k\rangle$. It follows that

$$\hat{\rho}_S = \sum_k p_k\,|\psi_k\rangle\langle\psi_k|\,, \tag{3.8}$$

which coincides with the definition in Eq. (3.4). We see that by applying the partial trace in Eq. (3.6), we lose all information encoded in the correlations between S and E, and thus introduce uncertainty about the state of S. Therefore, open systems are prime examples where we, in general, need the density matrix in order to describe the state of the system.

3.3   Dynamics

For a closed system described by a density matrix, as in Eq. (3.4), each state $|\psi_j\rangle$ evolves in time according to the Schrödinger equation (3.1). This implies that the density matrix can

be translated in time according to $\hat{\rho}(t) = \hat{U}(t, t_0)\hat{\rho}(t_0)\hat{U}^\dagger(t, t_0)$, where $\hat{\rho}(t_0)$ is the density matrix at time t_0, and $\hat{U}(t, t_0)$ is the time evolution operator in Eq. (3.3). Differentiating with respect to time, we find the von Neumann equation

$$\partial_t\hat{\rho}(t) = -i[\hat{H}(t), \hat{\rho}(t)]. \tag{3.9}$$

This equation determines the dynamics of $\hat{\rho}(t)$ for closed systems, and can be regarded as the Schrödinger equation for mixed states. Note that due to the unitary time evolution, the eigenvalues of $\hat{\rho}(t)$ and the probabilities p_j are stationary over time.

We now proceed with open quantum systems. As introduced above, an open system interacts with its environment – see Fig. 3.1. By environment, we typically refer to one or several thermal reservoirs, but it could also be a smaller system, such as a qubit. Due to the possibly large dimensions of the environment, it is difficult, or impossible, to carry out calculations with the composite density operator $\hat{\rho}_{SE}$ of $S+E$. For instance, for a bath with infinitely many energy modes, the von Neumann equation (3.9) of $\hat{\rho}_{SE}$ would result in an infinitely large hierarchy of coupled differential equations, which, in general, does not have an exact analytical solution. Instead, we aim to work with the reduced density operator $\hat{\rho}_S = \text{tr}_E\{\hat{\rho}_{SE}\}$ of S.

For the combined unit $S + E$, the total Hamiltonian reads

$$\hat{H}_{SE}(t) = \hat{H}_S(t) + \hat{H}_E + \hat{H}_{\text{int}}(t), \tag{3.10}$$

where $\hat{H}_S(t)$ and $\hat{H}_E$ are the bare Hamiltonians of S and E, respectively, and $\hat{H}_{\text{int}}(t)$ describes the interaction between S and E. The total density operator $\hat{\rho}_{SE}$ can be translated in time with the unitary operator (3.3). If $\hat{\rho}_{SE}(t_0)$ is the initial state of $S + E$, and $\hat{\rho}_S(t_0)$ is the initial state of S, the state of S at a later time t is given by

$$\hat{\rho}_S(t) = \text{tr}_E\{\hat{U}(t, t_0)\hat{\rho}_{SE}(t_0)\hat{U}^\dagger(t, t_0)\} \equiv \mathcal{K}_{(t,t_0)}\hat{\rho}_S(t_0), \tag{3.11}$$

where $\mathcal{K}_{(t,t_0)}$ is referred to as a dynamical map, and is always dependent on the unitary $\hat{U}(t, t_0)$ and the initial state of the environment, i.e., $\hat{\rho}_E(t_0) = \text{tr}_S\{\hat{\rho}_{SE}(t_0)\}$. As $\hat{\rho}_{SE}(t_0)$ might contain correlations between S and E, $\mathcal{K}_{(t,t_0)}$ is generally dependent on the initial state of S as well. This is unsatisfactory as the map $\mathcal{K}_{(t,t_0)}$ will be dependent on the state it acts on – we would like to have a map that is universal and can take any input state $\hat{\rho}_S(t_0)$ as its argument. In fact, by choosing an uncorrelated initial state $\hat{\rho}_{SE}(t_0) = \hat{\rho}_S(t_0) \otimes \hat{\rho}_E(t_0)$, we find a universal dynamical map (UDM)

$$\hat{\rho}_S(t) = \text{tr}_E\{\hat{U}(t, t_0)[\hat{\rho}_S(t_0) \otimes \hat{\rho}_E(t_0)]\hat{U}^\dagger(t, t_0)\} \equiv \mathcal{E}_{(t,t_0)}\hat{\rho}_S(t_0), \tag{3.12}$$

where $\mathcal{E}_{(t,t_0)}$ only depends on $\hat{U}(t, t_0)$ and the initial state $\hat{\rho}_E(t_0)$ of the environment. This map is independent on the initial state of S, and can therefore take any state $\hat{\rho}_S(t_0)$ as

its argument for a fixed $\hat{\rho}_E(t_0)$. As $\hat{\rho}_E(t_0)$ is a positive operator, it can be written in a spectral representation as $\hat{\rho}_E(t_0) = \sum_j \lambda_j |e_j\rangle\langle e_j|$ with eigenvalues λ_j, for which $0 \leq \lambda_j \leq 1$ and $\sum_j \lambda_j = 1$, and eigenstates $|e_j\rangle$. By computing the partial trace in Eq. (3.12) in this eigenbasis, the UDM can be written as [2, 68, 73]

$$\mathcal{E}_{(t,t_0)}\hat{\rho}_S = \sum_{kj} \hat{E}_{kj}(t, t_0)\hat{\rho}_S\hat{E}_{kj}^\dagger(t, t_0), \tag{3.13}$$

with Kraus operators $\hat{E}_{kj}(t, t_0) = \sqrt{\lambda_j}\,\langle e_k|\hat{U}(t, t_0)|e_j\rangle$, satisfying the completeness relation $\sum_{kj} \hat{E}_{kj}^\dagger(t, t_0)\hat{E}_{kj}(t, t_0) = 1$. The completeness relation ensures that $\mathcal{E}_{(t,t_0)}$ preserves the trace of $\hat{\rho}_S$. We further note that $\mathcal{E}_{(t,t_0)}$ is linear and completely positive. Complete positivity ensures that any map $\mathcal{E}_{(t,t_0)} \otimes 1_D$, with 1_D being the D-dimensional identity operator, acting on the composite system of S and any external D-dimensional system is also a positive map. Finally, a remark: In general, the initial state of $S + E$ contains correlations between the subsystems and cannot be written as a product state as in Eq. (3.12). However, when experimentally preparing the initial state of S, all correlations between S and E are destroyed, such that $\hat{\rho}_{SE}(t_0) = \hat{\rho}_S(t_0) \otimes \hat{\rho}_E(t_0)$ is no serious restriction.

In general, it is desirable to find a Markovian equation of motion for $\hat{\rho}_S$, like the von Neumann equation (3.9), rather than translating the state in time with $\mathcal{E}_{(t,t_0)}$. To this end, we begin to note that we typically have the indivisibility condition $\mathcal{E}_{(t,t_0)} \neq \mathcal{E}_{(t,\tau)}\mathcal{E}_{(\tau,t_0)}$ for $t_0 < \tau < t$. The maps $\mathcal{E}_{(t,t_0)}$ and $\mathcal{E}_{(\tau,t_0)}$ are UDMs, but $\mathcal{E}_{(t,\tau)}$ is not a UDM as $\hat{\rho}_{SE}(\tau)$, the joint state of $S + E$ at time τ, can contain correlations between S and E. Therefore, $\mathcal{E}_{(t,\tau)}$ depends on the the input state $\hat{\rho}_S(\tau) = \text{tr}_E\{\hat{\rho}_{SE}(\tau)\}$. However, when the correlations between S and E are weak, and have a negligible effect on the dynamics of S, we get the divisibility condition $\mathcal{E}_{(t,t_0)} = \mathcal{E}_{(t,\tau)}\mathcal{E}_{(\tau,t_0)}$, where all maps $\mathcal{E}_{(t,t_0)}$, $\mathcal{E}_{(t,\tau)}$, and $\mathcal{E}_{(\tau,t_0)}$ are UDMs – compare to the Chapman-Kolmogorov equation (2.8) for classical stochastic systems. The divisibility condition is typically justified when the coupling between S and E is weak. We can thus use the divisibility condition to write down a Markovian master equation [73]

$$\partial_t\hat{\rho}_S(t) = \lim_{\epsilon \to 0}\frac{\hat{\rho}_S(t+\epsilon) - \hat{\rho}_S(t)}{\epsilon} = \lim_{\epsilon \to 0}\frac{\mathcal{E}_{(t+\epsilon,t)} - 1}{\epsilon}\mathcal{E}_{(t,t_0)}\hat{\rho}_S(t_0) = \mathcal{L}(t)\hat{\rho}_S(t), \tag{3.14}$$

where we introduced the Liouville superoperator $\mathcal{L}(t) = \lim_{\epsilon \to 0}[\mathcal{E}_{(t+\epsilon,t)} - 1]/\epsilon$. Such a Markovian master equation can always be written on Lindblad (or GKLS) form (named after the persons that first derived it: Gorini, Kossakowski, Lindblad and Sudarshan) [68, 73–75] as

$$\partial_t\hat{\rho}_S(t) = \mathcal{L}(t)\hat{\rho}_S(t) = -i[\hat{H}(t), \hat{\rho}_S(t)]$$
$$+ \sum_k \gamma_k(t)\left[\hat{L}_k(t)\hat{\rho}_S(t)\hat{L}_k^\dagger(t) - \frac{1}{2}\{\hat{L}_k^\dagger(t)\hat{L}_k(t), \hat{\rho}_S(t)\}\right], \tag{3.15}$$

where $\hat{H}(t)$ is an Hermitian operator, the coefficients $\gamma_k(t) \geq 0$, and $\hat{L}_k(t)$ are referred to as Lindblad operators. We note that $\hat{H}(t)$, typically, do not exactly coincide with the bare Hamiltonian $\hat{H}_S(t)$ of S, but also contain terms originating from the coupling between S and E [68, 73]. If the extra terms are negligible, the first term of the Lindblad equation (3.15) corresponds to the von Neumann equation (3.9), and describes the coherent dynamics of S in the absence of E. The combinations of operators under the sum in the Lindblad equation are commonly written on the compact superoperator form $\mathcal{D}[\hat{L}_k(t)]\hat{\rho} = \hat{L}_k(t)\hat{\rho}\hat{L}_k^\dagger(t) - \frac{1}{2}\{\hat{L}_k^\dagger(t)\hat{L}_k(t), \hat{\rho}\}$, and describes how the environment affects the system. Typically, the Lindblad operators are ladder operators of the system, describing how the system gets excited or de-excited by interacting with the environment. In general, this interaction can be considered as incoherent, and does not involve the off-diagonals of the density matrix. The coefficients $\gamma_k(t)$ are transition rates and can be expressed in terms of the properties of the environment and the coupling between S and E – for an explicit example, see the classical toy model in Chapter 7.

The Liouville superoperator, or Liouvillian, $\mathcal{L}(t)$ is said to be a generator of the UDM $\mathcal{E}_{(t,t_0)}$, and we can write

$$\mathcal{E}_{(t,t_0)} = \mathcal{T}e^{\int_{t_0}^t ds \mathcal{L}(s)}, \tag{3.16}$$

where $\mathcal{T}$ is the time ordering operator. If $\mathcal{L}(t)$ is time independent, $\mathcal{E}_{(t,t_0)} = \exp\{\mathcal{L}(t-t_0)\}$ and only depends on the time difference $\tau = t - t_0$, such that $\mathcal{E}_{(t,t_0)} = \mathcal{E}_\tau$. This UDM satisfies the semigroup property $\mathcal{E}_t \mathcal{E}_\tau = \mathcal{E}_{t+\tau}$ [73]. Starting from this property, we may show the converse, i.e., that the semigroup property leads to a time independent Liouvillian $\mathcal{L}$ [73], where all time dependence in the Lindblad equation (3.15) can be removed. For such a time independent Liouvillian, we are typically interested in the stationary state of the dynamics when $t \to \infty$ [a time dependent $\mathcal{L}(t)$ does not necessarily have a stationary state]. To motivate why we focus only on the stationary state, we note that for quantum heat engines or feedback controlled devices, it is desirable that the system reaches a target state that is stable over time. That is, we want to find the state $\hat{\rho}_{ss}$ that satisfies $\mathcal{L}\hat{\rho}_{ss} = 0$. The total solution to the Lindblad equation can be written on the general form

$$\hat{\rho}_S(t) = \sum_j c_j e^{\lambda_j(t-t_0)}\hat{\sigma}_j, \tag{3.17}$$

where c_j are coefficients determined by the initial condition $\hat{\rho}_S(t_0)$, and λ_j are the eigenvalues of $\mathcal{L}$ with corresponding (linearly independent) eigenstates $\hat{\sigma}_j$. We thus see that there exists one eigenvalue $\lambda_0 = 0$ with $c_0\hat{\sigma}_0 = \hat{\rho}_{ss}$ corresponding to the stationary state, while the other eigenvalues must have a negative real part such that only the $j = 0$ term survives in the long time limit.
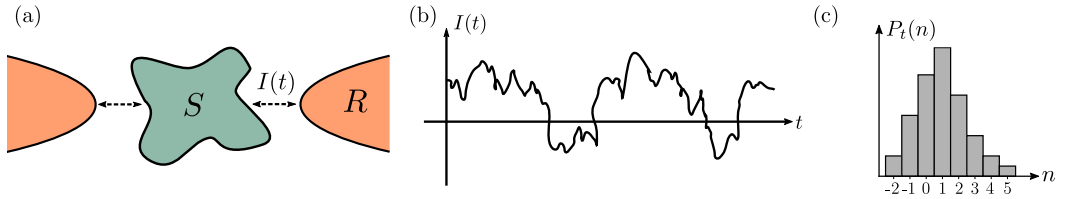
Figure 3.2: (a) A standard setup for nanoscale experiments. A system (*S*) is coupled to one or several environments. We are interested in investigating the intrinsic properties of *S* by measuring the particle exchange between *S* and the environment labeled by *R*. This exchange can be measured via the particle current $I(t)$, as marked in the figure. (b) A schematic sketch of how the current $I(t)$ changes over time. (c) The probability distribution $P_t(n)$ of the number of particles *n* exchanged between *S* and *R* after time *t*. By relating $n(t)$ and $I(t)$ as in Eq. (3.18), we may find the moments and cumulants of $P_t(n)$ directly from the current correlations.

3.4 Full counting statistics

The central idea of full counting statistics is to gain full knowledge about particle transport in nanoscale systems. The probability distribution $P_t(n)$ of having *n* transferred particles during a time interval *t* can reveal intrinsic properties of these systems. For instance, in electronic circuits on the microscopic scale, the role of current fluctuations becomes essential for understanding a large variety of microscopic concepts [67]. Motivated by this, we introduce full counting statistics with electronic transport [76] in mind, focusing especially on how $P_t(n)$ can be obtained for systems described by Markovian master equations [77, 78]. We note that this type of counting can be extended to any types of particles – for instance, photons [79] and phonons [80].

We begin by studying the setup depicted in Fig. 3.2(a), where a system *S* exchanges particles with one or several reservoirs – *S* is thereby an open quantum system. Our main objective is to measure the statistics of exchanged particles between *S* and the reservoir labeled by *R* during an arbitrary interaction time *t*. Such particle counting is, since roughly 20 years ago, possible to conduct in electronic systems, where single electron transitions can be detected [32, 44, 81–85]. As long as the response rate of the detector is much larger than the electron transition rate, one can accurately infer the transport statistics. When the electron transition rate is similar to, or larger than the detector response rate, it is no longer possible to resolve all electron transitions, and the recorded data would give inaccurate transport statistics. Instead, one could measure the current $I(t)$ (here interpreted as a particle current rather than an electronic current) to infer something about the transport statistics[1]. In Fig. 3.2(b), we have sketched a time trace of the current between *S* and *R*. The number of

---

[1]In this thesis, we interpret $I(t)$ as a classical current. This allows for straightforward manipulations when calculating higher order statistics as in Eq. (3.20). In a full quantum treatment, the current is introduced as an operator $\hat{I}(t)$. This raises some subtleties, such as time ordering. For instance, Eq. (3.20) does not, in general, hold when the current is an operator. For a full quantum treatment, see, for example, Refs. [76, 86, 87].

particles exchanged with R after time t is obtained via

$$n(t) = \int_0^t d\tau\, I(\tau).$$
(3.18)

Here we use the convention that $I(t) > 0$ when the current flows from S towards R, such that $n(t) > 0$ when particles enter R. Since $I(t)$ and $n(t)$ are random processes, it is difficult to draw general conclusions about the transport statistics from one single time trace. Instead, by repeating the experiment a large number of times N, and keeping track of $n(t)$ for each run, we can find the number of times K_n where we observe n exchanged particles after time t. The relative frequency of observing n particles is given by K_n/N, and in the limit of large N, we get

$$\lim_{N \to \infty} \frac{K_n}{N} = P_t(n),$$
(3.19)

the probability of observing n exchanged particles after time t. Figure 3.2(c) illustrates a typical distribution function $P_t(n)$.

Note that the moments of $P_t(n)$ may be calculated from the current as well. By taking an average $\langle \cdot \rangle$ over many experimental realizations [similar to Eq. (2.3)], we get

$$\langle n^k(t) \rangle = \int_0^t d\tau_1 \cdots \int_0^t d\tau_k \langle I(\tau_1) \cdots I(\tau_k) \rangle,$$
(3.20)

where we used Eq. (3.18). For $k = 1$, we get the average $\langle n(t) \rangle$. For long times t, the average current $\langle I(t) \rangle$ reaches a stationary state, and becomes independent on time. In that case, the average current can be moved outside the integral, and we get $\langle n(t) \rangle = \langle I \rangle_{\text{ss}} t$. The stationary current can thus be written on the intuitive form

$$\langle I \rangle_{\text{ss}} = \lim_{t \to \infty} \frac{\langle n(t) \rangle}{t}.$$
(3.21)

We can further calculate the variance of $P_t(n)$ via the current measurements as

$$\langle\!\langle n^2(t) \rangle\!\rangle = \langle n^2(t) \rangle - \langle n(t) \rangle^2 = \int_0^t d\tau_1 \int_0^t d\tau_2 \left[\langle I(\tau_2)I(\tau_1) \rangle - \langle I(\tau_2) \rangle \langle I(\tau_1) \rangle \right].$$
(3.22)

From this, we find the second order current cumulant

$$\langle\!\langle I^2(t) \rangle\!\rangle = \partial_t \langle\!\langle n^2(t) \rangle\!\rangle = 2 \int_0^t d\tau \left[\langle I(\tau)I(t) \rangle - \langle I(\tau) \rangle \langle I(t) \rangle \right].$$
(3.23)

From these expressions, we can define a current correlator $C_I(t, t') = \langle I(t)I(t') \rangle - \langle I(t) \rangle \langle I(t') \rangle$. We are interested in the stationary state of the current correlator, where it is translationally invariant in time and only depends on the difference $t - t'$, i.e., $C_I(t, t') = C_I(t - t')$. We further assume that the system is Markovian, meaning that the correlator quickly decays

to zero on some correlation time τ_c. Finally, we assume that the correlator is symmetric under the exchange $t \leftrightarrow t'$, such that all points separated by $t - t'$ are correlated identically. When the measurement time t greatly exceeds the correlation time τ_c, the variance of $P_t(n)$ becomes linear in time,

$$\langle\langle n^2(t) \rangle\rangle = t \int_{-\infty}^{\infty} d\tau \left[\langle I(\tau) I(0) \rangle - \langle I(\tau) \rangle \langle I(0) \rangle \right]. \tag{3.24}$$

This implies the stationary second current cumulant

$$\langle\langle I^2 \rangle\rangle_{\text{ss}} = \lim_{t \to \infty} \frac{\langle\langle n^2(t) \rangle\rangle}{t} = \int_{-\infty}^{\infty} d\tau \left[\langle I(\tau) I(0) \rangle - \langle I(\tau) \rangle \langle I(0) \rangle \right]. \tag{3.25}$$

With the noise spectrum of the stationary current correlator [see Eq. (2.6)]

$$S_I(\omega) = \int_{-\infty}^{\infty} d\tau e^{i\omega\tau} C_I(\tau), \tag{3.26}$$

we find that the zero frequency noise $S_I(0)$ coincides with Eq. (3.25). Therefore, we understand that the variance of n, in the long time limit, is given by

$$\langle\langle n^2(t) \rangle\rangle = S_I(0) t. \tag{3.27}$$

The variance thus grows linearly with time at a rate determined by the zero frequency noise of the current correlator. This linear increase reflects that different trajectories of $n(t)$ will be less similar the longer we measure. The uncertainty in the number of exchanged particles should therefore grow with time. This is similar to the variance of Brownian motion in Chapter 2.

3.4.1 Full counting statistics in Markovian master equations

In the previous section, we described how the moments of the distribution $P_t(n)$ can be calculated by measuring particle currents. Here we discuss how $P_t(n)$, and its moments and cumulants, may be calculated from a Markovian master equation.

Our starting point is the Markovian master equation

$$\partial_t \hat{\rho}_t = \mathcal{L} \hat{\rho}_t, \tag{3.28}$$

where the Liouville superoperator $\mathcal{L}$ is assumed to be on Lindblad form [see Eq. (3.15)]. This superoperator can be decomposed as $\mathcal{L} = \mathcal{L}_0 + \mathcal{J}_+ + \mathcal{J}_-$, where $\mathcal{L}_0$ describes all dynamics that leaves the number of exchanged particles with R unchanged, and the jump superoperators $\mathcal{J}_\pm$ describe how one particle is added ($+$) or removed ($-$) from R [see

Fig. 3.2(a)]. We are interested in the *n*-resolved density matrix $\hat{\rho}_t(n)$, representing the system state when n particles have been exchanged with R. In particular, we note that $P_t(n) = \mathrm{tr}\{\hat{\rho}_t(n)\}$ is the probability distribution of our interest, and that $\hat{\rho}_t = \sum_n \hat{\rho}_t(n)$. By taking the Laplace transform of the master equation (3.28), we can show (Appendix C) that the number resolved density matrix evolves according to

$$\partial_t \hat{\rho}_t(n) = \mathcal{L}_0 \hat{\rho}_t(n) + \mathcal{J}_+ \hat{\rho}_t(n-1) + \mathcal{J}_- \hat{\rho}_t(n+1), \qquad (3.29)$$

providing an infinitely large system of coupled differential equations. Typically, the initial condition is given by $\hat{\rho}_{t_0}(n) = \delta_{n,0}\hat{\rho}_{t_0}$, such that zero particles have been exchanged initially. To solve this set of equations, we introduce the counting field χ via the discrete Fourier transform

$$\hat{\rho}_t(\chi) = \sum_n \hat{\rho}_t(n) e^{in\chi}. \qquad (3.30)$$

Note that the system state is recovered for zero counting field, $\hat{\rho}_t = \hat{\rho}_t(\chi = 0)$. Fourier transforming Eq. (3.29) results in

$$\partial_t \hat{\rho}_t(\chi) = \mathcal{L}(\chi)\hat{\rho}_t(\chi), \qquad (3.31)$$

where the counting field dependent Liouvillian reads $\mathcal{L}(\chi) = \mathcal{L}_0 + e^{i\chi}\mathcal{J}_+ + e^{-i\chi}\mathcal{J}_-$, and the initial condition is given by $\hat{\rho}_{t_0}(\chi) = \hat{\rho}_{t_0}$. This master equation has the formal solution $\hat{\rho}_t(\chi) = e^{\mathcal{L}(\chi)t}\hat{\rho}_{t_0}$.

Since $P_t(n) = \mathrm{tr}\{\hat{\rho}_t(n)\}$, we can define a moment generating function

$$M_t(\chi) = \mathrm{tr}\{\hat{\rho}_t(\chi)\} = \sum_n P_t(n) e^{in\chi}, \qquad (3.32)$$

such that the moments of $P_t(n)$ can be calculated as

$$\langle n^k(t) \rangle = (-i)^k \partial_\chi^k M_t(\chi)\big|_{\chi=0}. \qquad (3.33)$$

In a strict mathematical sense, $M_t(\chi)$ is the characteristic function of $P_t(n)$, but as the characteristic function exists for all distributions, it is more beneficial to work with compared to the conventional moment generating function, which does not exist for all distributions [88]. Note that the first moment can conveniently be calculated as $\langle n \rangle = -it\,\mathrm{tr}\{\mathcal{L}'(\chi)|_{\chi=0}\hat{\rho}_t\}$, where the prime denotes the derivative with respect to χ. One can further define a cumulant generating function

$$C_t(\chi) = \ln[M_t(\chi)], \qquad (3.34)$$

which provides the cumulants of $P_t(n)$ via

$$\langle\!\langle n^k(t) \rangle\!\rangle = (-i)^k \partial_\chi^k C_t(\chi)\big|_{\chi=0}. \qquad (3.35)$$

As the moment and cumulant generating functions are related, one can write the cumulants in terms of the moments. In particular, $\langle\langle n(t)\rangle\rangle = \langle n(t)\rangle$ is the mean of $P_t(n)$, and $\langle\langle n^2(t)\rangle\rangle = \langle n^2(t)\rangle - \langle n(t)\rangle^2$ is the variance of $P_t(n)$. In fact, the second and third cumulants correspond exactly to the second and third central moments of $P_t(n)$. We also note that the third and fourth cumulants are related to the skewness and kurtosis of $P_t(n)$. The current cumulants are found by differentiating with respect to time,

$$\langle\langle I^k(t)\rangle\rangle = \partial_t\langle\langle n^k(t)\rangle\rangle. \tag{3.36}$$

With the definitions of the moment and cumulant generating functions, we can calculate the probability distribution according to

$$P_t(n) = \frac{1}{2\pi}\int_{-\pi}^{\pi}d\chi e^{C_t(\chi)-in\chi}. \tag{3.37}$$

In general, this must be calculated numerically, even if we know the cumulant generating function. However, the saddle point approximation [89–91] is useful for finding analytical expressions in the long time limit.

In many cases, we can find an approximate expression for the cumulant generating function in the long time limit. The solution of Eq. (3.31) can be written as

$$\hat{\rho}_t(\chi) = \sum_{j=0}^{N-1} c_j e^{\lambda_j(\chi)t}\hat{\sigma}_j(\chi), \tag{3.38}$$

where the coefficients c_j are determined by the initial condition $\hat{\rho}_0$ (we use $t_0 = 0$), $\lambda_j(\chi)$ are the eigenvalues of $\mathcal{L}(\chi)$ with corresponding eigenstates $\hat{\sigma}_j(\chi)$, and N is the dimension of $\mathcal{L}(\chi)$. We are interested in systems with a unique steady state. For such systems, there exists one single eigenvalue for which $\lambda_0(0) = 0$ (here labeled with $j = 0$), and where all other eigenvalues $\lambda_j(0) \neq 0$. Since the system tends to a stationary state, all eigenvalues with $j \neq 0$ must have negative real parts, such that all terms except $j = 0$ are vanishingly small when t is large [see discussion below Eq. (3.17)]. This means that all eigenvalues for finite χ must have negative real parts, with the real part of $\lambda_0(\chi)$ being the largest, such that we for large t find

$$\hat{\rho}_t(\chi) \approx c_0 e^{\lambda_0(\chi)t}\hat{\sigma}_0(\chi). \tag{3.39}$$

The moment generating function now reads $\text{tr}\{\hat{\rho}_t(\chi)\} \approx \text{tr}\{\hat{\sigma}_0(\chi)\}c_0 e^{\lambda_0(\chi)t}$, and we may approximate the cumulant generating function as

$$C_t(\chi) \approx \lambda_0(\chi)t, \tag{3.40}$$

up to a correction term $\ln[c_0\,\text{tr}\{\hat{\sigma}_0(\chi)\}]$ which has been neglected. In the long time limit, it is justified to neglect this term as it is small compared to $\lambda_0(\chi)t$. Consequently, the

number cumulants will have an error determined by the χ-derivatives of $\ln[c_0 \operatorname{tr}\{\hat{\sigma}_0(\chi)\}]$. However, in the current cumulants, this error will not be present as we take a time derivative in Eq. (3.36). We note that the approximate form in Eq. (3.40) reproduces the linear-in-time behavior of the number cumulants in Eq. (3.27). We emphasize that this formalism can be extended to multiple counting fields, keeping track of the counting statistics in multiple reservoirs simultaneously.

Chapter 4

Quantum measurements

In this chapter, we present the basic theory of quantum measurements that is required to describe continuous quantum measurements – this is later used in Chapter 6 to derive Eq. (1.1). We begin by briefly reviewing the concept of von Neumann measurements (projective measurements) that is commonly discussed in basic quantum mechanics courses. As this type of measurement often is an idealization of what can be performed in an actual experiment, we introduce generalized quantum measurements, providing a framework for describing any type of measurement, i.e., going beyond von Neumann measurements. Building on this, we discuss Gaussian and continuous measurements, which are central for the derivations in Chapter 6. As a measurement on a quantum system always affects the system dynamics, we briefly outline the quantum Zeno effect at the end of the section, and discuss how a continuous measurement may freeze, or prohibit, the dynamics of the measured system. Before closing this chapter, we introduce two central results from the field of continuous quantum feedback control that will be important references in the rest of the thesis.

4.1   von Neumann and generalized quantum measurements

Fundamental to measurements in quantum mechanics is the concept of *von Neumann measurements* – or projective measurements. This type of measurement describes how the state of a quantum system is collapsed (projected) onto one of the eigenstates of the measured observable after performing a measurement. More precisely, any observable $\hat{A}$ has a diagonal representation in some orthonormal basis $\{|a\rangle\}_{a=1}^{N}$, i.e., it can be written as $\hat{A} = \sum_{a=1}^{N} \xi_a |a\rangle\langle a|$, where $\{\xi_a\}_{a=1}^{N}$ are the (non-degenerate) eigenvalues of $\hat{A}$. In general, the eigenvalues can be degenerate. If that is the case, the system state is projected onto a

superposition of the corresponding eigenstates. In this thesis, however, we are interested in distinguishing the state of the system, and will therefore not deal with degenerate eigenvalues. Note that we assume that there is a finite number N of eigenvalues, as this typically will be the case in this thesis. Consider that we carry out a measurement on an arbitrary quantum system, whose state, when written in the eigenbasis of $\hat{A}$, is given by $|\psi\rangle = \sum_{a=1}^{N} c_a |a\rangle$, with complex coefficients c_a satisfying $\sum_{a=1}^{N} |c_a|^2 = 1$. Upon measuring, we obtain one of the eigenvalues $\xi_{a'}$ with probability $|c_{a'}|^2$, and the state collapses to $|a'\rangle$. That is, we are certain that the system is in this state after the measurement. In terms of the density operator formalism introduced in Chapter 3, we note that the pre-measurement state is given by some density operator $\hat{\rho}$ – pure or mixed – but the post-measurement state will with probability $|c_{a'}|^2$ be in the pure state $\hat{\rho}' = |a'\rangle\langle a'|$.

A von Neumann measurement does not fully describe a realistic procedure for quantum measurements. In reality, an experimenter rarely interacts directly with the system of interest, but rather measures on a probe that interacts with the system. In addition, the von Neumann measurement does not add any classical noise to the measurement outcome [57]. In general, this must be regarded as unrealistic as a measurement device typically adds noise to the measurement signal. The idea of the system-probe model is to build up correlations between the system and probe, and then perform a von Neumann measurement on the probe, such that we can infer something about the system without collapsing its state. As a first example of this, consider a nanowire quantum dot for which we want to measure the charge state, i.e., if there is an electron or not in the dot. In general, this is done by placing a probe in the vicinity of the dot – typically the probe is another quantum dot or a quantum point contact – and measure the electrical current through the probe. If the system-probe interaction is sensitive enough, the current will jump between discrete values when an electron jumps on or off the dot, see for instance Refs. [81] and [32]. As a second example, consider an atom interacting with an electromagnetic field. Here the field acts as the probe, and by measuring on the field, for instance with a photo detector, we can infer something about the state of the atom.

To find a mathematical description for the system-probe measurement, we consider the following model. Assume that the system and probe initially are uncorrelated, and that their joint state is given by $\hat{\rho}_{\text{tot}} = |0\rangle\langle 0| \otimes \hat{\rho}$, where the probe was prepared in some state $|0\rangle$ belonging to an orthonormal set $\{|m\rangle\}_m$ of probe states, and the system was prepared in an arbitrary state $\hat{\rho}$. By letting the system and probe interact under some unitary transformation $\hat{U}$, their states will become correlated. Now we make a von Neumann measurement on the probe, projecting it onto one of the states $|m\rangle$. After this procedure, the joint state is proportional to

$$\hat{\rho}'_{\text{tot}} \sim (|m\rangle\langle m| \otimes 1) \, \hat{U} (|0\rangle\langle 0| \otimes \hat{\rho}) \, \hat{U}^{\dagger} (|m\rangle\langle m| \otimes 1) = |m\rangle\langle m| \otimes \hat{K}_m \hat{\rho} \hat{K}_m^{\dagger}, \qquad (4.1)$$

where we in the second equality introduced operators $\hat{K}_m = \langle m|\hat{U}|0\rangle$ acting on the system state. This expression is only proportional to the true system-probe state as it is not

normalized. Especially note that the mathematical procedure resembles how the UDMs were introduced in Eq. (3.12) – in fact, any operation on an open quantum system may be written like this [2].

We can now define a generalized quantum measurement as follows. Consider a system with state $\hat{\rho}$ on which we perform a measurement described by a set of measurement operators $\{\hat{K}_m\}_m$, satisfying the completeness relation $\sum_m \hat{K}_m^\dagger \hat{K}_m = 1$. When observing outcome m, the state transforms as

$$\hat{\rho}' = \frac{\hat{K}_m \hat{\rho} \hat{K}_m^\dagger}{p_m}, \tag{4.2}$$

where $p_m = \mathrm{tr}\{\hat{K}_m^\dagger \hat{K}_m \hat{\rho}\}$ is the probability of observing outcome m, and the measurement operators are defined as in the previous paragraph. We emphasize here that Eq. (4.2) is obtained by tracing out the probe in Eq. (4.1), i.e., $\hat{\rho}' \sim \mathrm{tr}_P\{\hat{\rho}'_{\mathrm{tot}}\}$, and normalizing with p_m. The completeness relation $\sum_m \hat{K}_m^\dagger \hat{K}_m = 1$ follows from probability conservation for p_m, but also follows directly from the definition of $\hat{K}_m$. Sometimes, this type of measurement is referred to as a POVM (positive operator-valued measure) measurement [2, 57, 58], but in this thesis, we refer to it as a generalized quantum measurement. We stress here that the measurement operators $\hat{K}_m$ are completely general, and do not necessarily represent projective measurements. Below, in Sec. 4.2, we will discuss the special case of Gaussian measurements. However, by considering projective measurement operators $\hat{K}_m = |m\rangle\langle m|$ (where $|m\rangle$ now represents basis states of the system), Eq. (4.2) boils down to the von Neumann measurement discussed above.

It is important to note that $\hat{\rho}'$ in Eq. (4.2) is conditioned on the measurement outcome m. That is, it describes our state of knowledge of the system given that we observed m in the measurement. Interestingly, this transformation is nonlinear in $\hat{\rho}$. This is in contrast to the von Neumann equation (3.9) and the Lindblad equation (3.15) which are linear. This means that quantum measurements induce a nonlinear change in the system state. We will return to this in Chapter 4.3. However, a linear description is obtained by multiplying Eq. (4.2) by p_m, but at the cost of introducing the un-normalized joint system-outcome state $\hat{\rho}(m) = \hat{\rho}' p_m = \hat{K}_m \hat{\rho} \hat{K}_m^\dagger$. This will be used in Sec. 6 when we derive Eq. (1.1). We note that summing the joint system-outcome state over all outcomes m gives us the post-measurement state $\tilde{\rho} = \sum_m \hat{K}_m \hat{\rho} \hat{K}_m^\dagger$, which is the conditioned state $\hat{\rho}'$ [Eq. (4.2)] averaged over all outcomes. This is sometimes referred to as a non-selective measurement [68] as one can interpret $\tilde{\rho}$ as the state of the system if we ignored which outcome that was obtained. As an example, let us consider a two-level system with density operator $\hat{\rho} = p_0 |0\rangle\langle 0| + \alpha(|0\rangle\langle 1| + |1\rangle\langle 0|) + p_1 |1\rangle\langle 1|$, where p_0 and p_1 are the probabilities to be in state $|0\rangle$ or $|1\rangle$, respectively, and α represents the coherence. By performing a projective measurement, with measurement operators $\hat{K}_0 = |0\rangle\langle 0|$ and $\hat{K}_1 = |1\rangle\langle 1|$, the post-measurement state, averaged over all possible outcomes (0 or 1), is given by $\tilde{\rho} = p_0 |0\rangle\langle 0| + p_1 |1\rangle\langle 1|$. That is, after the measurement, the system will be in a statistical mixture of $|0\rangle$ and $|1\rangle$. This

illustrates that the measurement destroys all coherence, but we do not know the exact state of the system as we ignored the outcome.

Finally, we point out that quantum measurements induce a stochastic change to a system state. To illustrate this, we consider many copies of the same system on which we perform identical measurements. The state transformation in Eq. (4.2) depends on what outcome m that was observed, and since each outcome occurs with probability p_m, the measurement operators applied on a specific system is random. Therefore, the post-measurement state will not be the same for all copies. This implies that for a continuous measurement, the conditioned state $\hat{\rho}'$ evolves according to a stochastic master equation. This is further discussed in Sec. 4.3.

4.2 Gaussian measurement operator and weak continuous measurements

In many situations, it is common to perform a time-continuous measurement, rather than making one single measurement, and to use a measurement apparatus that outputs continuous outcomes, rather than discrete ones. Even though one measures a discrete observable, like a photon number operator, the measurement device adds noise to the signal, such that a continuous outcome space is more appropriate than a discrete one. The type of measurement, discrete or continuous in time, that is most suitable is determined by the type of system and experiment one is studying. For instance, in electronic systems, such as semiconductor quantum dots [32, 44, 92], it is possible to measure the charge occupation continuously, which suggests that a time-continuous measurement is most suitable. As another example, the state of superconducting qubits can also be monitored continuously [6]. On the other hand, when distinguishing spin states in semiconductor quantum dots, one is restricted to time-discrete measurements [93]. This is also the case when performing quantum state tomography in rare earth ion qubits [94]. However, many control procedures require continuous monitoring, such as certain schemes for quantum error correction [95], stabilizing Rabi oscillations [6], reversing quantum jumps [7], or implementing an electronic Szilard engine [28]. Therefore, we dedicate this section to time-continuous measurements with continuous outcomes. We begin by replacing the discrete outcomes m from the previous section by continuous outcomes z. The theory presented above for discrete outcomes still applies, but sums over m are typically replaced by integrals over all real values of z. In the second part of this section, we discuss how we theoretically can describe time-continuous measurements, and how the quantum Zeno effect emerges from this description.

In this thesis, we focus on Gaussian measurement operators [58, 96, 97]

$$\hat{K}(z) = \left(\frac{2\bar{\lambda}}{\pi}\right)^{1/4} e^{-\bar{\lambda}\left(z-\hat{A}\right)^2}, \tag{4.3}$$

where $\hat{A}$ is the measured observable (note that $\hat{A}^\dagger = \hat{A}$), and $\bar{\lambda}$ parameterizes the strength of the measurement. In the limit $\bar{\lambda} \to \infty$, Eq. (4.3) describes a projective von Neumann measurement, where all initial quantum coherence is destroyed, and where the post-measurement state is projected onto one of the eigenstates of $\hat{A}$. In the opposite limit, when $\bar{\lambda} \to 0$, Eq. (4.3) describes a weak, non-intrusive measurement, preserving all quantum coherence. It thus provides the possibility of describing measurements with a wide range of possible interaction strengths, and allows us to investigate how the strength affects the measured system. Additionally, Eq. (4.3) implies that the measurement noise in the outcome is Gaussian (see discussion below). This is commonly the case due to many independent random fluctuations in the electronic circuits of the measurement device. We also note (this will be shown below) that Eq. (4.3) is suitable for analytical manipulations as it simplifies many calculations, while still providing general results.

To illustrate the strong and weak measurement limits, we study a simple two-level system with states $|0\rangle$ and $|1\rangle$. In the $\{|0\rangle, |1\rangle\}$-basis, the system density operator reads $\hat{\rho} = p|0\rangle\langle 0| + \alpha(|0\rangle\langle 1| + |1\rangle\langle 0|) + (1-p)|1\rangle\langle 1|$, where p and $1-p$ are the probabilities of occupying $|0\rangle$ and $|1\rangle$, respectively, and α represents the coherence (here assumed to be real for simplicity, but without loss of generality). When measuring $\hat{A} = |1\rangle\langle 1| - |0\rangle\langle 0|$ [1], i.e., whether $|0\rangle$ or $|1\rangle$ is occupied, the state transformation is, according to Eq. (4.2), proportional to

$$\hat{K}(z)\hat{\rho}\hat{K}^\dagger(z) = \sqrt{\frac{2\bar{\lambda}}{\pi}}\Big[pe^{-2\bar{\lambda}(z+1)^2}|0\rangle\langle 0| \\ + \alpha e^{-2\bar{\lambda}(z^2+1)}(|0\rangle\langle 1| + |1\rangle\langle 0|) + (1-p)e^{-2\bar{\lambda}(z-1)^2}|1\rangle\langle 1|\Big]. \tag{4.4}$$

For simplicity, we neglect the normalizing factor $p(z) = \mathrm{tr}\{\hat{K}^\dagger(z)\hat{K}(z)\hat{\rho}\}$. The effect of the measurement is adding Gaussian weights, centered at $-1, 0,$ and 1, to the respective elements of $\hat{\rho}$, and the off-diagonal elements get suppressed by a factor $e^{-2\bar{\lambda}}$. The weights of the respective elements are sketched in Fig. 4.1. For a weak measurement, we note that a considerable amount of the coherence is preserved when the outcome lies in the range $-1 < z < 1$. In the infinitely weak limit, $\bar{\lambda} \to 0$, the Gaussian weights become uniform distributions over all z, and all coherence is preserved. As $\bar{\lambda}$ is increased in Fig. 4.1, the coherence is exponentially suppressed, and vanishes for strong measurements. For the strong measurement, we note that only the $|0\rangle\langle 0|$ or $|1\rangle\langle 1|$ matrix element survives. Treating this

---

[1]This corresponds to the Pauli-Z operator $\hat{\sigma}_z$.

rigorously in the limit $\bar{\lambda} \to \infty$, the diagonal Gaussian weights become Dirac delta functions $\delta(z \pm 1)$ centered at ± 1, while the off-diagonal weights vanish, corresponding to a projective measurement.
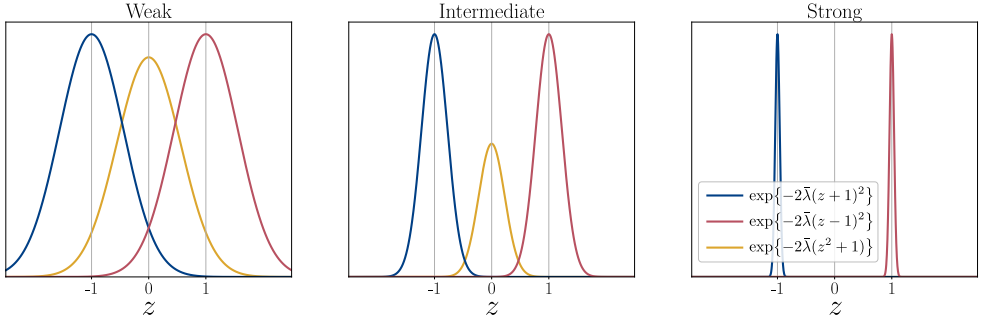

Figure 4.1: Qualitative sketch of how the Gaussian weights in Eq. (4.4) behave when going from a weak to a strong measurement (from left to right with increasing $\bar{\lambda}$). Note that for weak measurements, a substantial part of the coherence is preserved for a larger range of outcomes than in the strong measurement case. This is due to the factor $\exp\{-2\bar{\lambda}\}$ on the off-diagonal elements in Eq. (4.4).

For the example two-level system, the probability distribution of outcomes z is given by

$$p(z) = \mathrm{tr}\{\hat{K}^\dagger(z)\hat{K}(z)\hat{\rho}\} = \sqrt{\frac{2\bar{\lambda}}{\pi}} \left[p e^{-2\bar{\lambda}(z+1)^2} + (1-p) e^{-2\bar{\lambda}(z-1)^2} \right]. \qquad (4.5)$$

In the strong measurement limit, $\bar{\lambda} \to \infty$, the Gaussian weights become Dirac delta functions $\delta(z \pm 1)$. That is, the information we gain from the measurement is very exact. However, from Eq. (4.4), we noted that such a measurement destroys the coherence of the system. In the weak limit, $\bar{\lambda} \to 0$, the Gaussian weights become uniform distributions. Therefore, the measurement can yield any value for the outcome z, but without affecting the coherence of the system, as showed in Eq. (4.4) – this corresponds to not performing any measurement and randomly sampling the outcome from a uniform distribution. The strength of the measurement thus becomes a trade-off – a weak measurement preserves quantum coherence, but gives large measurement uncertainty, while a strong measurement destroys quantum coherence and gives low measurement uncertainty.

Equation (4.5) is a mixed distribution, and can be interpreted as follows. Consider a random variable $x = -1, 1$ for the system state, following a two-point distribution with $P(x = -1) = p$ and $P(x = 1) = 1 - p$ being the probabilities of occupying $|0\rangle$ and $|1\rangle$, respectively. Given that we know the system state x, the random variable $z|x$ represents the measurement outcome conditioned on the system state. This variable has a Gaussian distribution with mean value x and variance $1/4\bar{\lambda}$. The unconditioned outcome z has the distribution given in Eq. (4.5), and is obtained via the total law of probability according to

$$p(z) = \sum_{k=-1,1} f_{z|x=k}(z) P(x = k), \qquad (4.6)$$

40

where $f_{z|x}(z) = \sqrt{2\bar{\lambda}/\pi}e^{-2\bar{\lambda}(z-x)^2}$ is the probability density of $z|x$.

To describe a continuous measurement, we may use the measurement operator in Eq. (4.3). The continuous description is achieved by first discretizing time, and then making successive measurements at times separated by δt. To preserve the quantum coherence during the continuous measurement, each measurement must be weak. Otherwise, the coherence is quickly destroyed, prohibiting the system to evolve coherently – this is known as the quantum Zeno effect [68, 98, 99]. The Zeno effect is typically explained by considering the effect of repeated projective (strong) measurements on a Rabi oscillator – by repeatedly projecting a coherently driven system onto one of the eigenstates of the observable, the coherent transition is blocked and the system cannot evolve in time. To avoid such a situation, the measurement strength is postulated to be proportional to δt [58, 96, 97], i.e., $\bar{\lambda} = \lambda\delta t$, with λ being a fixed constant with units of inverse time, such that each measurement becomes infinitely weak in the continuous limit $\lambda\delta t \to 0$. For a continuous measurement, λ is referred to as the measurement strength.

Even though each measurement in this discretized sequence of measurements is infinitely weak, the system will be continuously disturbed when $\lambda\delta t \to 0$. That is, the vanishingly small backaction of each measurement accumulates over time, collectively having an influence on the system dynamics. To understand such measurement backaction, we consider a general system with Hamiltonian $\hat{H}$ and density operator $\hat{\rho}_t$, representing our state of knowledge of the system at time t. During one discrete timestep δt, the system evolves according to

$$\hat{\rho}_{t+\delta t}(z) = e^{\mathcal{L}\delta t}\mathcal{M}(z)\hat{\rho}_t, \tag{4.7}$$

where we introduced the compact superoperator notation $\mathcal{L}\hat{\rho} = -i[\hat{H}, \hat{\rho}]$ for the system time evolution, and $\mathcal{M}(z)\hat{\rho} = \hat{K}(z)\hat{\rho}\hat{K}^\dagger(z)$ for the measurement. Note that $\hat{\rho}_{t+\delta t}(z)$ is the joint system-outcome state at time $t + \delta t$. Expanding the right hand side to linear order in δt, using $\hat{\rho}_{t+\delta t} = \int dz \hat{\rho}_{t+\delta t}(z)$, and taking the continuous limit $\delta t \to 0$, provides the following master equation for the system state,

$$\partial_t\hat{\rho}_t = -i[\hat{H}, \hat{\rho}_t] + \lambda\mathcal{D}[\hat{A}]\hat{\rho}_t. \tag{4.8}$$

Note that this equation is written on Lindblad form [c.f. Eq. (3.15)]. The first term on the right hand side is the standard von Neumann equation [see Eq. (3.9)], describing the time evolution of the system in the absence of measurement. The second term represents the measurement backaction. Note that this master equation is not a consequence of using the Gaussian measurement operator in Eq. (4.3), but is rather a general result that holds for all continuous quantum measurements [53, 57, 68, 99]. To understand the effect of the backaction term, we ignore the first term of the master equation, and write the density matrix in the eigenbasis of $\hat{A}$, and get, for element $\rho_{aa'}(t) = \langle a|\hat{\rho}_t|a'\rangle$,

$$\dot{\rho}_{aa'}(t) = -\frac{\lambda}{2}(\xi_a - \xi_{a'})^2\rho_{aa'}(t). \tag{4.9}$$

We thus see that the effect of the measurement is to exponentially dampen all coherences for non-degenerate eigenvalues ($\xi_a \neq \xi_{a'}$) at a rate proportional to the measurement strength λ. The continuous measurement thus dephases the system, and in the long time limit, the coherence vanishes. The coherent dynamics generated by the Hamiltonian in Eq. (4.8) is thus blocked, and we observe the quantum Zeno effect. Note that if the dynamics were incoherent, the backaction term would have no effect on the system.

Finally, we discuss measurement noise for the continuous measurement. For simplicity, we focus on the two-level system in Eq. (4.4) and put $p = 1$. Equation (4.5) then becomes a single Gaussian distribution centered around -1. The measurement noise is thus Gaussian, and the outcome may be written as a random variable

$$z(t) = -1 + \frac{1}{\sqrt{4\lambda\delta t}}\delta W(t), \tag{4.10}$$

where $\delta W(t)$ is a normal distributed random variable with mean 0 and variance δt, which is independent (and thereby uncorrelated) with itself at other times t', i.e., $\langle \delta W(t)\delta W(t')\rangle = \delta t\delta_{t,t'}$, with $\delta_{t,t'}$ being the Kronecker delta function. In Chapter 2, we refered to $\delta W(t)$ as a Wiener increment, and as discussed in that chapter, when $\delta t \to 0$, the ratio $\delta W(t)/\delta t$ is interpreted as a white noise process $\xi(t)$ for which $\langle \xi(t)\xi(t')\rangle = \delta(t - t')$.

The Gaussian noise profile resulting from Eq. (4.3) may appear restrictive as it is a very specific type of noise. Let us instead look at another timescale $\delta t' \ll \delta t$, where we can use a measurement operator $\hat{K}'(\alpha)$, assumed to give an arbitrary noise profile in the measured signal $\alpha(t)$. Coarse graining over the larger timescale δt at any time t results in $\delta t^{-1}\int_t^{t+\delta t} ds\alpha(s)$ which is, by the central limit theorem, a Gaussian random variable. We thus see that a Gaussian noise profile can be obtained at any timescale, and is, therefore, not a restrictive choice [96].

4.3   Measurement and feedback in quantum systems

To put the results of this thesis into a wider perspective, this section introduces two of the central results in the field of measurement and feedback in quantum systems – namely, the Belavkin equation and the Wiseman-Milburn equation. To this end, we will use the rule of Itô calculus (see Chapter 2).

Our starting point is the update rule [see Eqs. (3.16) and (4.2)]

$$\hat{\rho}_c(t + \delta t) = e^{\mathcal{L}(D)\delta t}\frac{\hat{K}(z)\hat{\rho}_c(t)\hat{K}^\dagger(z)}{p_t(z)}, \tag{4.11}$$

where $\hat{\rho}_c(t)$ is the system state at time t conditioned on the complete history of previous measurement outcomes $z(t)$, i.e., it may be written as $\hat{\rho}_c(t) = \hat{\rho}[t|\mathbf{z}]$, where $\mathbf{z}$ denotes a

trajectory of the outcomes. The measurement operator $\hat{K}(z)$ is given in Eq. (4.3). The denominator $p_t(z) = \mathrm{tr}\{\hat{K}^\dagger(z)\hat{K}(z)\hat{\rho}_c(t)\}$ is the conditional probability distribution for obtaining outcome z at time t given the complete history of previous outcomes. From this distribution, we find the average

$$\langle z \rangle_c = \int z\,\mathrm{tr}\{\hat{K}^\dagger(z)\hat{K}(z)\hat{\rho}_c(t)\}dz = \langle \hat{A} \rangle_c, \qquad (4.12)$$

where $\langle \hat{A} \rangle_c = \mathrm{tr}\{\hat{A}\hat{\rho}_c(t)\}$ is the average of the measured observable $\hat{A}$ [see Eq. (4.3)] with respect to $\hat{\rho}_c(t)$. This implies, as discussed in Sec. 4.2, that the outcome can be written as a random variable as

$$z = \langle \hat{A} \rangle_c + \frac{\delta W}{\sqrt{4\lambda}\delta t}, \qquad (4.13)$$

where δW is a Wiener increment. Feedback is incorporated in Eq. (4.11) via the Liouville superoperator $\mathcal{L}(D)$, where D is the outcome observed on the detector at time t, see Fig. 1.1. Note that $\mathcal{L}(D)$ has a completely general (and unspecified) dependence on D, and may depend linearly as well as nonlinearly on D. The observed outcome D is related to z via [57, 62, 63, 95, 100–103]

$$D(t) = \int_{-\infty}^{t} ds\,\gamma e^{-\gamma(t-s)} z(s), \qquad (4.14)$$

where γ is the bandwidth of the detector (see Fig. 1.1). The bandwidth of a detector determines the range of frequencies that are present in the detector signal. For an infinite bandwidth, all frequencies are transmitted with equal weight, and thus contains diverging frequencies. This corresponds to a white noise process, see Fig. 2.1(b) in Chapter 2. For finite bandwidths, higher frequencies are filtered out, and the signal is less noisy. Note that Eq. (4.14) adds a delay time $1/\gamma$ to the detector. As any real detector has a finite bandwidth and delay time, i.e., we never observe diverging frequencies in reality, Eq. (4.14) adds a realistic element to the theory. Note that by differentiating Eq. (4.14) with respect to time, and employing Eq. (4.13), we get the Langevin equation

$$\dot{D}(t) = \gamma\left[\langle \hat{A} \rangle_c - D(t)\right] + \frac{\gamma}{\sqrt{4\lambda}}\xi(t), \qquad (4.15)$$

using that $\xi(t) = \lim_{\delta t \to 0} \delta W/\delta t$, as discussed in Chapter 2. That is, $D(t)$ is an Ornstein-Uhlenbeck process with Itô equation

$$dD = \gamma\left(\langle \hat{A} \rangle_c - D\right)dt + \frac{\gamma}{\sqrt{4\lambda}}dW, \qquad (4.16)$$

and thus describes a noisy relaxation towards $\langle \hat{A} \rangle_c$ on a timescale set by $1/\gamma$. The detector noise is determined by $\gamma/8\lambda$ – see Chapter 2. We depict this in Fig. 4.2(a) for the example two-level system in Sec. 4.2 undergoing a transition $|0\rangle \to |1\rangle$. Figure 4.2(b) illustrates how the outcome D may be thought of as a Brownian particle in a harmonic potential,
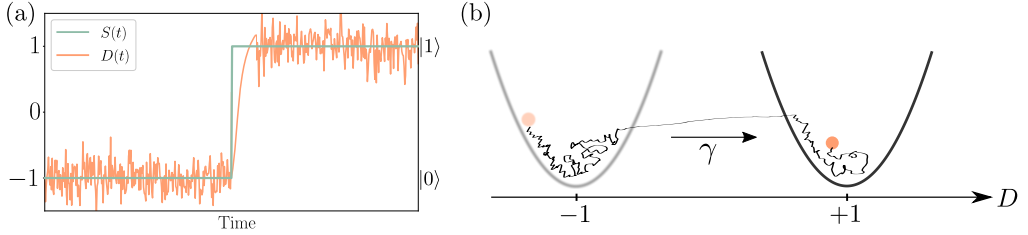
Figure 4.2: (a) Time traces of the system state $S(t)$ and the outcome $D(t)$ as observed on the detector screen during the state transition $|0\rangle \rightarrow |1\rangle$ for the example two-level system in Sec. 4.2. Due to a finite bandwidth γ, the detector signal lags behind the system state. (b) Illustration of D as a Browninan particle in a harmonic potential during the same state transition as in (a). As the transition occurs, the potential moves from -1 to $+1$. The particle follows with speed γ.

see discussion in Chapter 2. When the system jumps $|0\rangle \rightarrow |1\rangle$, the potential is moved instantly from -1 to 1, and the detector outcome follows with speed γ.

Our goal is to use Eqs. (4.11) and (4.13) to derive a master equation for $\hat{\rho}_c(t)$. To this end, we aim to linearize the RHS of Eq. (4.11) in δt. The time evolution operator can be written as $e^{\mathcal{L}(D)\delta t} \approx 1 + \mathcal{L}(D)\delta t$, and by using Eqs. (4.3) and (4.13), and the Itô rule, we get [58, 96]

$$\frac{\hat{K}(z)\hat{\rho}_c\hat{K}^\dagger(z)}{p_t(z)} = \hat{\rho}_c + \lambda\delta t \mathcal{D}[\hat{A}]\hat{\rho}_c + \sqrt{\lambda}\delta W\{\hat{A} - \langle\hat{A}\rangle_c, \hat{\rho}_c\}, \tag{4.17}$$

where the time arguments were omitted for brevity. From these linearizations, we can take the continuous limit $\delta t \rightarrow dt$ and $\delta W \rightarrow dW$ to find the Belavkin equation [49] (see also Refs. [57, 58, 96])

$$d\hat{\rho}_c = dt\mathcal{L}(D)\hat{\rho}_c + \lambda dt \mathcal{D}[\hat{A}]\hat{\rho}_c + \sqrt{\lambda}dW\{\hat{A} - \langle\hat{A}\rangle_c, \hat{\rho}_c\}. \tag{4.18}$$

This stochastic master equation is one of the central results in the field of continuous measurement and feedback control. The first term describes the feedback controlled time evolution of the system, the second term describes measurement backaction, and the third term describes how noise is induced into the system due to the randomness of the measurement. We note that the equation is nonlinear in $\hat{\rho}_c$ because of the average $\langle\hat{A}\rangle_c$ in the anti-commutator in the noise term. This is in contrast to the von Neumann equation (3.9), and is a result from the nonlinear transformation that describes a quantum measurement, see Eqs. (4.2) and (4.11). The Belavkin equation, together with Eq. (4.16), can be used to model any type of continuous feedback protocols, linear as well as nonlinear in D, but must, in general, be solved numerically due to the stochastic noise term. We note that since there exists infinitely many realizations of the noise process dW, the Belavkin equation has infinitely many solutions, where each solution defines a quantum trajectory of $\hat{\rho}_c$. In Fig. 4.3, we show such a trajectory for a qubit in the absence of feedback control, illustrating how noise is induced into our state of knowledge (the density matrix) given that we observed the trajectory of $D(t)$ in the rightmost panel.
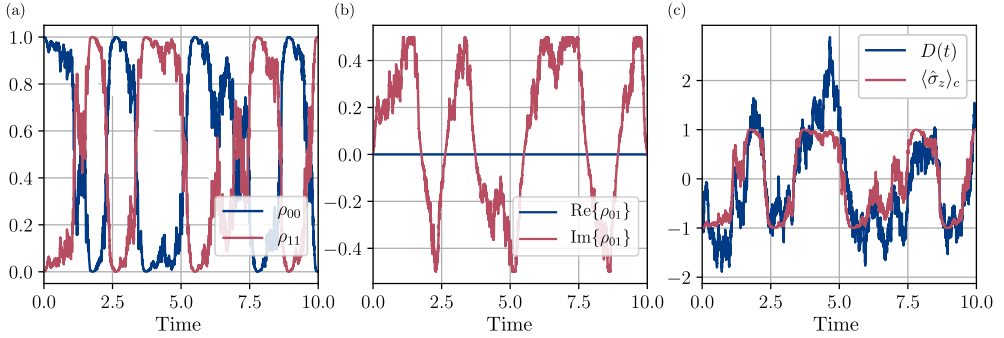
Figure 4.3: A solution to the Belavkin equation (4.18) and Eq. (4.16) for an uncontrolled qubit when measuring the Pauli-Z operator $\hat{\sigma}_z = |1\rangle\langle 1| - |0\rangle\langle 0|$. The qubit has Hamiltonian $\hat{H} = g\hat{\sigma}_x$, where $\hat{\sigma}_x$ is the Pauli-X operator. (a) The leftmost panel visualizes the diagonal density matrix elements $\rho_{aa} = \langle a|\hat{\rho}_c(t)|a\rangle$ of the conditioned density matrix $\hat{\rho}_c(t)$. (b) The middle panel shows the real and imaginary parts of the off-diagonal density matrix element $\rho_{01} = \langle 0|\hat{\rho}_c(t)|1\rangle$. (c) The rightmost panel is the corresponding time trace of the detector signal $D(t)$ [see Eq. (4.16)], and the expectation value $\langle\hat{\sigma}_z\rangle_c = \text{tr}\{\hat{\sigma}_z\hat{\rho}_c\}$. Here we used $\gamma/g = 2$, $\lambda/g = 1/2$, and $dt/g = 10^{-3}$.

The stochastic evolution of the quantum trajectory in Fig. 4.3 makes it difficult to draw conclusions about general trends in the system dynamics. By averaging over many trajectories $\boldsymbol{z} = \{z(t_0), z(t_0 + dt), \ldots, z(t)\}$, we obtain an unconditioned state $\hat{\rho}_t = \langle\hat{\rho}_c(t)\rangle_{\boldsymbol{z}}$ where such trends can be distinguished – by $\langle\cdot\rangle_{\boldsymbol{z}}$, we denote an average over all possible trajectories of $\boldsymbol{z}$. As discussed in Chapter 2, this average can be evaluated as

$$\langle\hat{\rho}_c(t)\rangle_{\boldsymbol{z}} = \int \mathcal{D}[\boldsymbol{z}]\hat{\rho}_c(t)P[\boldsymbol{z}] = \int \mathcal{D}[\boldsymbol{z}]\hat{\rho}_t[\boldsymbol{z}] = \hat{\rho}_t, \tag{4.19}$$

using that $\hat{\rho}_t[\boldsymbol{z}] = \hat{\rho}_c(t)P[\boldsymbol{z}]$, with $P[\boldsymbol{z}]$ being the probability of observing trajectory $\boldsymbol{z}$. Such averaging is always feasible in numerical simulations. Unfortunately, calculating this averaging analytically is more complicated because of the unspecified dependence of D in $\mathcal{L}(D)$. Here we consider two cases where the average is possible to compute.

In the absence of feedback, i.e., when $\mathcal{L}(D) \rightarrow \mathcal{L}$, the Belavkin equation reduces to Eq. (4.8) when averaging over all trajectories $\boldsymbol{z}$. This average is possible to compute because the noise dW at time t is independent of $\hat{\rho}_c(t)$, see Appendix A.

The second case is linear feedback based on a white noise detector signal [52, 57]. This is sometimes referred to as Markovian feedback as it is possible to find a deterministic Markovian master equation for the unconditioned system state $\hat{\rho}_t$. To this end, we use the Liouville superoperator $\mathcal{L}(z) = \mathcal{L}_0 + z\mathcal{K}$, where $\mathcal{L}_0$ describes the system dynamics in the absence of feedback, and $\mathcal{K}$ is a Liouville superoperator describing the feedback forces. Note that we feed back z [Eq. (4.13)] (as opposed to a nonlinear function thereof) because of its white noise spectrum, see Chapter 2. To find the corresponding Belavkin equation, we use the Itô rule to find that $e^{\mathcal{L}(z)\delta t} \approx 1 + \delta t\mathcal{L}_0 + \langle\hat{A}\rangle_c\delta t\mathcal{K} + \delta t\mathcal{K}^2/8\lambda + \delta W\mathcal{K}/\sqrt{4\lambda}$,

and get

$$d\hat{\rho}_c = dt\mathcal{L}_0\hat{\rho}_c + \lambda dt\mathcal{D}[\hat{A}]\hat{\rho}_c + \frac{dt}{2}\mathcal{K}\{\hat{A}, \hat{\rho}_c\}$$
$$+ \frac{dt}{8\lambda}\mathcal{K}^2\hat{\rho}_c + dW\left[\sqrt{\lambda}\{\hat{A} - \langle\hat{A}\rangle_c, \hat{\rho}_c\} + \frac{1}{\sqrt{4\lambda}}\mathcal{K}\hat{\rho}_c\right]. \tag{4.20}$$

This is a stochastic master equation for the conditioned state $\hat{\rho}_c$ under linear feedback control, where the measured signal has a white noise power spectrum. Averaging over all possible trajectories $\mathbf{z}$, we get the Wiseman-Milburn equation [52, 57]

$$\partial_t\hat{\rho} = \mathcal{L}_0\hat{\rho} + \lambda\mathcal{D}[\hat{A}]\hat{\rho} + \frac{1}{2}\mathcal{K}\{\hat{A}, \hat{\rho}\} + \frac{1}{8\lambda}\mathcal{K}^2\hat{\rho}, \tag{4.21}$$

which is another central result in the field of continuous measurement and feedback control. The first and second terms on the RHS corresponds to Eq. (4.8). The third term describes how the feedback forces acts on the system. The fourth term, originating from the noise term dW in $\mathcal{L}(z)$, describes how measurement noise is fed back to the system and causes diffusion in the dynamics [57]. When λ is large, this diffusion effect is reduced, as the detector noise becomes small – the magnitude of the noise scales as $1/\lambda$ as discussed in Secs. 4.2. This equation has been applied in numerous contexts, including stabilizing qubit states [104], manipulating entanglement [105–110], retarding decoherence [111, 112], producing squeezed states [113–116], and charging quantum batteries [117]. Finding a corresponding Markovian master equation description for a general $\mathcal{L}(D)$ is possible, but with an alternative method. This method is one of the central results of this thesis, and is introduced in Chapter 6.

Chapter 5

Stochastic and information thermodynamics

Stochastic thermodynamics [118–127] deals with small, fluctuating systems far from equilibrium. Building on the prominent discoveries of the Jarzynski relation [128, 129] and Crooks' fluctuation theorem [130, 131], the last 25 years have resulted in many general laws applicable to non-equilibrium systems. As such, stochastic thermodynamics extends its conventional (macroscopic) counterpart beyond close-to-equilibrium scenarios. By defining quantities such as work, heat, and entropy at the level of single microscopic trajectories, it is possible to understand how fluctuations affect the thermodynamics of small systems. In particular, the second law is generalized to fluctuation theorems, stating that entropy production is a fluctuating quantity which only needs to be non-negative on average. This stands in contrast to classical thermodynamics, where entropy should always increase, and where fluctuations are negligible. Stochastic thermodynamics is thus particularly good at describing the thermodynamics of small systems such as colloidal particles [132], DNA molecules [133], molecular motors [134], and nanosized electronic systems [135, 136], where fluctuations play an important role. The experimental advancements over the last 20 years [137] have made it possible to implement Maxwell's demon [9–11], where measurement and feedback is used to rectify thermal fluctuations. This concept ties together the fields of information theory and thermodynamics, and has fueled the field of information thermodynamics [23–25], where information processing is incorporated into the laws of stochastic thermodynamics.

In this chapter, we begin by introducing some of the results from classical thermodynamics in Sec. 5.1 that will be important for comparison in the proceeding sections. Section 5.2 is devoted to stochastic thermodynamics, and defines entropy, work, and heat on the level of single microscopic trajectories. Especially, we introduce fluctuation theorems. Section

5.3 introduces information thermodynamics, and we discuss a selection of results that are important for understanding the thermodynamics of Maxwell's demon.

5.1 Classical thermodynamics

With classical thermodynamics, we can describe the energetics and dynamics of macroscopic systems that are in equilibrium. With linear response theory, it is possible to get some insights into non-equilibrium thermodynamics, but the results are only valid close to equilibrium.

The first law of thermodynamics reads

$$\Delta E = W + Q, \tag{5.1}$$

stating that a change in internal energy ΔE of a system can be decomposed into work W and heat Q. While work is energy that is provided macroscopically, heat is energy that is transferred by microscopic degrees of freedom. Here we use the sign convention that $W > 0$ ($W < 0$) when work is done on (by) the system. Similarly, $Q > 0$ ($Q < 0$) when heat is absorbed (released) by the system.

The second law of thermodynamics states that the entropy S of an isolated system (not exchanging energy or particles with its environment) never decreases. Mathematically, we write

$$\Delta S \geq 0. \tag{5.2}$$

If the system makes a transition between two states for which $\Delta S = 0$, the process is said to be reversible, and the system can jump back and forth between these states without restriction. A system transition with $\Delta S > 0$ is said to be irreversible. That is, if the transition $x_0 \rightarrow x_1$, between system states x_0 and x_1, increases the system entropy, the reverse process, $x_1 \rightarrow x_0$, is prohibited by the second law, and will never be observed. This notion of reversibility will be widened in Sec. 5.2 when we study thermodynamics on the microscopic scale.

An equilibrium state can be described by the function $E(S, V, N)$ for the internal energy E, where S is entropy, V the volume of the system, and N the number of particles of a given species. To avoid clutter, we only write out these three variables, but E could, in principle, depend on other variables as well. Let us assume that we perform an experiment where we cannot measure the entropy, but only have access to the temperature T, as well as V and N. In this case, it is difficult to describe our observations with $E(S, V, N)$. Instead, we can make use of the Legendre transform [138] to make the following change variables, $S, V, N \rightarrow T, V, N$. Mathematically, this is done by introducing Helmholtz free energy

(typically referred to as the free energy) as

$$F = E - ST, \tag{5.3}$$

where $F(T, V, N)$ depends on the temperature instead of the entropy. The free energy is a thermodynamic potential, which means that it can be used to reconstruct all information that we can derive from $E(S, V, N)$. Note that the second law implies that the free energy should be minimized in an isolated system, i.e., $\Delta F \leq 0$. Another example of a thermodynamic potential is Gibbs free energy $G = E - ST + pV$ which depends on T, p (pressure), and N.

Before closing this section, we study work extraction under isothermal transformations. We consider a system that is in contact with an equilibrium heat bath at constant temperature T. By assuming that the bath is much larger than the system, the system can only weakly perturb the bath. Additionally, we assume that the bath relaxation time (to return to equilibrium) due to a small perturbation is much faster than the system timescale, such that the bath effectively remains in equilibrium at all times. We now drive the system between two equilibrium states. Since the bath effectively is in equilibrium, the bath and system are uncorrelated, and the total entropy change can be written as $\Delta S_{\text{tot}} = \Delta S_{\text{sys}} + \Delta S_{\text{B}} \geq 0$, where ΔS_{sys} and ΔS_{B} are the entropy changes associated to the system and the bath, respectively. As the bath is much larger than the system, the entropy production associated to the bath can be written as $\Delta S_{\text{B}} = -Q/T$, with Q being the system heat. By using the first law, we can express the second law for isothermal processes as

$$W \geq \Delta F. \tag{5.4}$$

This establishes a minimal bound on the work that we need to do on the system to drive it between the two states. Alternatively, by defining the extracted work as $W_{\text{ext}} = -W$, having a positive sign when the system do work on its environment, we find the upper bound $W_{\text{ext}} \leq -\Delta F$. The change in free energy thus puts a fundamental limit on how much work that can be extracted from a system under isothermal transformations. Note that equality only holds for reversible processes.

5.2   Stochastic thermodynamics

In this section, we discuss stochastic thermodynamics by studying systems described by Markovian rate equations [139], but the results are general, and are typically applicable for other systems as well – for instance, systems obeying Langevin dynamics [121].

We consider systems with discrete states x, each with an energy ε_x and number of particles n_x. For the purposes of this thesis, we involve only one particle species, but the results can

be extended to include several species. The energies can be controlled by an external, time dependent control variable $\lambda(t)$, such that $\varepsilon_x = \varepsilon_x[\lambda(t)]$. The control variable could, for instance, be an electric field. Here we assume that n_x is fixed for all states x, and cannot be controlled externally. The system is coupled to an arbitrary number of equilibrium reservoirs, labeled with indexes ν, having well-defined temperatures T_ν and chemical potentials μ_ν [see Fig. 5.1(a)]. The system exchanges energy and particles with the reservoirs. The reservoirs are assumed to be so large that the system can only perturb the reservoirs weakly, and that their thermal relaxation time is so short compared to the system timescale that the reservoirs effectively remain in equilibrium at all times. To describe the system dynamics, we will use the following Markovian rate equation,

$$\dot{p}_x(t) = \sum_{x'} \sum_\nu \left[M_{xx'}^{(\nu)} p_{x'}(t) - M_{x'x}^{(\nu)} p_x(t) \right], \tag{5.5}$$

where $p_x(t)$ is the probability to occupy state x at time t (typically, we will not write out the time dependence unless necessary), and $M_{xx'}^{(\nu)} = M_{xx'}^{(\nu)}[\lambda(t)]$ is the transition rate for the transition $x' \to x$ mediated by reservoir ν. As indicated, the transition rates will, in general, be dependent on $\lambda(t)$, but to avoid clutter, we will only write out the explicit dependence on $\lambda(t)$ when necessary.
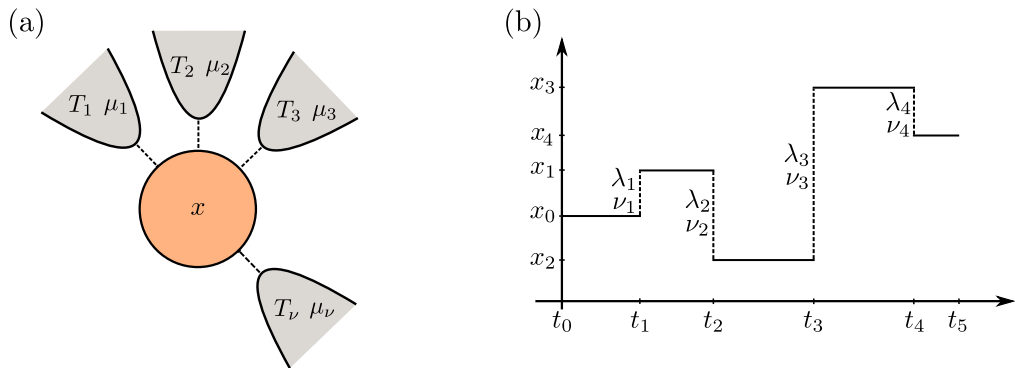
Figure 5.1: (a) A microscopic system in state x coupled to an arbitrary number of equilibrium reservoirs with which the system can exchange energy and particles. Each reservoir has a well-defined temperature T_ν and chemical potential μ_ν. (b) Example trajectory of the system state [see trajectory definition in Eq. (5.10)]. Each state transition $x_{j-1} \to x_j$ is mediated by a reservoir ν_j for a fixed control parameter λ_j. Note that the control parameter can vary continuously between transitions.

To incorporate thermodynamics into our model, we assume that the transition rates obey local detailed balance, i.e.,

$$\ln \left(\frac{M_{xx'}^{(\nu)}}{M_{x'x}^{(\nu)}} \right) = \frac{\varepsilon_{x'} - \varepsilon_x - \mu_\nu(n_{x'} - n_x)}{k_B T_\nu}, \tag{5.6}$$

where k_B is the Boltzmann constant. This assumption is justified as long as the timescale of $\lambda(t)$ is much slower than the thermal relaxation time of the reservoirs, such that the system

effectively interacts with equilibrium reservoirs at all times. To understand the origin and physical meaning of local detailed balance, we begin to consider the case where the system only interacts with one single reservoir. In the long time limit, the system thermalizes with the bath, and reaches an equilibrium distribution

$$p_x^{(\mathrm{eq})} = \frac{e^{-(\varepsilon_x - \mu_\nu n_x)/k_B T_\nu}}{Z}, \qquad\qquad Z = \sum_x e^{-(\varepsilon_x - \mu_n u n_x)/k_B T_\nu}, \qquad (5.7)$$

with Z being the partition function. In equilibrium, there should, on average, be no net flow of energy or particles. The probability current $J_{xx'}^{(\nu)} = M_{xx'}^{(\nu)} p_{x'} - M_{x'x}^{(\nu)} p_x$ should, therefore, vanish, giving the detailed balance condition

$$M_{xx'}^{(\nu)} p_{x'}^{(\mathrm{eq})} = M_{x'x}^{(\nu)} p_x^{(\mathrm{eq})}, \qquad (5.8)$$

and we recover Eq. (5.6). We thus see that the local detailed balance condition leads to a proper description of thermalization, where we recover the equilibrium distributions from statistical mechanics.

In the presence of several reservoirs, all with different temperatures and chemical potentials, the situation is different. All reservoirs will try to impose an equilibrium distribution on the system, but will fail due to the presence of the other reservoirs. Because of this non-equilibrium setting, there will, on average, be a net flow of energy and particles between the system and the reservoirs, and the stationary probability currents $J_{xx'}^{(\nu)} \neq 0$. This is referred to as a non-equilibrium steady state. As we, on a general level, do not know either the stationary distribution $p_x^{(\mathrm{st})}$ nor the stationary currents $J_{xx'}^{(\nu)}$, it is at this point difficult to justify that the local detailed balance condition holds also for non-equilibrium scenarios. For now, we claim that it holds, and show in the upcoming paragraphs that it leads to a thermodynamically consistent definition of a non-equilibrium entropy, motivating why local detailed balance should hold for both equilibrium and non-equilibrium scenarios.

Once we know the distribution $p_x(t)$, we can calculate the average energy $E = \sum_x \varepsilon_x p_x$ and the average number of particles $N = \sum_x n_x p_x$ of the system. The average energy changes at a rate

$$\dot{E} = \dot{W} + \dot{W}_{\mathrm{chem}} + \dot{Q}, \qquad (5.9)$$

where $\dot{W} = \sum_x p_x(t) \partial_t \varepsilon_x[\lambda(t)] = \sum_x p_x(t) \dot{\lambda}(t) \partial_\lambda \varepsilon_x[\lambda(t)]$ is the external work applied on the system, $\dot{W}_{\mathrm{chem}} = \sum_\nu \sum_{xx'} \mu_\nu n_x J_{xx'}^{(\nu)}$ is the chemical work rate associated with the particle exchange between system and reservoirs, and $\dot{Q} = \sum_\nu \sum_{xx'} (\varepsilon_x - \mu_\nu n_x) J_{xx'}^{(\nu)}$ is the system heat current. Equation (5.9) thus shows that the first law of thermodynamics holds for the average system energy E. Note that the additional chemical work term was baked into one single term in Eq. (5.1).

We now define system trajectories. Since the state of the system fluctuates randomly over time, two separate measurements of the state trajectory would yield different results, see the example trajectory in Fig. 5.1(b). To fully understand how these fluctuations affect the thermodynamics of the system, we need to properly define work, heat, and entropy on the level of single system trajectories. We define a trajectory starting in state x_0 at time t_0 with control parameter λ_0 and ending in state x_{n-1} at time t_n with control parameter λ_n as

$$X = \{(t_j, \lambda_j, \nu_j, x_j)\}_{j=1}^{n-1}, \tag{5.10}$$

where t_j specifies the time when the system jumps to a new state x_j, by doing the transition $x_{j-1} \to x_j$, λ_j is the value of the control parameter when the transition occurs, and ν_j is the reservoir responsible for the transition. Note that the control variable $\lambda(t)$ varies continuously between transitions, but as we will see, we only need to care about its value at the times the system undergoes transitions. The rate of external work applied on the system at time t is given by $\partial_t \varepsilon_x[\lambda(t)] = \dot{\lambda}(t)\partial_\lambda \varepsilon_x[\lambda(t)]$ if the system is in state x. If the system remains in this state during the interval $[t, t+\Delta t]$, the work applied on the system is given by $\int_t^{t+\Delta t} ds \dot{\lambda}(s)\partial_\lambda \varepsilon_x[\lambda(s)] = \varepsilon_x[\lambda(t+\Delta t)] - \varepsilon_x[\lambda(t)]$. That is, we only need to know the initial and final position of the energy level. The external work applied along trajectory X may thus be written as

$$w[X] = \sum_{j=0}^{n-1} \left[\varepsilon_{x_j}(t_{j+1}) - \varepsilon_{x_j}(t_j) \right]. \tag{5.11}$$

For transition $x_{j-1} \to x_j$ mediated by reservoir ν_j at time t_j, the system heat is given by $\varepsilon_{x_j}(t_j) - \varepsilon_{x_{j-1}}(t_j) - \mu_{\nu_j}(n_{x_j} - n_{x_{j-1}})$, and along X, we get the trajectory heat

$$q[X] = \sum_{j=1}^{n-1} \left[\varepsilon_{x_j}(t_j) - \varepsilon_{x_{j-1}}(t_j) - \mu_{\nu_j}(n_{x_j} - n_{x_{j-1}}) \right]. \tag{5.12}$$

With this definition, we follow our convention that $q[X] > 0$ when the system absorbs heat, and $q[X] < 0$ when releasing heat. The chemical work done on the system along X reads

$$w_{\text{chem}}[X] = \sum_{j=1}^{n-1} \mu_{\nu_j}(n_{x_j} - n_{x_{j-1}}). \tag{5.13}$$

Adding these contributions together, we get the first law of stochastic thermodynamics,

$$w[X] + w_{\text{chem}}[X] + q[X] = \varepsilon_{x_{n-1}}(t_n) - \varepsilon_{x_0}(t_0), \tag{5.14}$$

resembling Eq. (5.1).

Next we want to define a non-equilibrium entropy for the system. We aim to use the Shannon entropy

$$S_{\text{sys}}(t) = -k_B \sum_x p_x(t) \ln[p_x(t)], \tag{5.15}$$

and show that it gives reasonable results. If we interpret $S_{\mathrm{sys}}(t)$ as the system entropy at time t, averaged over all possible trajectories X, we can define a stochastic entropy [140]

$$s_{\mathrm{sys}}(t) = -k_B \ln[p_x(t)], \tag{5.16}$$

evaluated at time t when the system state is x. Averaging over all possible trajectories X, we recover the Shannon entropy $S_{\mathrm{sys}}(t) = \langle s_{\mathrm{sys}}(t) \rangle_X$. To evaluate whether these definitions give sensible results, it is useful to study the entropy change related to a single transition $x' \to x$ mediated by reservoir ν. During this jump, the system exchanges heat with the reservoir, which can be calculated as $q_{xx'}^{(\nu)} = \varepsilon_x - \varepsilon_{x'} - \mu_\nu(n_x - n_{x'})$. As the reservoir is in equilibrium, the change of entropy in the reservoir is given by

$$\Delta s_{xx'}^{(\mathrm{res})} = -\frac{q_{xx'}^{(\nu)}}{T_\nu} = k_B \ln\left(\frac{M_{xx'}^{(\nu)}}{M_{x'x}^{(\nu)}}\right), \tag{5.17}$$

where we used the local detailed balance condition in Eq. (5.6). From our definition of stochastic entropy (5.16), the change in system entropy can be written as

$$\Delta_{xx'}^{(\mathrm{sys})} = k_B \ln\left(\frac{p_{x'}}{p_x}\right), \tag{5.18}$$

and we find the total change of entropy

$$\Delta s_{xx'}^{(\mathrm{tot})} = \Delta s_{xx'}^{(\mathrm{sys})} + \Delta s_{xx'}^{(\mathrm{res})} = k_B \ln\left(\frac{M_{xx'}^{(\nu)} p_{x'}}{M_{x'x}^{(\nu)} p_x}\right). \tag{5.19}$$

From the definition of the Shannon entropy (5.15) and the definition of the rate equation (5.5), the average system entropy production may be written as

$$\dot{S}_{\mathrm{sys}}(t) = \frac{k_B}{2}\sum_\nu\sum_{xx'} J_{xx'}^{(\nu)} \ln\left(\frac{M_{xx'}^{(\nu)} p_{x'}(t)}{M_{x'x}^{(\nu)} p_x(t)}\right) - \frac{k_B}{2}\sum_\nu\sum_{xx'} J_{xx'}^{(\nu)} \ln\left(\frac{M_{xx'}^{(\nu)}}{M_{x'x}^{(\nu)}}\right), \tag{5.20}$$

where the factor of $1/2$ accounts for counting each jump twice in the double sums. With the help of Eqs. (5.17) and (5.19), we identify the total entropy production rate

$$\dot{S}_{\mathrm{tot}}(t) = \frac{k_B}{2}\sum_\nu\sum_{xx'} J_{xx'}^{(\nu)} \ln\left(\frac{M_{xx'}^{(\nu)} p_{x'}(t)}{M_{x'x}^{(\nu)} p_x(t)}\right), \tag{5.21}$$

and the reservoir entropy production rate

$$\dot{S}_{\mathrm{res}}(t) = \frac{k_B}{2}\sum_\nu\sum_{xx'} J_{xx'}^{(\nu)} \ln\left(\frac{M_{xx'}^{(\nu)}}{M_{x'x}^{(\nu)}}\right), \tag{5.22}$$

such that $\dot{S}_{\text{tot}}(t) = \dot{S}_{\text{sys}}(t) + \dot{S}_{\text{res}}(t)$. First, we note that $J_{xx'}^{(\nu)}$ and $\ln[M_{xx'}^{(\nu)} p_{x'}(t)/M_{x'x}^{(\nu)} p_x(t)]$ always have the same sign, implying that $\dot{S}_{\text{tot}} \geq 0$ at all times. Second, when all reservoirs have the same temperatures and chemical potentials, i.e., being in thermal equilibrium, we get the stationary condition in Eq. (5.8), and $\dot{S}_{\text{tot}}(t)$ vanishes in the long time limit when the system have thermalized to the reservoirs. Finally, the detailed balance condition in Eq. (5.6) implies that the entropy production rate in the reservoirs reads

$$\dot{S}_{\text{res}}(t) = \frac{1}{2} \sum_{\nu} \sum_{xx'} J_{xx'}^{(\nu)} \frac{\left(-q_{xx'}^{(\nu)}\right)}{T_\nu}, \tag{5.23}$$

as we would expect for a set of equilibrium reservoirs. These results show that the Shannon entropy (5.15) is a sensible candidate for being a non-equilibrium entropy, and that the assumption of local detailed balance (5.6) leads to a reasonable expression for the reservoir entropy production.

We can now define a trajectory entropy production for X in Eq. (5.10) as [140]

$$\Delta s_{\text{tot}}[X] = k_B \ln \left[\frac{p_{x_0}(t_0)}{p_{x_{n-1}}(t_n)} \right] + k_B \sum_{j=1}^{n-1} \ln \left(\frac{M_{x_j x_{j-1}}^{(\nu_j)}}{M_{x_{j-1} x_j}^{(\nu_j)}} \right), \tag{5.24}$$

where we used Eqs. (5.17) and (5.18).

With the definitions from the previous paragraphs, it is possible to introduce a non-equilibrium free energy. To this end, we consider a system exchanging energy with a single reservoir at temperature T – we neglect particle exchanges between the system and the reservoir for simplicity. With the first and second law for averages, Eqs. (5.9) and (5.21), we get that $\dot{W} \geq \dot{F}$, where we introduced the (trajectory averaged) non-equilibrium free energy $F = E - S_{\text{sys}} T$. By integrating over time, we get the non-equilibrium inequality

$$W \geq \Delta F, \tag{5.25}$$

resembling the classical equilibrium case in Eq. (5.4). This motivates us to define a stochastic free energy $f = \varepsilon_x - T s_{\text{sys}}$, with ε_x being the energy of the occupied system state x, and $s_{\text{sys}} = -k_B \ln(p_x)$ the stochastic entropy of the system. In equilibrium, we have $p_x = \exp\{(F^{(\text{eq})} - \varepsilon_x)/k_B T\}$, where $F^{(\text{eq})}$ is the equilibrium free energy of the system, implying that $f^{(\text{eq})} = F^{(\text{eq})}$, such that the stochastic equilibrium free energy coincides with the equilibrium free energy. Driving the system isothermally thus gives us the total trajectory entropy production

$$T \Delta s_{\text{tot}}[X] = w[X] - \Delta f[X], \tag{5.26}$$

where $w[X]$ is the work applied along the trajectory, and $\Delta f[X]$ is the difference in stochastic free energy between the initial and final states of trajectory X. To obtain this relation, we

used Eqs. (5.11), (5.24), and (5.6). If the initial and finial states are in thermal equilibrium, we get $\Delta f[X] = \Delta F^{(eq)}$, which is independent on the initial and final states – see the equilibrium distribution above Eq. (5.26).

We have now reached the heart of stochastic thermodynamics; fluctuation theorems. To begin, we define a forward trajectory X of the system as specified in Eq. (5.10). To carry out calculations, we discretize time into N steps and define a time increment $\delta t = (t_n - t_0)/N$. Between two system transitions, let us say t_{j-1} and t_j, we get $N_j = (t_j - t_{j-1})/\delta t$ time increments. Since time is discretized, the jump $x_{j-1} \to x_j$ occurs at $t_j - \delta t$, such that the system dwells in x_{j-1} during $N_j - 1$ timesteps before making the transition. By using the definitions of Markov processes (see Chapter 2), and that transition probabilities can be calculated as $P(x_j|x_{j-1}) = M_{x_j x_{j-1}}^{(\nu)} \delta t$, the probability of observing the forward trajectory reads

$$P[X] = [P(x_{n-1}|x_{n-1})]^{N_n} \left[\prod_{j=0}^{n-2} M_{x_{j+1}x_j}^{(\nu_{j+1})}(\lambda_{j+1})\delta t [P(x_j|x_j)]^{N_{j+1}-1} \right] p_{x_0}(t_0), \qquad (5.27)$$

where $P(x|x)$ is the probability to dwell in state x during a time interval δt, and $p_{x_0}(t_0)$ is the probability to initially occupy x_0. To derive a fluctuation theorem, we must consider a time reversed trajectory as well, where we consider the time reversed versions of both the system state and the control protocol. The time reversed trajectory of X is given by

$$X^{tr} = \{t_{n-1}, \lambda_{n-j}, \nu_{n-j}, x_{n-j-1}\}_{j=1}^{n-1}, \qquad (5.28)$$

starting in x_{n-1} at t_n with control variable λ_n, and ending in x_0 at t_0 with control variable λ_0, passing through the same system states and values of the control parameter as in the forward trajectory, but in reversed order. Note that this corresponds to a scenario where both x and λ are even under time reversal. The trajectory work and heat are odd under the time reversed operation, i.e., $w[X^{tr}] = -w[X]$, $q[X^{tr}] = -q[X]$. The probability of observing the time reversed trajectory reads

$$P^{tr}[X^{tr}] = \left[\prod_{j=0}^{n-2} [P(x_j|x_j)]^{N_{j+1}-1} M_{x_j x_{j+1}}^{(\nu_{j+1})}(\lambda_{j+1})\delta t \right] [P(x_{n-1}|x_{n-1})]^{N_n} \tilde{p}_{x_{n-1}}(t_n), \qquad (5.29)$$

where the superscript 'tr' on P^{tr} expresses the fact that we consider a time reversed experiment. Note that the initial distribution $\tilde{p}_{x_{n-1}}(t_n)$ of X^{tr} not necessarily coincides with the final distribution $p_{x_{n-1}}(t_n)$ to be in x_{n-1} at time t_n in the forward trajectory X. Experimentally, these distributions are typically different as the experimenter first runs a series of forward experiments, and then performs a series of backward experiments (time-reversing the driving). The distributions thus depend on the preparation of the experiment. The special case where the distributions coincide can, for example, be achieved by either letting

the forward (backward) trajectory end (start) in a stationary state for a fixed control parameter, or letting the system thermalize to some environment after (before) the driving in the forward (backward) experiment.

Here we consider the situation where $\tilde{p}_{x_{n-1}}(t_n) = p_{x_{n-1}}(t_n)$, and use the definitions of Eqs. (5.27), (5.29), and (5.24) to find the detailed fluctuation theorem

$$\frac{P[X]}{P^{\mathrm{tr}}[X^{\mathrm{tr}}]} = e^{\Delta s_{\mathrm{tot}}[X]/k_B}. \tag{5.30}$$

This theorem relates the probabilities of observing the forward and time reversed trajectories with the entropy production of the forward trajectory $\Delta s_{\mathrm{tot}}[X]$ as defined in Eq. (5.24). For trajectories where $P[X] = P^{\mathrm{tr}}[X^{\mathrm{tr}}]$, $\Delta s_{\mathrm{tot}}[X] = 0$, and there is no bias towards either of the trajectories, implying full microscopic reversibility. For $\Delta s_{\mathrm{tot}}[X] > 0$, $P[X] > P^{\mathrm{tr}}[X^{\mathrm{tr}}]$, and there is a bias towards observing the forward trajectory. We stress that there still is a finite probability to observe the time reversed trajectory, but it is less likely. When $\Delta s_{\mathrm{tot}}[X] \gg 1$, $P^{\mathrm{tr}}[X^{\mathrm{tr}}]$ becomes vanishingly small compared to $P[X]$, indicating absolute microscopic irreversibility. By averaging over all possible trajectories X, the detailed fluctuation theorem (5.30) implies an integral fluctuation theorem

$$\left\langle e^{-\Delta s_{\mathrm{tot}}[X]/k_B} \right\rangle = 1, \tag{5.31}$$

where the average is taken with respect to $P[X]$, and $\sum_X P^{\mathrm{tr}}[X^{\mathrm{tr}}] = 1$. Jensen's inequality further provides the second law of stochastic thermodynamics,

$$\left\langle \Delta s_{\mathrm{tot}}[X] \right\rangle \geq 0. \tag{5.32}$$

That is, averaged over all possible trajectories, the entropy must be non-negative. This coincides with the conventional second law of thermodynamics. Further note that as $0 < e^{-\Delta s_{\mathrm{tot}}[X]/k_B} < 1$ for all trajectories with $\Delta s_{\mathrm{tot}}[X] > 0$, it is necessary that there exist trajectories with $\Delta s_{\mathrm{tot}}[X] < 0$ such that the average in Eq. (5.31) holds. We thus understand that these fluctuation theorems are generalizations of the second law that hold for microscopic systems far from equilibrium. In particular, we note that the second law is probabilistic on the microscopic scale, allowing for observations of trajectories with negative entropy production. It is only on average that the entropy production must be non-negative.

When isothermally driving a system coupled to a single reservoir between two equilibrium states, Eqs. (5.26) and (5.31) can be used to recover the Jarzynski relation [128]

$$\left\langle e^{-w[X]/k_B T} \right\rangle = e^{-\Delta F^{(\mathrm{eq})}/k_B T}. \tag{5.33}$$

The power of this relation lies in its ability to determine the free energy difference $\Delta F^{(\mathrm{eq})}$ between two equilibrium states by performing measurements on a non-equilibrium system. The Jarzynski relation further implies that $\langle w[X] \rangle \geq \Delta F^{(\mathrm{eq})}$, a generalization of Eq. (5.4).

Finally, we make some remarks. First, fluctuation theorems can be obtained by considering alternative time reversed trajectories as well. The scenario discussed here, when restricting ourselves to a system and a driving that are even under time reversal, is a special case. In fact, it is possible to derive fluctuation theorems for systems and control protocols that are odd under time reversal [127]. Note that this introduces several subtleties in the derivations. The reason for studying the special case of even functions under time reversal is because of its direct applicability on the classical toy model discussed in Chapter 7. Second, during the course of last decades, many of the non-equilibrium theorems of stochastic thermodynamics have been verified in various experimental platforms [137].

5.3 Information thermodynamics

The acquisition and processing of information come with a thermodynamic cost. This is famously illustrated by Maxwell's demon [9–11], where the acquisition of information about the velocities of gas molecules can be used to rectify their thermal fluctuations, seemingly violating the second law of thermodynamics. By considering the thermodynamics of information processing, i.e., accounting for the energy and entropy required to gather, store, and erase information, one finds that Maxwell's demon does not violate the second law. This was first realized by Bennett [141], who argued, based on the Landauer principle [142], that the apparent violation is resolved when the demon erases its memory, increasing the entropy of its environment such that the second law is restored. During the past decades, the thermodynamics of information [23–25] has been incorporated into stochastic thermodynamics. This has resulted in several generalizations of the second law, showing that processes like Maxwell's demon are not thermodynamically forbidden. In fact, several experimental implementations of the demon have been demonstrated over the last decade [26–32]. The purpose of this section is to introduce some of the results from information thermodynamics in order to clearly motivate why Maxwell's demon does not violate the second law.

To begin, we will shortly review some key concepts from information theory that will be useful throughout this section. Our average uncertainty of a random variable X with distribution $p(x)$ can be quantified via the (information theoretic) Shannon entropy

$$H[p(x)] = -\sum_x p(x) \ln[p(x)]. \tag{5.34}$$

We call this the "information theoretic entropy" since it differs by a factor of k_B from the one defined in Eq. (5.15). In the case where $p(x) = 1$ for one specific x, our uncertainty vanishes. That is, we will always know the value of X. When X is uniformly distributed over N different values, each with probability $p(x) = 1/N$, the Shannon entropy is maximized, corresponding to maximal uncertainty about X. Second, for two distributions $p(x)$ and
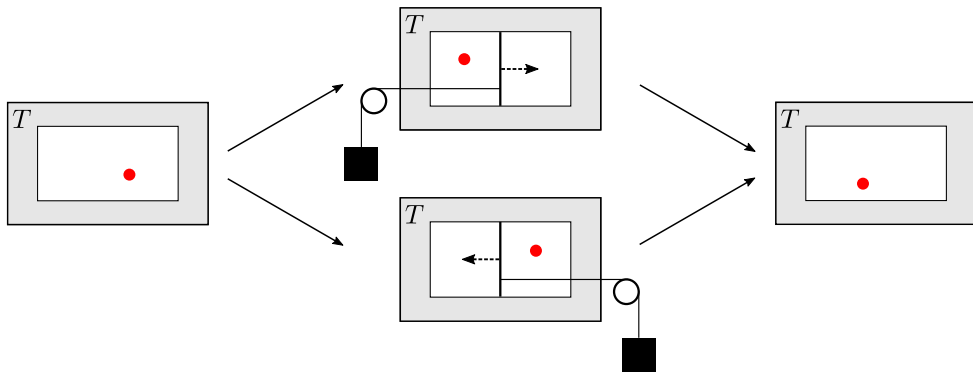
Figure 5.2: Illustration of the Szilard engine. A container with a single gas particle is in contact with a heat bath at temperature T. (left) Initially, the gas is in thermal equilibrium. (middle) A demon (experimenter) inserts a partition in the middle of the container, and measures on which side the particle is. Depending on the outcome, the demon applies feedback by attaching a weight on the same side of the partition as the particle is. Via isothermal expansion, the gas can lift the weight, extracting $k_B T \ln(2)$ of work from the bath (dashed arrow). (right) As the expansion ends, the gas returns to its initial state.

$q(x)$ defined over the same outcomes x, we introduce the Kullback-Leibler divergence

$$D(p||q) = \sum_x p(x) \ln \left[\frac{p(x)}{q(x)} \right] . \tag{5.35}$$

We note that $D(p||q) \geq 0$, with equality if $p(x)$ and $q(x)$ are the same distribution. The Kullback-Leibler divergence can thus be used as a measure of how similar two distributions are. It vanishes for identical distributions and takes finite values otherwise. Finally, we define the mutual information between two random variables X and Y as

$$I[X : Y] = \sum_{x,y} p(x,y) \ln \left[\frac{p(x,y)}{p(x)p(y)} \right] , \tag{5.36}$$

where $p(x,y)$ is the joint distribution of the random variables, and $p(x)$ and $p(y)$ are the marginal distributions for X and Y, respectively. By definition, the mutual information coincides with the Kullback-Leibler divergence for $p(x,y)$ and $p(x)p(y)$, and we thus get that $I[X : Y] \geq 0$. The mutual information gives a measure on how correlated the variables X and Y are. If they are completely uncorrelated, $p(x,y) = p(x)p(y)$ and $I[X : Y] = 0$. Therefore, the mutual information is useful in measurement theory where the correlation between a system observable X and the measurement outcomes Y is of interest.

To illustrate the issues of apparent violations of the second law, we will study the Szilard engine – a simplified version of Maxwell's demon. Its working cycle is visualized in Fig. 5.2. A single gas particle is trapped inside a container of fixed volume, and is in contact with a heat bath of temperature T. That is, the gas is initially in thermal equilibrium. A demon (or experimenter) inserts a partition in the middle of the container, and measures whether

the particle is on the left or the right side of the partition. Based on the outcome, the demon performs feedback by attaching a weight to the partition. By quasistatic, isothermal expansion, the gas particle can lift the weight, extracting work

$$W_{\text{ext}} = -W = \int_{V_{\text{tot}}/2}^{V_{\text{tot}}} p dV = k_B T \ln(2), \tag{5.37}$$

where V_{tot} is the volume of the container, and $p = k_B T / V$ is the pressure of the gas at volume V and temperature T (ideal gas law for one particle). Finally, the demon removes the partition, and lets the particle return to its initial state. As the container returns to its initial state, the first law implies that the bath must have provided an amount of heat $Q = k_B T \ln(2)$ to the container, implying that the change of entropy in the bath $\Delta S_{\text{B}} = -Q/T$ is negative. Since the gas returns to its initial equilibrium state, the entropy of the container does not change, and the total entropy, of both bath and container, is negative, appearing as a clear violation of the second law. To resolve this issue, the demon must be treated as a physical system whose entropy increases by an amount that at least matches the decrease in the bath. To motivate why this is the case, we will now discuss the thermodynamics of measuring, storing, and erasing information.

In the Szilard engine, the gas particle is initially in an equilibrium state with probability distribution $p(x = L) = p(x = R) = 1/2$ (x denotes the state of the gas). That is, we find the particle with equal probability on either side of the container. By measuring the state of the gas, we obtain an outcome $y = L, R$, and update our knowledge of the gas according to Bayes' rule,

$$p(x|y) = \frac{p(y|x)p(x)}{p(y)}, \qquad x, y = L, R, \tag{5.38}$$

where $p(y|x)$ is the likelihood function to get outcome y given that the state is x, $p(x)$ is the initial equilibrium distribution from above, and $p(y)$ is the probability to obtain outcome y. As $p(x|y)$ does not necessarily coincide with the equilibrium distribution, a measurement typically drives the system out of equilibrium. Therefore, the act of measuring should be considered as a non-equilibrium process. To calculate the change of system entropy due to the measurement, we use the Shannon entropy (5.34). Since $H[p(x|y)] - H[p(x)]$ depends on a specific value of y, we average this over all possible outcomes, and get

$$\Delta S_{\text{sys}} = k_B \sum_y p(y) \Big(H[p(x|y)] - H[p(x)] \Big) = -k_B I[S : M], \tag{5.39}$$

where $I[S : M]$ is the mutual information between the system and the measurement outcome. Since the mutual information is non-negative, $\Delta S_{\text{sys}} \leq 0$, implying that by measuring, our uncertainty of the system must at least stay the same or decrease. Assuming that the measurement does not change the internal system energy, i.e., $\Delta E = 0$, the free energy change in the system becomes

$$\Delta F = \Delta E - T \Delta S_{\text{sys}} = k_B T I[S : M] \geq 0, \tag{5.40}$$

where T is the temperature of the environment of the system. We thus see that the effect of the measurement is to increase the free energy of the system, increasing the amount of work that can be extracted isothermally. In fact, for a system initially at equilibrium and coupled to a reservoir at temperature T, the following inequality holds true when feedback controlling the system based on a single measurement [12]

$$W \geq -k_B T I[S:M] + \Delta F. \tag{5.41}$$

Here W is the average system work, and ΔF the change in free energy of the system. This generalizes the result in Eq. (5.25) to feedback controlled systems. If $\Delta F = 0$, we get the following upper bound for the extracted work,

$$W_{\text{ext}} = -W \leq k_B T I[S:M]. \tag{5.42}$$

That is, the decrease in uncertainty about the system sets the limit on how much work that can be extracted by doing feedback. For the Szilard engine, the system is described by the equilibrium distribution $p(x = L) = p(x = R) = 1/2$. For an error free measurement, the likelihood function is given by $p(y = L|x = L) = p(y = R|x = R) = 1$, and $p(y = L|x = R) = p(y = R|x = L) = 0$. We thus get that $I[S:M] = \ln(2)$, i.e., the measurement obtains one bit of information. In the end of the cycle, the system returns to its initial state and $\Delta F = 0$. Therefore, the work that can be extracted by the Szilard engine obeys $W_{\text{ext}} \leq k_B T \ln(2)$, providing an upper bound on how much work that is possible to extract. This inequality was saturated in Eq. (5.37).

We now consider the work required to do a measurement. The information acquired during the measurement will be stored in a memory M. Again, we obtain some outcome y that has probability distribution $p(y)$. The memory is in contact with a heat bath at temperature T. Initially, the system, the memory, and the bath are uncorrelated, and the memory is in thermal equilibrium. To perform the measurement, the memory interacts with the system. By assuming that this interaction does not involve any heat exchange, the average work [with respect to $p(y)$] performed on M during the measurement is bounded by [143]

$$W_{\text{M}}^{(\text{meas})} \geq -k_B T (H - I[S:M]) + \Delta F_{\text{M}}, \tag{5.43}$$

where $H = H[p(y)]$ is the Shannon entropy for the measurement outcome, and ΔF_{M} is the change of free energy in the memory during the measurement. This inequality states that the work on the memory must at least be the change of free energy in the memory, as expected from Eq. (5.25), plus an additional energetic cost due to the information acquisition. The first term obeys the inequality $0 \leq H - I[S:M] \leq H$, where the lower bound is obtained for an error free measurement, and the upper bound when no information is extracted, i.e., when $I[S:M] = 0$. We note that when $H = I[S:M]$ (error free measurement) and $\Delta F_{\text{M}} = 0$, $W_{\text{M}}^{(\text{meas})} \geq 0$. There are thus scenarios when no energy is needed to do the measurement. Note that there also exist scenarios where the lower bound

on the work is negative, meaning that work can be extracted from the memory by doing the measurement.

By assuming that M is in thermal equilibrium with its environment before resetting it to the standard state, i.e., erasing it, the average work [with respect to $p(y)$] required to erase the memory is bounded by [143]

$$W_{\mathrm{M}}^{(\mathrm{eras})} \geq k_B T H - \Delta F_M. \tag{5.44}$$

It is interesting to study the case for which $\Delta F_{\mathrm{M}} = 0$. For a measurement with two outcomes where $p(y = 0) = p(y = 1) = 1/2$, $W_{\mathrm{M}}^{(\mathrm{eras})} \geq k_B T \ln(2)$. That is, to erase the memory, at least $k_B T \ln(2)$ of energy is required – this is the Landauer principle [142].

Combining Eqs. (5.41), (5.43) and (5.44) results in

$$W_{\mathrm{SM}} = W + W_{\mathrm{M}}^{(\mathrm{meas})} + W_{\mathrm{M}}^{(\mathrm{eras})} \geq \Delta F_{\mathrm{S}}, \tag{5.45}$$

where W_{SM} is the average work for the combined unit of system and memory. This inequality is in agreement with the conventional second law (5.4). We thus understand that the apparent violation of the second law for the Szilard engine only appears when considering the thermodynamics of the system alone. As the information processing must be performed by a physical system (demon), that system must also be included in the thermodynamic book-keeping. By doing accordingly, no violations of the second law are observed.

The above discussion focused on feedback processes where only one single measurement was made, and illustrated how information processing comes with a thermodynamic cost. As this thesis concentrates on continuous measurement and feedback, we will now review a few important fluctuation theorems valid for continuous information processing.

In the absence of measurement and feedback, backward or time reversed trajectories are rather straightforward to define. However, when including measurement and feedback, it is not clear how to define a backwards trajectory. In Fig. 4.2(a), we visualize a trajectory X [marked as $S(t)$] of a two-level system together with a trajectory Y [marked as $D(t)$] of the measurement outcomes from a continuous measurement. We note that the time reversed trajectories of X and Y, going from right to left in the figure, yield an unphysical picture; the measurement outcome will predict a system transition before it happens. Similarly, a feedback protocol, with measurement dependent trajectory $\Lambda(Y)$, will therefore be able to act before a system transition occurs. This motivates why there exists no clear definition of backward dynamics under feedback control. In fact, the backward trajectory can be defined in different ways. This implies that each definition leads to a different fluctuation theorem [22]. It is, however, possible to always write down a general detailed fluctuation theorem for continuous feedback control [22]

$$\frac{P_{\mathrm{B}}[X^{\mathrm{tr}}, Y^{\mathrm{tr}}]}{P[X, Y]} = e^{-\sigma[X, \Lambda(Y)] - \left(I_t[X:Y] - I_t^{\mathrm{tr}}[X^{\mathrm{tr}}:Y^{\mathrm{tr}}]\right)}, \tag{5.46}$$

where $P[X, Y]$ is the probability following the forward trajectories X and Y, $P_B[X^{tr}, Y^{tr}]$ is the probability for the (undefined) backward experiment following backward trajectories X^{tr} and Y^{tr}, $\sigma[X, \Lambda(Y)]$ is the unitless entropy production along the forward trajectory when applying feedback protocol $\Lambda(Y)$, $I_t[X : Y]$ is the transfer entropy for the forward experiment, and $I_t^{tr}[X^{tr} : Y^{tr}]$ is the transfer entropy of the backwards experiment. The power of Eq. (5.46) lies in that it is valid for any choice of backward experiment. This indicates that each choice of backward experiment implies a choice-dependent fluctuation theorem, rather than a universal theorem that holds for all scenarios.

As an instructive example, we consider the backward trajectory of Ref. [18]. The experiment is executed as follows. First, we perform the forward experiment with feedback protocol $\Lambda(Y)$. Then, we run the backward experiment by randomly choosing an outcome trajectory Y, and applying the time reversed protocol of $\Lambda(Y)$, but do not perform any feedback. For this type of experiment, one can derive the integral fluctuation theorem [18]

$$\left\langle e^{-\sigma - I_t} \right\rangle = 1. \tag{5.47}$$

Jensen's inequality implies that

$$\langle \sigma \rangle \geq -\langle I_t \rangle. \tag{5.48}$$

This is a generalization of the second law, showing that under continuous measurement and feedback, it is possible to observe a negative system entropy production. Again, including the thermodynamics of the feedback controller would give a non-negative total entropy production. One may also find a generalized Jarzynski relation [18]

$$\left\langle e^{-(w - \Delta F)/k_B T - I_t} \right\rangle = 1, \tag{5.49}$$

where w is the system work, and ΔF the free energy change of the system. For the average work, we get

$$\langle w \rangle \geq -k_B T \langle I_t \rangle + \Delta F, \tag{5.50}$$

resembling the single measurement inequality in Eq. (5.41).

Before closing this section, we review the special case where the presence of feedback control modifies the local detailed balance as [144]

$$\ln\left(\frac{M_{xx'}^{(\nu)}}{M_{x'x}^{(\nu)}}\right) = \frac{\varepsilon_{x'} - \varepsilon_x - \mu_\nu(n_{x'} - n_x)}{k_B T_\nu} + f_{xx'}^{(\nu)}. \tag{5.51}$$

Here $f_{xx'}^{(\nu)}$ is a feedback parameter assumed to be independent on the system energies ε_x. In the absence of feedback, $f_{xx'}^{(\nu)} = 0$, and we recover the standard local detailed balance. It is assumed that the timescale of the feedback is much faster than the system, but much slower than the thermal relaxation time of the reservoirs. Again, so that the system always

interacts with equilibrium reservoirs. This type of modified local detailed balance may arise from deriving a Markovian master equation from the QFPME (1.1) by using the separation of timescales technique introduced in Chapter 6. This is the case for the classical toy model presented in Chapter 7. We note that this type of modified detailed balance also was observed in Ref. [145]. A difference from the cases discussed above is that we do not consider any trajectory for the measurement outcomes or the control protocol – measurement and feedback are effectively incorporated into the rates $M_{xx'}^{(\nu)}$. The modified local detailed balance (5.51) leads to the integral fluctuation theorem [144]

$$\left\langle e^{-(\Delta S_{\text{tot}} + I)/k_B} \right\rangle = 1, \tag{5.52}$$

where I is an information term depending on the feedback parameters $f_{xx'}^{(\nu)}$. In the absence of feedback, the information term vanishes, and we recover the standard fluctuation theorem for non-equilibrium systems (5.31). With Jensen's inequality, we get

$$\langle \Delta S_{\text{tot}} \rangle \geq -\langle I \rangle, \tag{5.53}$$

similar to Eq. (5.48). Again, the entropy production is bounded from below by an information term.

Chapter 6

Results I: Derivations

Having introduced all the theoretical background of this thesis in the preceding chapters, we are now ready to derive the main result of the thesis, Eq. (1.1). We present two different derivations, one based on conventional calculus in Sec. 6.1, and one based on stochastic calculus in Sec. 6.2. In Sec. 6.3, we show how a Markovian master equation for the system, independent of the detector, can be derived from Eq. (1.1) in the limit of a large detector bandwidth. We provide two derivations of this. For linear feedback, we show that the Markovian master equation reduces to the Wiseman-Milburn equation. For threshold (bang-bang) feedback, we derive some general formulas that will be important in Chapter 7.

6.1   Derivation I: Conventional calculus

We may now derive the QFPME (1.1). To this end, we will use the compact measurement superoperator notation $\mathcal{M}(z)\hat{\rho} = \hat{K}(z)\hat{\rho}\hat{K}^{\dagger}(z)$, where $\hat{K}(z)$ is the Gaussian measurement operator in Eq. (4.3). To describe a continuous measurement, time is discretized into n intervals of length $\delta t = (t - t_0)/n$, where t_0 and t are the initial and final times of the measurement, respectively. The initial state of the system in Fig. 1.1 is $\hat{\rho}_{t_0}$. To feedback control the system, the outcome D observed on the detector (see Fig. 1.1) is used to control the Liouville superoperator $\mathcal{L}(D)$ of the system. In this thesis, $\mathcal{L}(D)$ is assumed to be of standard Lindblad form, as discussed in Chapter 3. The control is typically implemented in the system Hamiltonian, or in the coupling rates between the system and its environment.

By successively applying measurement and feedback-controlled time evolutions on the ini-

tial state, we obtain

$$\hat{\rho}_t(\{z_j\}_{j=1}^n) = \mathcal{M}(z_n)e^{\mathcal{L}(D_{n-1})\delta t}\cdots\mathcal{M}(z_2)e^{\mathcal{L}(D_1)\delta t}\mathcal{M}(z_1)e^{\mathcal{L}\delta t}\hat{\rho}_{t_0}, \qquad (6.1)$$

representing the joint state of system and the sequence of outcomes $\{z_j\}_{j=1}^n$, where z_j is the outcome at time $t_j = t_0 + j\delta t$. Note that $z(t) = \lim_{\delta t \to 0}\{z_j\}_{j=1}^n$ is the continuous stream of outcomes produced in the measurement apparatus, while $D(t) = \lim_{\delta t \to 0}\{D_j\}_{j=1}^n$ is the stream of outcomes observed on the detector screen. These signals are connected via the low-pass frequency filter (see Chapter 4.3)

$$D(t) = \int_{-\infty}^t ds\gamma e^{-\gamma(t-s)}z(s), \qquad (6.2)$$

where the detector bandwidth γ (see Fig. 1.1) is introduced[1]. As discussed in Chapter 4, all detectors have a finite bandwidth, and as such, Eq. (6.2) adds a realistic element to our model, eliminating high frequency measurement noise, and introduces a detector delay scaling as $1/\gamma$. Furthermore, the frequency filtering makes it possible to execute feedback protocols that depend nonlinearly on D. Due to the white noise of $z(t)$ [see Eq. (4.10)], higher orders of $z(t)$ are ill-defined because of the diverging frequencies in the power spectrum of $z(t)$ [95, 100, 102] – this is further discussed in Sec. 6.1.1 below.

Since the observer only has access to the sequence $\{D_j\}_{j=1}^n$ from the measurement, it is more favorable to work with the density operator $\hat{\rho}_t(\{D_j\}_{j=1}^n)$ rather than $\hat{\rho}_t(\{z_j\}_{j=1}^n)$. To this end, we discretize Eq. (6.2),

$$D_j = \gamma\delta t\sum_{k=0}^j e^{-\gamma\delta t(j-k)}z_k, \qquad (6.3)$$

and change variables $\hat{\rho}_t(\{z_j\}_{j=1}^n) \to \hat{\rho}_t(\{D_j\}_{j=1}^n)$ via

$$\hat{\rho}_t(\{D_j\}_{j=1}^n) = \int d\mathbf{z}\prod_{r=0}^n \delta\left(D_r - \gamma\delta t\sum_{k=0}^r e^{-\gamma\delta t(r-k)}z_k\right)\hat{\rho}_t(\{z_j\}_{j=1}^n), \qquad (6.4)$$

where $d\mathbf{z} = dz_1\cdots dz_n$, and z_0 is the initial value of $z(t)$. Carrying out the integrals in order, one by one, starting with z_1, and using the standard properties of the Dirac delta function, we get

$$\hat{\rho}_t(\{D_j\}_{j=1}^n) = M(D_n|D_{n-1})e^{\mathcal{L}(D_{n-1})\delta t}\cdots e^{\mathcal{L}(D_1)\delta t}M(D_1|D_0)e^{\mathcal{L}\delta t}\hat{\rho}_{t_0}, \qquad (6.5)$$

---

[1]More generally, the filtering can be introduced as $D(t) = \int_{-\infty}^t ds f(t,s)z(s)$, where $f(t,s)$ is an arbitrary filter function. The choice of this function determines whether it is possible to derive a Markovian master equation as in Eq. (1.1). In this section, we show that the choice $f(t,s) = \gamma e^{-\gamma(t-s)}$, as done in Eq. (6.2), yields a Markovian master equation [Eq. (1.1)]. Note that there might exist other choices of $f(t,s)$ that result in Markovian dynamics. This is not investigated in this thesis.

with new measurement superoperators

$$M(D|D') = \frac{1}{\gamma\delta t}\mathcal{M}\left(\frac{D - D'e^{-\gamma\delta t}}{\gamma\delta t}\right),$$ (6.6)

for outcome D given that D' was observed in the previous timestep.

The property $\int dD_{n-1}\cdots dD_1\hat{\rho}_t(\{D_j\}_{j=1}^n) = \hat{\rho}_t(D_n)$ reduces Eq. (6.5) to

$$\hat{\rho}_{t+\delta t}(D) = \int dD' M(D|D')e^{\mathcal{L}(D')\delta t}\hat{\rho}_t(D'),$$ (6.7)

where we have substituted $D_{n-1} \to D'$ and $D_n \to D$. This provides an update rule for the measurement and feedback process, including the effect of a finite detector bandwidth. To derive Eq. (1.1), we use that $M(D|D')$ may be written, to first order in δt, as

$$M(D|D')\hat{\rho} \approx \delta(D - D')\hat{\rho}$$
$$+ \delta t\left[\lambda\delta(D - D')\mathcal{D}[\hat{A}]\hat{\rho} - \gamma\delta'(D - D')\mathcal{A}(D)\hat{\rho} + \frac{\gamma^2}{8\lambda}\delta''(D - D')\hat{\rho}\right],$$ (6.8)

where $\delta'(D - D')$ and $\delta''(D - D')$ denote the first and second derivative on $\delta(D - D')$ with respect to D. To obtain this expansion, we wrote $M(D|D')$ in the eigenbasis of the observable $\hat{A}$, note that $\hat{A}|a\rangle = \xi_a|a\rangle$, and used the identity

$$\sqrt{\frac{2\lambda}{\pi\gamma^2\delta t}}e^{-2\lambda\delta t\left(\frac{D - D'e^{-\gamma\delta t}}{\gamma\delta t} - \frac{\xi_a + \xi_{a'}}{2}\right)^2}$$
$$\approx \frac{1}{2\pi}\int_{-\infty}^{\infty} d\omega\, e^{-i\omega(D-D')}e^{\frac{1}{8}\gamma\omega\delta t\left[4i(\xi_a + \xi_{a'}) - \frac{\gamma}{\lambda}\omega - 8iD'\right]},$$ (6.9)

where the LHS is expressed in terms of its inverse Fourier transform on the RHS. The '$\approx$' sign represents that we made use of the linearization $e^{-\gamma\delta t} \approx 1 - \gamma\delta t$ on the RHS. Equation (6.8) follows from first expanding the second exponential under the integral in Eq. (6.9) to first order in δt, and then carrying out the integration. Plugging Eq. (6.8) into the update rule (6.7), using $e^{\mathcal{L}(D')} \approx 1 + \mathcal{L}(D')\delta t$, and taking the continuous limit $\delta t \to 0$ yields Eq. (1.1).

6.1.1 Motivation for Eq. (6.2)

We can now motivate why Eq. (6.2) makes it possible to execute nonlinear feedback protocols. To begin, we note that the correlation functions for $z(t)$ and $D(t)$ are given by

$$C_z(t', t) = \frac{1}{4\lambda}\delta(t - t'), \qquad \text{and} \qquad C_D(t', t) = \frac{\gamma}{8\lambda}e^{-\gamma|t-t'|}, \quad (6.10)$$

where we used Eqs. (4.13) [in the continuous limit, with $\xi(t) = \lim_{\delta t \to 0} \delta W/\delta t$] and (6.2). Because of the white noise process $\xi(t)$, we know that the variance of $z(t)$ is given by $\langle z^2(t) \rangle - \langle z(t) \rangle^2 = C_z(t,t) = \delta(0)/4\lambda$. That is, the measurement noise diverges. This reflects the uncertainty of an infinitely weak measurement – quantum coherence is preserved, but at the cost of getting infinite uncertainty, see Eqs. (4.4) and (4.5). The singularity in the variance explains why higher orders of $z(t)$ are ill-defined. In fact, this stems from the white noise process $\xi(t)$ being an idealization – see Chapter 2.

To illustrate this further, we consider the useful example of bang-bang control, typically referred to as threshold control in this thesis, which is the optimal control strategy in many scenarios [60, 61]. For this type of control, the strategy is to apply two different protocols depending on whether the measurement signal is above or below a predetermined threshold value. For instance, in our example two-level system in Chapter 4, the system can be controlled differently whether $|0\rangle$ or $|1\rangle$ is occupied. The natural threshold value for distinguishing the two states would be 0, in-between -1 and $+1$ in Fig. 4.2(a).

Because of the singularity in the variance of $z(t)$, it cannot be used for threshold control in any meaningful way. The infinitely large fluctuations of $z(t)$ makes it impossible to tell whether $|0\rangle$ or $|1\rangle$ is occupied, leading to randomly applied feedback. On the other hand, to understand why $D(t)$ can be used for threshold feedback, we begin by noting that its variance $\langle D^2(t) \rangle - \langle D(t) \rangle^2 = C_D(t,t) = \gamma/8\lambda$ is finite. By tuning the ratio γ/λ, the noise of $D(t)$ can be adjusted such that it always is possible to distinguish which state the system is in, see Fig. 4.2(a), where we clearly can see when $|0\rangle$ or $|1\rangle$ is occupied. Furthermore, the power spectra of $z(t)$ and $D(t)$ are given by [see Eqs. (2.6) and (2.28)]

$$S_z(\omega) = \frac{1}{4\lambda}, \qquad \text{and} \qquad S_D(\omega) = \frac{1}{4\lambda}\frac{\gamma^2}{\gamma^2 + \omega^2}. \qquad (6.11)$$

The white noise spectrum $S_z(\omega)$ for $z(t)$ contains diverging frequencies and explains the singularity in the variance. For $D(t)$, on the other hand, $S_D(\omega)$ is a Lorentzian spectrum, where high frequency noise is filtered out. This explains the finite variance of $D(t)$. Because this type of frequency filtering always occurs in any electronic circuitry, Eq. (6.2) provides a realistic model for signal processing. We note that in the infinite bandwidth limit, $\gamma \to \infty$, $D(t) \to z(t)$ as expected when diverging frequencies are allowed in the spectrum of $D(t)$.

6.2 Derivation II: Stochastic calculus

In this section, we derive Eq. (1.1) by starting from the Belavkin equation (4.18). To establish a connection between the conditional state $\hat{\rho}_c(t)$ and the joint system-detector state $\hat{\rho}_t(D)$, we introduce the average

$$\mathrm{E}[\cdot] \equiv \int \mathcal{D}[\boldsymbol{D}] \langle \tilde{\delta}[\boldsymbol{D}, \boldsymbol{z}] \cdot \rangle_{\boldsymbol{z}}, \qquad (6.12)$$

where $\boldsymbol{D} = \{D_j\}_{j=1}^n$ is a trajectory of outcome D, $\langle \cdot \rangle_{\boldsymbol{z}}$ is an average over all trajectories of the outcome z [see Eq. (4.19)], the path integral $\int \mathcal{D}[\boldsymbol{D}]$, with $\mathcal{D}[\boldsymbol{D}] = dD_1 \cdots dD_n$, is taken over all possible trajectories of the observed outcome D, and

$$\tilde{\delta}[\boldsymbol{D}, \boldsymbol{z}] = \prod_{j=0}^{n-1} \delta\left[D(t_j) - \int_{-\infty}^{t_j} ds \gamma e^{-\gamma(t_j - s)} z(s)\right] \tag{6.13}$$

ensures that the low-pass filter in Eq. (6.2) is incorporated, where $t_j = t_0 + jdt$. Note that $\langle \tilde{\delta}[\boldsymbol{D}, \boldsymbol{z}] \cdot \rangle_{\boldsymbol{z}}$ corresponds to Eq. (6.4), and that $\hat{\rho}_t(\boldsymbol{D}) = \langle \tilde{\delta}[\boldsymbol{D}, \boldsymbol{z}] \hat{\rho}_c(t) \rangle_{\boldsymbol{z}}$. This implies that

$$\hat{\rho}_t(D) = \mathrm{E}\left[\delta[D(t) - D]\hat{\rho}_c(t)\right], \tag{6.14}$$

where the delta function ensures that the last (current) value of $D(t)$ is preserved. From these definitions, we see that taking the trace of Eq. (6.14) gives the detector probability distribution $P_t(D) = E[\delta[D(t) - D]]$, and when integrating (6.14) over D we get the system state $\hat{\rho}_t = \mathrm{E}[\hat{\rho}_c(t)]$.

By using Eq. (6.14), we find the increment

$$d\hat{\rho}_t(D) = \mathrm{E}\left[d\left(\delta[D(t) - D]\hat{\rho}_c(t)\right)\right]. \tag{6.15}$$

To evaluate the RHS of this equation, we note that for functions $f(D)$ and $g(D)$, we get a stochastic product rule $d(fg) = (df)g + f(dg) + (df)(dg)$, where the last term $(df)(dg)$ scales as dt because df and dg contain terms proportional to the Wiener increment dW. We further need the increment

$$d\delta[D(t) - D] = \gamma dt \left[\langle \hat{A} \rangle_c - D(t)\right] \delta'[D(t) - D]$$
$$+ \frac{\gamma^2 dt}{8\lambda} \delta''[D(t) - D] + \frac{\gamma}{\sqrt{4\lambda}} dW(t) \delta'[D(t) - D], \tag{6.16}$$

which can be obtained from Eqs. (2.14) and (4.16). Together with the Belavkin equation (4.18), we may evaluate the RHS of Eq. (6.15) and get (details in Appendix A),

$$d\hat{\rho}_t(D) = dt\mathcal{L}(D)\hat{\rho}_t(D) + \lambda dt\mathcal{D}[\hat{A}]\hat{\rho}_t(D) - \gamma dt\partial_D\mathcal{A}(D)\hat{\rho}_t(D) + \frac{\gamma^2 dt}{8\lambda}\partial_D^2\hat{\rho}_t(D), \tag{6.17}$$

which is Eq. (1.1).

6.3 Separation of timescales

As Eq. (1.1) includes the dynamics of both system and detector, it is typically difficult to solve it analytically. In general, we are restricted to numerical solutions, where our qualitative

insight is limited. This restriction is common in the field of continuous feedback control as discussed in Chapter 4.3, where we pointed out that the Belvakin equation (4.18) can describe any type of feedback numerically, but analytical tools are only available for linear feedback [see the Wiseman-Milburn equation (4.21)].

In this Chapter, we show that Eq. (1.1) reduces to a Markovian master equation for the system state $\hat{\rho}_t$ when there exists a large separation in the system and detector timescales. In particular, this equation allows for analytical treatment of nonlinear feedback protocols, generalizing the Wiseman-Milburn equation (4.21), and makes qualitative investigations of any type of continuous feedback possible.

The dominating timescale of the system $1/\Gamma$ is established by the first two terms of Eq. (1.1), $\mathcal{L}(D) + \lambda\mathcal{D}[\hat{A}]$, while the detector timescale is given by $1/\gamma$, as discussed in Chapter 4.3. When $\gamma \gg \Gamma$, i.e., when changes in the system occur at a rate much smaller than the inverse relaxation time of the detector, the system evolves, to first order in γ^{-1}, according to

$$\partial_t\hat{\rho}_t = \left[\mathcal{L}_0 + \lambda\mathcal{D}[\hat{A}] + \gamma^{-1}\mathcal{L}_{\mathrm{corr}}\right]\hat{\rho}_t, \tag{6.18}$$

where $\mathcal{L}_0$ describes the system dynamics in the limit of an infinitely fast detector, $\lambda\mathcal{D}[\hat{A}]$ describes the effect of measurement backaction, and $\mathcal{L}_{\mathrm{corr}}$ provides a correction to $\mathcal{L}_0$ when there is a small but finite detector delay time γ^{-1}. Explicit expressions and derivations of $\mathcal{L}_0$ and $\mathcal{L}_{\mathrm{corr}}$ are provided in Secs. 6.3.2 and 6.3.3. We emphasize that the measurement strength λ plays a subtle role in the timescales hierarchy. In general, it is required that also $\gamma \gg \lambda$, but there are cases where this requirement can be relaxed. Typically, this is related to the dynamics of the system. In an effectively classical system, where the dynamics of the diagonal and off-diagonal terms of the density matrix are uncoupled in the eigenbasis of $\hat{A}$, $\mathcal{D}[\hat{A}]$, and thereby λ, does not affect the dynamics of the diagonal elements. The measurement strength λ thus only affect the magnitude of the detector noise, as can be seen in the last term of Eq. (1.1). Under these conditions, the ratio λ/γ may be chosen arbitrarily without affecting the system dynamics. However, under a dynamical map where diagonal and off-diagonal elements are coupled, we must keep $\gamma \gg \lambda$ to justify Eq. (6.18).

Finally, we stress that Eq. (6.18) holds for any type of feedback, linear as well as nonlinear. In particular, it simplifies to the Wiseman-Milburn equation (4.21) for a linear (in D) $\mathcal{L}(D)$ when taking the infinite bandwidth limit $\gamma \to \infty$ as shown in Sec. 6.3.4. Therefore, equation (6.18) generalizes the Wiseman-Milburn equation to nonlinear feedback.

Section 6.3.1, provides the basic formalism for deriving Eq. (6.18), while Secs. 6.3.2 and 6.3.3 detail two different derivations – the first using a multiple timescales perturbation approach, and the second using Nakajima-Zwanzig projection operators. Section 6.3.4 provides general expressions of $\mathcal{L}_0$ and $\mathcal{L}_{\mathrm{corr}}$ for linear and threshold feedback.

6.3.1 Mathematical tools

We begin by defining a Fokker-Planck superoperator for the last two terms of Eq. (1.1),

$$\mathcal{F}(D) \equiv -\gamma \partial_D \mathcal{A}(D) + \frac{\gamma^2}{8\lambda} \partial_D^2. \tag{6.19}$$

By introducing a projection superoperator $\mathcal{V}_{bb',aa'}\,\hat{\rho} = \langle a|\hat{\rho}|a'\rangle\,|b\rangle\langle b'|$, for eigenstates $|a\rangle$ and $|b\rangle$ of the observable $\hat{A}$, such that $\hat{A}|j\rangle = \xi_j|j\rangle$ with eigenvalue ξ_j $(j = a, b)$, we may write the Fokker-Planck superoperator as

$$\mathcal{F}(D) = \sum_{aa'} \mathcal{F}_{aa'}(D)\mathcal{V}_{aa',aa'}, \qquad \mathcal{F}_{aa'}(D) = \gamma\partial_D\left(D - \frac{\xi_a + \xi_{a'}}{2}\right) + \frac{\gamma^2}{8\lambda}\partial_D^2, \tag{6.20}$$

where $\mathcal{F}_{aa'}(D)$ are differential operators for Ornstein-Uhlenbeck processes with drift coefficients $D - (\xi_a + \xi_{a'})/2$, see Chapter 2. This illustrates how the superoperator $\mathcal{A}(D)$ couples the system and the detector such that the detector relaxes towards values determined by the eigenvalues of $\hat{A}$.

Next, we introduce the generalized Hermite polynomials of variance $\sigma = \gamma/8\lambda$ as

$$He_n^{[\sigma]}(x) = \left(\frac{\sigma}{2}\right)^{n/2} H_n\left(\frac{x}{\sqrt{2\sigma}}\right), \tag{6.21}$$

where $H_n(x) = (-1)^n e^{x^2}\partial_x^n e^{-x^2}$ are the standard physicist's Hermite polynomials. The generalized Hermite polynomials obey the orthogonality condition

$$\int_{-\infty}^{\infty} dx \frac{He_m^{[\sigma]}(x)}{\sqrt{m!\sigma^m}} \frac{He_n^{[\sigma]}(x)}{\sqrt{n!\sigma^n}} \frac{e^{-x^2/2\sigma}}{\sqrt{2\pi\sigma}} = \delta_{mn}. \tag{6.22}$$

We will, furthermore, make use of the following properties,

$$He_n^{[\sigma]}(x + y) = \sum_{k=0}^{n} \binom{n}{k} He_n^{[\sigma]}(x)y^{n-k}, \tag{6.23}$$

for shifting the polynomials,

$$xHe_n^{[\sigma]}(x) = He_{n+1}^{[\sigma]}(x) + n\sigma He_{n-1}^{[\sigma]}(x), \tag{6.24}$$

and

$$\partial_x\left[He_n^{[\sigma]}(x)e^{-x^2/2\sigma}\right] = -\frac{1}{\sigma}He_{n+1}^{[\sigma]}(x)e^{-x^2/2\sigma}. \tag{6.25}$$

We are particularly interested in the generalized Hermite polynomials as these constitute the left and right eigenfunctions of $\mathcal{F}_{aa'}(D)$ with

$$
\mathcal{F}_{aa'}(D) \left[\frac{He_n^{[\sigma]}\left(D - \frac{\xi_a + \xi_{a'}}{2}\right)}{\sqrt{n!\sigma^n}} \frac{e^{-\left(D - \frac{\xi_a + \xi_{a'}}{2}\right)^2/2\sigma}}{\sqrt{2\pi\sigma}} \right]
$$
$$
= -n\gamma \left[\frac{He_n^{[\sigma]}\left(D - \frac{\xi_a + \xi_{a'}}{2}\right)}{\sqrt{n!\sigma^n}} \frac{e^{-\left(D - \frac{\xi_a + \xi_{a'}}{2}\right)^2/2\sigma}}{\sqrt{2\pi\sigma}} \right]
\tag{6.26}
$$

defining the right eigenfunctions of $\mathcal{F}_{aa'}(D)$ with eigenvalues $-n\gamma$. The eigenfunction for $n = 0$, i.e., the eigenfunction with eigenvalue equal to zero, will be of special interest, and is denoted as

$$
\pi_{aa'}(D) = \frac{e^{-\left(D - \frac{\xi_a + \xi_{a'}}{2}\right)^2/2\sigma}}{\sqrt{2\pi\sigma}}.
\tag{6.27}
$$

The left eigenfunctions of $\mathcal{F}_{aa'}(D)$ are defined by

$$
\left[\frac{He_n^{[\sigma]}\left(D - \frac{\xi_a + \xi_{a'}}{2}\right)}{\sqrt{n!\sigma^n}} \right] \mathcal{F}_{aa'}(D) = -n\gamma \left[\frac{He_n^{[\sigma]}\left(D - \frac{\xi_a + \xi_{a'}}{2}\right)}{\sqrt{n!\sigma^n}} \right],
\tag{6.28}
$$

also with eigenvalues $-n\gamma$.

For our derivations of Eq. (6.18), it is useful to introduce a projection superoperator

$$
\mathcal{P}\hat{\rho}(D) \equiv \mathcal{G}(D) \int_{-\infty}^{\infty} dD\hat{\rho}(D),
\tag{6.29}
$$

where

$$
\mathcal{G}(D) = \sum_{aa'} \pi_{aa'}(D)\mathcal{V}_{aa',aa'}.
\tag{6.30}
$$

The property $\mathcal{P}^2 = \mathcal{P}$ illustrates that $\mathcal{P}$ is a projection. From the definition of $\pi_{aa'}(D)$, we understand that $\mathcal{P}$ projects density matrices onto the eigensubspace of $\mathcal{F}(D)$ corresponding to the eigenvalue equal to zero. Therefore, all states $\mathcal{P}\hat{\rho}(D)$ describes a stationary state with respect to $\mathcal{F}(D)$. In particular, we note that $\mathcal{F}(D)\mathcal{P} = \mathcal{P}\mathcal{F}(D) = 0$. Similarly, we define

$$
\mathcal{Q} = 1 - \mathcal{P}
\tag{6.31}
$$

which is a projection onto the eigensubspace of $\mathcal{F}(D)$ corresponding to all nonzero eigenvalues. Again, we have $\mathcal{Q}^2 = \mathcal{Q}$ as expected for a projection operator. We can, furthermore, show that $\mathcal{P}\mathcal{Q} = \mathcal{Q}\mathcal{P} = 0$, illustrating that $\mathcal{P}$ and $\mathcal{Q}$ are projecting onto subspaces that are each other's orthogonal complements.

6.3.2 Multiple timescales approach

Whenever there is more than one timescale involved in a problem, it is usually beneficial to apply a multiple timescales approach when performing perturbative calculations [146, 147]. When ignoring the presence of several timescales, regular perturbation theory can lead to unphysical solutions with secular terms that grow linearly with time. The source of these terms can usually be removed when taking the multiple timescales into account, prohibiting unphysical solutions. In this section, we apply a multiple timescales perturbation approach to derive Eq. (6.18).

Our starting point is to write the QFPME (1.1) as

$$\partial_t \hat{\rho}_t(D) = \tilde{\mathcal{L}}(D)\hat{\rho}_t(D) + \gamma \tilde{\mathcal{F}}(D)\hat{\rho}_t(D) \tag{6.32}$$

such that $\tilde{\mathcal{L}}(D) = \mathcal{L}(D) + \lambda \mathcal{D}[\hat{A}]$, and $\gamma \tilde{\mathcal{F}}(D) = \mathcal{F}(D)$. The characteristic timescale of the system $1/\Gamma$ is determined by $\tilde{\mathcal{L}}(D)$, and the detector timescale is given by $1/\gamma$. We now define two timescales, one slow, $\tau_1 = t$, and one fast, $\tau_2 = t/\epsilon$, where $\epsilon = \Gamma/\gamma \ll 1$, assuming that the detector is much faster than the system. By replacing $\hat{\rho}_t(D)$ with its two-timed analogue $\hat{\rho}(D, \tau_1, \tau_2)$ [146], and using the chain rule to write $\partial_t = \partial_{\tau_1} + \epsilon^{-1}\partial_{\tau_2}$, the QFPME (6.32) transforms to

$$\epsilon \left[\partial_{\tau_1} - \tilde{\mathcal{L}}(D) \right] \hat{\rho}(D, \tau_1, \tau_2) = - \left[\partial_{\tau_2} - \Gamma\tilde{\mathcal{F}}(D) \right] \hat{\rho}(D, \tau_1, \tau_2). \tag{6.33}$$

By expanding the density matrix in powers of ϵ as $\hat{\rho}(D, \tau_1, \tau_2) = \hat{\rho}^{(0)}(D, \tau_1, \tau_2) + \epsilon\hat{\rho}^{(1)}(D, \tau_1, \tau_2) + \epsilon^2\hat{\rho}^{(2)}(D, \tau_1, \tau_2) + \ldots$, Eq. (6.33) can be written as a recursive set of differential equations,

$$\left[\partial_{\tau_2} - \Gamma\tilde{\mathcal{F}}(D) \right] \hat{\rho}^{(0)}(D, \tau_1, \tau_2) = 0, \tag{6.34a}$$

$$\left[\partial_{\tau_2} - \Gamma\tilde{\mathcal{F}}(D) \right] \hat{\rho}^{(k)}(D, \tau_1, \tau_2) = - \left[\partial_{\tau_1} - \tilde{\mathcal{L}}(D) \right] \hat{\rho}^{(k-1)}(D, \tau_1, \tau_2), \quad k \geq 1. \tag{6.34b}$$

The solutions to these equations can be written as

$$\hat{\rho}^{(0)}(D, \tau_1, \tau_2) = e^{\Gamma\tau_2\tilde{\mathcal{F}}(D)}\hat{\rho}^{(0)}(D, \tau_1, 0), \tag{6.35a}$$

$$\hat{\rho}^{(k)}(D, \tau_1, \tau_2) = e^{\Gamma\tau_2\tilde{\mathcal{F}}(D)}\hat{\rho}^{(k)}(D, \tau_1, 0) - \int_0^{\tau_2} ds\, e^{\Gamma(\tau_2-s)\tilde{\mathcal{F}}(D)} \left[\partial_{\tau_1} - \tilde{\mathcal{L}}(D) \right] \hat{\rho}^{(k-1)}(D, \tau_1, s). \tag{6.35b}$$

By inserting $1 = \mathcal{P} + \mathcal{Q}$ after the exponential superoperator in Eq. (6.35a), the zeroth order solution is split into $\mathcal{P}$- and $\mathcal{Q}$-space. Since all eigenvalues of $\tilde{\mathcal{F}}(D)$ in $\mathcal{Q}$-space are negative, and since we are interested in the limit $\epsilon \ll 1$, where τ_2 is large, the $\mathcal{Q}$-space contribution becomes vanishingly small, such that $\hat{\rho}^{(0)}(D, \tau_1, \tau_2) = \mathcal{P}\hat{\rho}^{(0)}(D, \tau_1, 0)$

as shown in Appendix B.1. The zeroth order solution thus becomes independent on the fast timescale τ_2, and we understand that a fast detector quickly reaches and remains in a stationary state with respect to $\tilde{\mathcal{F}}(D)$ before any system changes have time to occur. Substituting back $\tau_1 = t$, we get the zeroth order solution

$$\hat{\rho}_t^{(0)}(D) = \mathcal{G}(D)\hat{\rho}_t^{(0)}, \tag{6.36}$$

where $\hat{\rho}_t^{(0)} = \int_{-\infty}^{\infty} dD\hat{\rho}_t^{(0)}(D)$.

For $k = 1$ in Eq. (6.35b), the first term becomes independent on the fast timescale τ_2, similar to the zeroth order solution. Since the zeroth order solution also is independent on τ_2, it is only the exponential superoperator that is affected by the integral in the second term. By inserting $1 = \mathcal{P} + \mathcal{Q}$ after the exponential, the integral can be split into $\mathcal{P}$- and $\mathcal{Q}$-space. Since the eigenvalue of $\tilde{\mathcal{F}}(D)$ is zero in $\mathcal{P}$-space, the integral in $\mathcal{P}$-space becomes linear in τ_2, giving rise to a secular term. This term leads to an unphysical behavior in the long time limit. The secular terms are removed by requiring that $\mathcal{P}[\partial_{\tau_1} - \tilde{\mathcal{L}}(D)]\hat{\rho}^{(0)}(D, \tau_1, \tau_2) = 0$, leading to the removal condition

$$\int_{-\infty}^{\infty} dD \left[\partial_{\tau_1} - \tilde{\mathcal{L}}(D) \right] \hat{\rho}^{(k-1)}(D, \tau_1, \tau_2) = 0. \tag{6.37}$$

Note that we have stated the removal condition for a general $k \geq 1$. This may be done as the solutions to Eq. (6.35) will be independent of τ_2 when $\epsilon \ll 1$, as motivated in the following paragraph.

Under the condition $\epsilon \ll 1$, we know that τ_2 is so large that the exponential superoperator under the integral quickly decays to zero in $\mathcal{Q}$-space. Therefore, we may substitute variables $z = \tau_2 - s$ and replace the upper integration limit to $+\infty$, such that the first order solution becomes completely independent of τ_2. Substituting back to $\tau_1 = t$, the first order solution of Eq. (6.35) reads

$$\hat{\rho}_t^{(1)}(D) = \mathcal{G}(D)\hat{\rho}_t^{(1)} + \Gamma^{-1}\tilde{\mathcal{F}}^{-1}(D)\mathcal{Q}\left[\partial_t - \tilde{\mathcal{L}}(D)\right]\mathcal{G}(D)\hat{\rho}_t^{(0)}, \tag{6.38}$$

where we have defined the Drazin inverse [148, 149] of $\tilde{\mathcal{F}}(D)$ as

$$\tilde{\mathcal{F}}^{-1}(D) = -\int_0^{\infty} dz e^{z\tilde{\mathcal{F}}(D)}\mathcal{Q}. \tag{6.39}$$

Since all eigenvalues of $\tilde{\mathcal{F}}(D)$ are nonzero in $\mathcal{Q}$-space, this inverse is well-defined. Note that $\mathcal{Q}$ may be added between $\tilde{\mathcal{F}}^{-1}(D)$ and $[\partial_t - \tilde{\mathcal{L}}(D)]$ in Eq. (6.38) because $\mathcal{Q}^2 = \mathcal{Q}$.

Substituting back $\tau_1 = t$, and using that the solutions in Eq. (6.35) are independent of τ_2, the removal condition (6.37) leads to master equations

$$\partial_t \hat{\rho}_t^{(k)} = \int_{-\infty}^{\infty} dD \tilde{\mathcal{L}}(D)\hat{\rho}_t^{(k)}(D), \qquad k \geq 0, \tag{6.40}$$

for the system state $\hat{\rho}_t^{(k)}$, where the detector has been integrated out. For $k = 0$, we get, by using Eq. (6.36),

$$\partial_t \hat{\rho}_t^{(0)} = \tilde{\mathcal{L}}_0 \hat{\rho}_t^{(0)}, \qquad\qquad \tilde{\mathcal{L}}_0 = \int_{-\infty}^{\infty} dD \tilde{\mathcal{L}}(D) \mathcal{G}(D). \qquad (6.41)$$

For $k = 1$, we begin to note that Eqs. (6.38) and (6.41) give that

$$\hat{\rho}_t^{(1)}(D) = \mathcal{G}(D) \hat{\rho}_t^{(1)} - \Gamma^{-1} \tilde{\mathcal{F}}^{-1}(D) \mathcal{Q} \tilde{\mathcal{L}}(D) \mathcal{G}(D) \hat{\rho}_t^{(0)} \qquad (6.42)$$

because $\mathcal{Q}\mathcal{G}(D) = 0$, as shown in Appendix B.2. Equations (6.40), (6.41) and (6.42) now provides the following master equation for $k = 1$,

$$\begin{aligned} \partial_t \hat{\rho}_t^{(1)} &= \tilde{\mathcal{L}}_0 \hat{\rho}_t^{(1)} + \Gamma^{-1} \tilde{\mathcal{L}}_{\mathrm{corr}} \hat{\rho}_t^{(0)}, \\ \tilde{\mathcal{L}}_{\mathrm{corr}} &= - \int_{-\infty}^{\infty} dD \tilde{\mathcal{L}}(D) \tilde{\mathcal{F}}^{-1}(D) \mathcal{Q} \tilde{\mathcal{L}}(D) \mathcal{G}(D). \end{aligned} \qquad (6.43)$$

With $\hat{\rho}_t = \hat{\rho}_t^{(0)} + \epsilon \hat{\rho}_t^{(1)} + \mathcal{O}(\epsilon^2)$, and Eqs. (6.41) and (6.43), we can derive Eq. (6.18) to first order in ϵ, with

$$\mathcal{L}_0 = \int_{-\infty}^{\infty} dD \mathcal{L}(D) \mathcal{G}(D), \qquad (6.44)$$

and

$$\mathcal{L}_{\mathrm{corr}} = - \int_{-\infty}^{\infty} dD \mathcal{L}(D) \tilde{\mathcal{F}}^{-1}(D) \mathcal{Q} \mathcal{L}(D) \mathcal{G}(D), \qquad (6.45)$$

where we for $\mathcal{L}_{\mathrm{corr}}$ used that $\int_{-\infty}^{\infty} dD \hat{\rho}(D) = \int_{-\infty}^{\infty} dD \mathcal{P} \hat{\rho}(D)$, $\mathcal{P} \tilde{\mathcal{F}}^{-1}(D) \mathcal{Q} = 0$ (see Appendix B.2), and that $[\mathcal{P}, \mathcal{D}[\hat{A}]] = [\mathcal{Q}, \mathcal{D}[\hat{A}]] = 0$. Finally, we note that the joint system-detector state to first order in ϵ reads

$$\hat{\rho}_t(D) = \left[1 - \gamma^{-1} \tilde{\mathcal{F}}^{-1}(D) \mathcal{Q} \mathcal{L}(D) \right] \mathcal{G}(D) \hat{\rho}_t, \qquad (6.46)$$

where we used Eqs. (6.36) and (6.42), and that $\mathcal{Q}\mathcal{G}(D) = 0$. Note that the dynamics of $\hat{\rho}_t$ in this equation are determined by Eq. (6.18). That is, we can always recover the joint system-detector state $\hat{\rho}_t(D)$ to first order in ϵ provided that the system state $\hat{\rho}_t$ is known.

6.3.3 Nakajima-Zwanzig approach

In this section, we provide an alternative derivation of Eq. (6.18), making use of Nakajima-Zwanzig projection superoperators [68, 150, 151]. While the multiple timescales approach systematically evaluates the effect of a finite detector bandwidth order by order in a perturbation scheme, the Nakajima-Zwanzig approach provides a more straightforward treatment

of the perturbation calculations. Despite the methods being different, they provide equivalent expressions for $\mathcal{L}_0$ and $\mathcal{L}_{\text{corr}}$ [see Eq. (6.18)] as shown below.

We begin by writing the QFPME (1.1) as

$$\partial_t \hat{\rho}_t(D) = \tilde{\mathcal{L}}(D)\hat{\rho}_t(D) + \mathcal{F}(D)\hat{\rho}_t(D), \tag{6.47}$$

where $\tilde{\mathcal{L}}(D) = \mathcal{L}(D) + \lambda\mathcal{D}[\hat{A}]$. By making use of Eqs. (6.29) and (6.31), we may split Eq. (6.47) into two coupled differential equations,

$$\partial_t \mathcal{P}\hat{\rho}_t(D) = \mathcal{P}\tilde{\mathcal{L}}(D)\mathcal{P}\hat{\rho}_t(D) + \mathcal{P}\tilde{\mathcal{L}}(D)\mathcal{Q}\hat{\rho}_t(D), \tag{6.48a}$$

$$\partial_t \mathcal{Q}\hat{\rho}_t(D) = \mathcal{Q}\tilde{\mathcal{L}}(D)\mathcal{P}\hat{\rho}_t(D) + \mathcal{Q}\tilde{\mathcal{L}}(D)\mathcal{Q}\hat{\rho}_t(D) + \mathcal{Q}\mathcal{F}(D)\mathcal{Q}\hat{\rho}_t(D). \tag{6.48b}$$

To arrive at these equations, we used that $\mathcal{P}\mathcal{F}(D) = \mathcal{F}(D)\mathcal{P} = 0$ and $1 = \mathcal{P} + \mathcal{Q}$. The formal solution to Eq. (6.48b) reads

$$\begin{aligned}
\mathcal{Q}\hat{\rho}_t(D) &= e^{\mathcal{Q}[\tilde{\mathcal{L}}(D)+\mathcal{F}(D)]\mathcal{Q}(t-t_0)}\mathcal{Q}\hat{\rho}_{t_0}(D) \\
&\quad + \int_{t_0}^t ds\, e^{\mathcal{Q}[\tilde{\mathcal{L}}(D)+\mathcal{F}(D)]\mathcal{Q}(t-s)}\mathcal{Q}\tilde{\mathcal{L}}(D)\mathcal{P}\hat{\rho}_s(D),
\end{aligned} \tag{6.49}$$

where $\mathcal{Q}\hat{\rho}_{t_0}(D)$ specifies the initial state in $\mathcal{Q}$-space. As specified above, $\tilde{\mathcal{L}}(D) \sim \Gamma$ and $\mathcal{F}(D) \sim \gamma$, where $1/\Gamma$ and $1/\gamma$ determines the timescales of the system and the detector, respectively. Here, we assume that $\gamma \gg \Gamma$, such that the effect of $\tilde{\mathcal{L}}(D)$ in the exponentials in Eq. (6.49) is vanishingly small, and thus can be removed to leading order. Since the exponentials only act in $\mathcal{Q}$-space, they will decay with time in the eigenbasis of $\mathcal{F}(D)$ (see Appendix B.1). Therefore, we can put $\mathcal{Q}\hat{\rho}_{t_0}(D) = 0$, as we, typically, only are interested in the long time limit. Plugging this back into Eq. (6.48a) gives

$$\partial_t \mathcal{P}\hat{\rho}_t(D) = \mathcal{P}\tilde{\mathcal{L}}(D)\mathcal{P}\hat{\rho}_t(D) + \mathcal{P}\tilde{\mathcal{L}}(D)\mathcal{Q}\int_{t_0}^t ds\, e^{\mathcal{Q}\mathcal{F}(D)\mathcal{Q}(t-s)}\mathcal{Q}\tilde{\mathcal{L}}(D)\mathcal{P}\hat{\rho}_s(D). \tag{6.50}$$

If the state $\mathcal{P}\hat{\rho}_t(D)$ remains constant over the timescale $1/\gamma$, during which the exponential under the integral decays to zero, we may change variables $t - s = z$, extend the upper integration limit to $+\infty$, and replace $\hat{\rho}_s(D) \to \hat{\rho}_t(D)$. We now get

$$\partial_t \mathcal{P}\hat{\rho}_t(D) = \mathcal{P}\tilde{\mathcal{L}}(D)\mathcal{P}\hat{\rho}_t(D) - \mathcal{P}\tilde{\mathcal{L}}(D)\mathcal{Q}\mathcal{F}^{-1}(D)\mathcal{Q}\tilde{\mathcal{L}}(D)\mathcal{P}\hat{\rho}_t(D), \tag{6.51}$$

where the (Drazin) inverse of $\mathcal{F}(D)$ is defined as

$$\mathcal{F}^{-1}(D) = -\int_0^\infty dz\, e^{\mathcal{Q}\mathcal{F}(D)\mathcal{Q}z}\mathcal{Q}. \tag{6.52}$$

In Appendix B.3, we show that this inverse is equivalent to the one in Eq. (6.39) – note that we put a tilde on top of the superoperator $\mathcal{F}$ depending on whether the factor of γ

is included or excluded in the operator, see definition below Eq. (6.32). Equation (6.51) provides a Markovian master equation for the joint system-detector state $\mathcal{P}\hat{\rho}_t(D)$. As the first term scales as Γ, and the second as Γ^2/γ, we may think of the first term as the leading order term for an infinitely quick detector ($\gamma \to \infty$), while the second term can be thought of as a correction due to a finite detector response time γ^{-1}. By integrating Eq. (6.51) over D, we find Eq. (6.18) with

$$\mathcal{L}_0 = \int_{-\infty}^{\infty} dD \mathcal{L}(D)\mathcal{G}(D), \tag{6.53}$$

and

$$\mathcal{L}_{\mathrm{corr}} = -\gamma \int_{-\infty}^{\infty} dD \mathcal{L}(D)\mathcal{Q}\mathcal{F}^{-1}(D)\mathcal{Q}\mathcal{L}(D)\mathcal{G}(D). \tag{6.54}$$

Equation (6.53) is presented in an identical form as in Eq. (6.44), while Eq. (6.54) appears slightly different compared to Eq. (6.45). These two representations of $\mathcal{L}_{\mathrm{corr}}$ are, however, identical – note that $\mathcal{F}(D) = \gamma\tilde{\mathcal{F}}(D)$, and that the leftmost $\mathcal{Q}$ in Eq. (6.54) can be absorbed into the inverse $\mathcal{F}^{-1}(D)$ as demonstrated in Appendix B.3.

6.3.4 Explicit expressions for linear and threshold feedback

Equations (6.44), (6.45), (6.53), and (6.54) are general expressions for the leading order and first order correction of the system dynamics when the relaxation time of the detector is small. While $\mathcal{L}_0$ can be calculated straightforwardly, the inverse of the Fokker-Planck superoperator in $\mathcal{L}_{\mathrm{corr}}$ complicates the evaluation of the correction term. In this section, we provide a general method for evaluating this term. In particular, we focus on the special cases of linear and threshold (bang-bang) feedback. For linear feedback, we recover the Wiseman-Milburn equation (4.21) with additional correction terms due to a finite detector bandwidth. For threshold feedback, we demonstrate how Eq. (6.18) can be used for nonlinear feedback – this will be important for the results presented in Chapter 7.

The feedback Liouville superoperator $\mathcal{L}(D)$ can be written as

$$\mathcal{L}(D) = \sum_{aa',bb'} \mathcal{L}_{bb',aa'}(D)\mathcal{V}_{bb',aa'}, \tag{6.55}$$

where $\mathcal{L}_{bb',aa'}(D)$ are the matrix elements in the Liouville space representation [152] of $\mathcal{L}(D)$, evaluated in the eigenbasis of the observable $\hat{A}$. These matrix elements can be expanded in terms of the left eigenfunctions (6.28) as

$$\mathcal{L}_{bb',aa'}(D) = \sum_{n=0}^{\infty} \mathcal{L}_{bb',aa'}^{(n)} \frac{He_n^{[\sigma]}\left(D - \frac{\xi_a + \xi_{a'}}{2}\right)}{\sqrt{n!\sigma^n}}, \tag{6.56}$$

where Eq. (6.22) provides the following expression for the expansion coefficients,

$$\mathcal{L}^{(n)}_{bb',aa'} = \int_{-\infty}^{\infty} dD \frac{\mathcal{L}_{bb',aa'}(D)}{\sqrt{2\pi n!}\sigma^{n+1}} He_n^{[\sigma]}\left(D - \frac{\xi_a + \xi_{a'}}{2}\right) e^{-\left(D - \frac{\xi_a + \xi_{a'}}{2}\right)^2/2\sigma}. \tag{6.57}$$

With these definitions, the correction term [here we use Eq. (6.54)] may be written as

$$\mathcal{L}_{\text{corr}} = \sum_{n=1}^{\infty} \frac{1}{n} \sum_{k=0}^{n} \frac{\sqrt{n!/k!}}{(n-k)!} \sum_{aa',bb',cc'} \frac{(\xi_a + \xi_{a'} - \xi_c - \xi_{c'})^{n-k}}{(2\sqrt{\sigma})^{n-k}}$$
$$\times \mathcal{L}^{(n)}_{bb',cc'} \mathcal{L}^{(k)}_{cc',aa'} \mathcal{V}_{bb',aa'}, \tag{6.58}$$

where ξ_j are the eigenvalues of $\hat{A}$ corresponding to the eigenstate $|j\rangle$. To obtain this expression, we made use of Eqs. (6.22) and (6.23). Note that the sum over n starts at 1 – this is due to the $\mathcal{Q}$ projectors in Eq. (6.54), making sure that the inverse only is taken in the eigensubspace of $\mathcal{F}(D)$ with nonzero eigenvalues. This equation specifies a general expression for $\mathcal{L}_{\text{corr}}$ for arbitrary feedback protocols $\mathcal{L}(D)$, linear as well as nonlinear in D.

Linear feedback

For the special case of linear feedback, we consider a feedback Liouvillian

$$\mathcal{L}(D) = \mathcal{L} + D\mathcal{K}, \tag{6.59}$$

where $\mathcal{L}$ is the Liouville operator of the system in the absence of feedback, and $\mathcal{K}$ is a Liouville superoperator describing the feedback forces applied on the system. The measurement outcome D can here be considered as the strength at which these forces are applied. For linear feedback, Eq. (6.57) becomes

$$\mathcal{L}^{(n)}_{bb',aa'} = \mathcal{L}_{bb',aa'}\delta_{0,n} + \sqrt{\sigma}\mathcal{K}_{bb',aa'}\delta_{0,n-1} + \frac{\xi_a + \xi_{a'}}{2}\mathcal{K}_{bb',aa'}\delta_{0,n}, \tag{6.60}$$

where we employed Eqs. (6.22) and (6.24). Together with Eqs. (6.53) and (6.58), this provides

$$\mathcal{L}_0 = \mathcal{L} + \mathcal{K}\mathcal{A}(0), \qquad \mathcal{L}_{\text{corr}} = \frac{\gamma}{8\lambda}\mathcal{K}^2 + \mathcal{K}[\mathcal{L}, \mathcal{A}(0)] + \mathcal{K}[\mathcal{K}, \mathcal{A}(0)]\mathcal{A}(0), \tag{6.61}$$

where $\mathcal{A}(0)\hat{\rho} = \frac{1}{2}\{\hat{A}, \hat{\rho}\}$. Plugging this into Eq. (6.18) gives us the Markovian master equation

$$\partial_t \hat{\rho}_t = \mathcal{L}\hat{\rho}_t + \lambda \mathcal{D}[\hat{A}]\hat{\rho}_t + \mathcal{K}\mathcal{A}(0)\hat{\rho}_t + \frac{1}{8\lambda}\mathcal{K}^2\hat{\rho}_t$$
$$+ \gamma^{-1}\mathcal{K}[\mathcal{L}, \mathcal{A}(0)]\hat{\rho}_t + \gamma^{-1}\mathcal{K}[\mathcal{K}, \mathcal{A}(0)]\mathcal{A}(0)\hat{\rho}_t. \tag{6.62}$$

This is the Wiseman-Milburn equation (4.21) with two additional correction terms due to a finite detector bandwidth γ. In the infinite bandwidth limit, we recover Eq. (4.21). The fact that we may recover the result of Wiseman and Milburn indicates that there is a clear connection between the main results of this thesis and earlier work [52]. As detailed before, Eqs. (1.1) and (6.18) thus provides a generalization of the result in Ref. [52], able to describe arbitrary feedback protocols, linear as well as nonlinear in D.

Finally, we make a remark. The separation of timescales approach assumes that γ is the largest parameter in the problem, such that $\mathcal{F}(D)$ dominates over $\mathcal{L}(D)$. As the increment dD in Eq. (4.16) scales as γ, the Liouville superoperator in Eq. (6.59) is unbounded, breaking the assumption of $\mathcal{F}(D)$ being the dominant contribution in Eq. (1.1)[2]. Because of this, there is one term in $\mathcal{L}_{\text{corr}}$ that scales with γ, contributing to leading order in γ^{-1}. We thus stress that the separation of timescales technique should be treated with care for linear feedback. However, in the infinite bandwidth limit, we recovered the Wiseman-Milburn equation, which is a sensible result.

Threshold feedback

Threshold feedback, or bang-bang control, is a special case of nonlinear feedback, where the controller instantaneously switches between two different protocols, $\mathcal{J}$ and $\mathcal{K}$, dependent on whether the measurement outcome D is above or below a predetermined threshold value. Using $D = 0$ as threshold, the feedback Liouville superoperator can be written as

$$\mathcal{L}(D) = \theta(D)\mathcal{J} + [1 - \theta(D)]\mathcal{K}, \tag{6.63}$$

where $\theta(D)$ is the Heaviside step function. We begin to note that the leading order term (6.53) is given by

$$\mathcal{L}_0 = \sum_{aa'} [(1 - \eta_{aa'})\mathcal{J} + \eta_{aa'}\mathcal{K}] \mathcal{V}_{aa',aa'}, \tag{6.64}$$

where

$$\eta_{aa'} = \frac{1}{2}\left(1 - \text{erf}\left[\sqrt{\frac{\lambda}{\gamma}}(\xi_a + \xi_{a'})\right]\right), \tag{6.65}$$

with $\text{erf}(\cdot)$ being the error function.

To find the correction term (6.58), we use Eq. (6.57) to show that $\mathcal{L}^{(0)}_{bb',aa'} = [\mathcal{L}_0]_{bb',aa'}$ for $n = 0$, while nonzero n gives

$$\mathcal{L}^{(n)}_{bb',aa'} = (\mathcal{J} - \mathcal{K})_{bb',aa'} \frac{(-1)^{n-1}}{\sqrt{2^n n!\pi}} e^{-\frac{(\xi_a+\xi_{a'})^2}{8\sigma}} H_{n-1}\left(\frac{\xi_a + \xi_{a'}}{\sqrt{8\sigma}}\right), \tag{6.66}$$

---

[2]Note that this assumption breaks down for all feedback protocols where $\mathcal{L}(D) = \mathcal{L} + f(D)\mathcal{K}$ contains an unbounded function $f(D)$. Therefore, one needs to treat the separation of timescales technique with care for unbounded feedback protocols.

where $H_n(\cdot)$ is the standard physicist's Hermite polynomials. This was derived using Eq. (6.25) and the fact that $He_n^{[\sigma]}(-x) = (-1)^n He_n^{[\sigma]}(x)$. Plugging this into Eq. (6.58), gives the correction superoperator

$$\mathcal{L}_{\mathrm{corr}} = (\mathcal{J} - \mathcal{K})(\tilde{\mathcal{J}} - \tilde{\mathcal{K}} - \tilde{\mathcal{L}}_0), \tag{6.67}$$

where the matrix elements of $\tilde{\mathcal{L}}_0$ are given by

$$
[\tilde{\mathcal{L}}_0]_{bb',aa'} = [\mathcal{L}_0]_{bb',aa'} \sum_{n=0}^{\infty} \frac{\left[\sqrt{\frac{\lambda}{\gamma}}\left(\xi_b + \xi_{b'} - \xi_a - \xi_{a'}\right)\right]^{n+1}}{(n+1)(n+1)!\sqrt{\pi}}
$$
$$
\times e^{-\frac{\lambda}{\gamma}(\xi_b + \xi_{b'})^2} H_n\left[\sqrt{\frac{\lambda}{\gamma}}(\xi_b + \xi_{b'})\right], \tag{6.68}
$$

and the elements of $\tilde{\mathcal{J}} - \tilde{\mathcal{K}}$ are given by

$$
(\tilde{\mathcal{J}} - \tilde{\mathcal{K}})_{bb',aa'} = (\mathcal{J} - \mathcal{K})_{bb',aa'} \sum_{n=0}^{\infty} \sum_{k=0}^{n} \binom{n}{k} \frac{\left[\sqrt{\frac{\lambda}{\gamma}}\left(\xi_b + \xi_{b'} - \xi_a - \xi_{a'}\right)\right]^{n-k}}{2^{k+1}(k+1)(n+1)!\pi}
$$
$$
\times e^{-\frac{\lambda}{\gamma}\left[(\xi_a + \xi_{a'})^2 + (\xi_b + \xi_{b'})^2\right]} H_k\left[\sqrt{\frac{\lambda}{\gamma}}(\xi_a + \xi_{a'})\right] H_n\left[\sqrt{\frac{\lambda}{\gamma}}(\xi_b + \xi_{b'})\right]. \tag{6.69}
$$

We note that the sums appearing in Eqs. (6.68) and (6.69) can be converted into integrals that are straightforward to evaluate numerically. For the single sum in Eq. (6.68), we get

$$
\sum_{n=0}^{\infty} \frac{[\sqrt{\alpha}(b-a)]^{n+1}}{(n+1)(n+1)!\sqrt{\pi}} e^{-\alpha b^2} H_n\left[\sqrt{\alpha}b\right] = \frac{1}{2}\int_0^1 dy \frac{\mathrm{erf}\left[\sqrt{\alpha}b\right] - \mathrm{erf}\left[\sqrt{\alpha}(b[1-y] + ay)\right]}{y},
$$
$$\tag{6.70}$$

for $\alpha > 0$ and arbitrary constants a and b. This was obtained using $1/(n+1) = \int_0^1 dy\, y^n$ twice, and that $\exp\{2xt - t^2\} = \sum_{n=0}^{\infty} t^n H_n(x)/n!$. The double sum in Eq. (6.69) can be converted into the following integrals,

$$
\sum_{n=0}^{\infty} \sum_{k=0}^{n} \binom{n}{k} \frac{[\sqrt{\alpha}(b-a)]^{n-k}}{2^{k+1}(k+1)(n+1)!\pi} e^{-\alpha(a^2+b^2)} H_k\left[\sqrt{\alpha}a\right] H_n\left[\sqrt{\alpha}b\right] =
$$
$$
= \frac{\mathrm{sgn}(a) - \mathrm{erf}(\sqrt{\alpha}a)}{4} \int_0^1 dy \frac{\mathrm{erf}\{\sqrt{\alpha}[b(1-y) + ay]\} - \mathrm{erf}\{\sqrt{\alpha}b(1-y)\}}{y} +
$$
$$
+ \frac{1}{2\pi}\int_0^1 dy \int_0^1 dz \left\{ \frac{e^{-\alpha\left[a^2 + b^2\frac{(1-y)^2}{1-y^2z^2}\right]}}{\sqrt{1-y^2z^2}} - \sqrt{\pi\alpha}e^{-\alpha[b(1-y)+ayz]^2} \right.
$$
$$
\left. \times \left[|a| + a\,\mathrm{erf}\left(\sqrt{\alpha}\frac{-by(1-y)z - a(1-y^2z^2)}{\sqrt{1-y^2z^2}}\right)\right]\right\}. \tag{6.71}
$$

In Appendix B.4, we provide details on how to find this integral representation.

Chapter 7

Results II: Toy models

In this chapter, we illustrate how the QFPME (1.1) and the separation of timescales technique (Chapter 6.3) can be applied on specific systems. To this end, we consider two simple information engines using measurement and feedback for producing power. First, we consider a classical two-level system coupled to a thermal environment that can excite and de-excite the system. Through a simple feedback protocol, energy can be extracted from the thermal environment. Second, we study a coherently driven qubit. By applying the same feedback protocol as in the classical model, it is possible to extract energy from the drive in the long time limit, while simultaneously preserving the quantum coherence of the system.

7.1 Full counting statistics

We begin by showing how full counting statistics can be used in the QFPME (1.1). By extending the system-detector density matrix to include the number of transported particles as $\hat{\rho}_t(D) \to \hat{\rho}_t(D, n)$, we find the probability distribution over n via

$$P_t(n) = \int_{-\infty}^{\infty} dD \operatorname{tr}\{\hat{\rho}_t(D, n)\}. \tag{7.1}$$

The joint system-detector density matrix is recovered by summing over all possible n, $\hat{\rho}_t(D) = \sum_n \hat{\rho}_t(D, n)$. By introducing a counting field χ, we can find the counting field dependent density matrix $\hat{\rho}_t(D, \chi) = \sum_n \hat{\rho}_t(D, n)e^{in\chi}$. The QFPME can now be written as

$$\partial_t \hat{\rho}_t(D, \chi) = \mathcal{L}(D, \chi)\hat{\rho}_t(D, \chi) + \lambda \mathcal{D}[\hat{A}]\hat{\rho}_t(D, \chi) - \gamma \partial_D \mathcal{A}(D)\hat{\rho}_t(D, \chi) + \frac{\gamma^2}{8\lambda}\partial_D^2 \hat{\rho}_t(D, \chi), \tag{7.2}$$

with the counting field dependent Liouville superoperator $\mathcal{L}(D, \chi)$. The moment generating function can be defined as

$$M_t(\chi) = \int_{-\infty}^{\infty} dD \operatorname{tr}\{\hat{\rho}_t(D, \chi)\}. \tag{7.3}$$

In steady state, we find

$$\langle n \rangle = -i\partial_\chi M_t(\chi)|_{\chi=0} = -it \int_{-\infty}^{\infty} dD \operatorname{tr}\left\{[\partial_\chi \mathcal{L}(D, \chi)]_{\chi=0} \hat{\rho}_{ss}(D)\right\}, \tag{7.4}$$

where $\hat{\rho}_{ss}(D)$ is the stationary joint system-detector density matrix.

7.2 Classical toy model

We consider a classical two-level system with states $|0\rangle$ and $|1\rangle$ separated by energy Δ as depicted in the inset of Fig. 7.1(a). The system is in contact with a thermal reservoir at temperature T, with which the system can exchange energy quanta at a rate given by Γ. We continuously monitor the state of the system by measuring the observable $\hat{A} = \hat{\sigma}_z = |1\rangle\langle 1| - |0\rangle\langle 0|$. For an ideal detector, with low noise and delay, this means that whenever the measurement outcome $D < 0$, the system resides in $|0\rangle$, while the system resides in $|1\rangle$ for $D \geq 0$. Note that while we use the notation of quantum mechanics, the diagonal and off-diagonal elements of the system density matrix $\hat{\rho}_t(D)$ are decoupled, such that $[\hat{\rho}_t(D), \hat{\sigma}_z] = 0$ at all times, and the backaction term of Eq. (1.1) has no effect on the system dynamics. Therefore, we refer to the system as classical.

The feedback protocol works as follows. Upon detecting an excitation in the system, i.e., by observing a change of sign for D, the levels are immediately flipped according to the solid arrows in the inset of Fig. 7.1(a), extracting energy from the reservoir. The Hamiltonian under this feedback is given by

$$\hat{H}(D) = [1 - \theta(D)]\Delta |1\rangle\langle 1| + \theta(D)\Delta |0\rangle\langle 0|, \tag{7.5}$$

with $\theta(D)$ being the Heaviside step function. Since $[\hat{H}(D), \hat{\sigma}_z] = 0$, the density matrix remains diagonal in the energy basis at all times. The feedback protocol is thus represented by the following Liouville superoperator,

$$\mathcal{L}(D) = [1 - \theta(D)]\mathcal{L}_- + \theta(D)\mathcal{L}_+. \tag{7.6}$$

Here $\mathcal{L}_-\hat{\rho} = \Gamma n_B \mathcal{D}[\hat{\sigma}^\dagger]\hat{\rho} + \Gamma[n_B + 1]\mathcal{D}[\hat{\sigma}]\hat{\rho}$ is the protocol applied for $D < 0$, and $\mathcal{L}_+\hat{\rho} = \Gamma[n_B + 1]\mathcal{D}[\hat{\sigma}^\dagger]\hat{\rho} + \Gamma n_B \mathcal{D}[\hat{\sigma}]\hat{\rho}$ is the protocol applied for $D \geq 0$, with $\mathcal{D}[\hat{c}]\hat{\rho} = \hat{c}\hat{\rho}\hat{c}^\dagger - \{\hat{c}^\dagger\hat{c}, \hat{\rho}\}/2$ for an arbitrary operator $\hat{c}$, $\hat{\sigma} = |0\rangle\langle 1|$, and $n_B = [\exp(\Delta/k_B T) - 1]^{-1}$
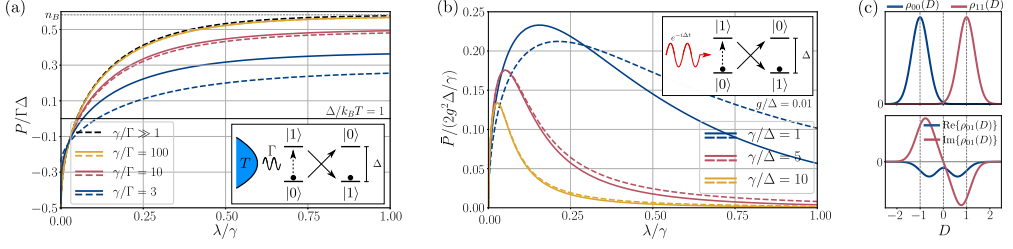
Figure 7.1: Power production of the classical (a) and quantum (b) toy model as a function of λ/γ. Dashed lines correspond to analytical calculations, solid lines to numerical calculations. (a) The inset visualizes the classical toy model and its feedback protocol. When an excitation (dashed arrow) is detected, the levels are flipped according to the solid arrows. The black, dashed line corresponds to Eq. (7.11), while the colored dashed lines correspond to Eq. (7.25). For $\lambda \gg \gamma$ (strong measurement), feedback is consistently applied correctly, and n_B sets an upper bound on how much energy that can be extracted from the bath (grey, dashed line). For $\lambda \ll \gamma$ (weak measurement), feedback is applied randomly, leading to dissipation of energy. Here we used $\Delta/k_B T = 1$. (b) The inset illustrates the quantum toy model, where a qubit is driven by an external semiclassical field. Measurement and feedback are performed exactly as in the classical model. The dashed lines correspond to Eq. (7.34). For $\lambda \gg \gamma$, the power vanishes – this illustrates the quantum Zeno effect. For $\lambda \ll \gamma$, feedback is applied randomly, and no power can be extracted due to the symmetric driving (see discussion in Sec. 7.3). From the numerics, we note that the separation of timescales approximation breaks down when γ is comparable in size to all other timescales. (c) Visualization of the numerically calculated $\hat{\rho}_t(D)$ for the quantum toy model in steady state for $t = \tau = 2\pi/\Delta$ (period of driving field), with matrix elements $\rho_{ab}(D) = \langle a|\hat{\rho}_t(D)|b\rangle$. Here we use $g/\Delta = 0.01$ and $\gamma = \Delta = \lambda$. Upper panel shows the diagonal elements of $\hat{\rho}_t(D)$. Bottom panel visualizes the real and imaginary part of $\rho_{01}(D)$. Figure taken from Paper I.

is the Bose-Einstein distribution giving the average occupation of the reservoir at energy Δ. By writing the density matrix as a vector $\rho = (\rho_{00}, \rho_{11})^T$, with $\rho_{aa} = \langle a|\hat{\rho}|a\rangle$, we can write $\mathcal{L}_-$ and $\mathcal{L}_+$ in matrix representation, including counting fields (see Sec. 3.4), as

$$
\mathcal{L}_-(\chi) = \begin{pmatrix} -\Gamma n_B & \Gamma(n_B+1)e^{-i\chi} \\ \Gamma n_B e^{i\chi} & -\Gamma(n_B+1) \end{pmatrix}, \qquad \mathcal{L}_+(\chi) = \begin{pmatrix} -\Gamma(n_B+1) & \Gamma n_B e^{i\chi} \\ \Gamma(n_B+1)e^{-i\chi} & -\Gamma n_B \end{pmatrix}.
$$
(7.7)

We recover $\mathcal{L}_-$ and $\mathcal{L}_+$ in Eq. (7.6) by putting $\chi = 0$ in these matrices.

To find the system dynamics under feedback, we use the separation of timescales technique from Chapter 6, and find, by using Eqs. (6.63) and (6.64), the following counting field dependent feedback Liouvillian to leading order in γ^{-1},

$$
\mathcal{L}_0(\chi) = [(1-\eta)\mathcal{L}_-(\chi) + \eta\mathcal{L}_+]\mathcal{V}_{00,00} + [\eta\mathcal{L}_-(\chi) + (1-\eta)\mathcal{L}_+(\chi)]\mathcal{V}_{11,11} =
$$
$$
= \Gamma \begin{pmatrix} -(1-\eta)n_B - \eta(n_B+1) & (1-\eta)n_B e^{i\chi} + \eta(n_B+1)e^{-i\chi} \\ (1-\eta)n_B e^{i\chi} + \eta(n_B+1)e^{-i\chi} & -(1-\eta)n_B - \eta(n_B+1) \end{pmatrix}.
$$
(7.8)

Here we have introduced the feedback error probability

$$
\eta = \frac{1}{2}\left[1 - \mathrm{erf}\left(2\sqrt{\frac{\lambda}{\gamma}}\right)\right].
$$
(7.9)

The error probability is bounded by $0 \leq \eta \leq 1/2$, and depends solely on the ratio λ/γ, which directly determines the magnitude of the detector noise, see Chapter (6). For strong

measurements ($\lambda \gg \gamma$), the detector noise becomes infinitesimal and the error probability vanishes. This makes intuitive sense, for a detector with low noise, the feedback protocol will be applied correctly at all times. For a weak measurement ($\lambda \ll \gamma$), the measurement outcome fluctuates violently, and the error probability is maximized ($\eta = 1/2$). That is, for a noisy signal, it is difficult to distinguish the system state, and feedback is applied randomly. We thus see that Eq. (7.8) provides an effective description of the system dynamics under feedback, where each transition rate is weighted in a way corresponding to how probable it is to occur.

By counting the number of extracted and dissipated energy quanta n, we can evaluate the average power as $P = \partial_t \Delta \langle n \rangle$. Employing the techniques presented in Chapter 3.4, Eq. (7.8) provides the following cumulant generating function to leading order in γ^{-1},

$$C_t(\chi) = \lambda_0(\chi)t = \Gamma t \left[\left(e^{i\chi} - 1 \right) (1 - \eta)n_B + \left(e^{-i\chi} - 1 \right) \eta(n_B + 1) \right], \qquad (7.10)$$

where $\lambda_0(\chi)$ is the eigenvalue of $\mathcal{L}_0(\chi)$ which vanishes for $\chi = 0$. This cumulant generating function corresponds to a bidirectional Poisson process [124]. From Eq. (3.35), we find the average steady state power production to leading order,

$$P_0 = \Gamma\Delta \left[(1 - \eta)n_B - \eta(n_B + 1) \right], \qquad (7.11)$$

where the subscript '0' denotes that this is the power corresponding to the leading order separation of timescales Liouvillian in Eq. (7.8). Note that $P_0 > 0$ when extracting energy from the reservoir. When measuring strongly, the error probability vanishes ($\eta \to 0$), and the feedback is always applied as intended. In this limit, we reach the maximum power production $P_0 = \Gamma\Delta n_B$, which is limited by the rate Γ and the average occupation of the bath n_B. In the weak measurement regime ($\eta \to 1/2$), feedback is applied randomly, and as the excitation and de-excitation rates are asymmetric, energy is dissipated to the bath in this limit. The maximum dissipation rate is given by $P_0 = -\Gamma\Delta/2$. Equation (7.11) is plotted in Fig. 7.1(a) as the black, dashed line.

With Eqs. (3.37) and (7.10), we find the probability distribution $P_t(n)$, giving the probability to have n extracted energy quanta after time t. The distribution is visualized in Fig. 7.2 for various values of Γt and η. For $\eta = 0$, the probability distribution traverses in the direction of positive n, always being 0 for $n < 0$. That is, with no feedback errors, energy is only extracted. For $\eta \neq 0$, the distribution spreads over negative n as well, illustrating that feedback errors lead to dissipation. This effect is most pronounced for $\eta = 1/2$, where the average of the distribution becomes negative, as discussed below Eq. (7.11).

We may also calculate the second power cumulant to leading order in γ^{-1} as

$$\langle\langle P_0^2 \rangle\rangle = \Gamma\Delta^2 \left(\eta + n_B \right), \qquad (7.12)$$

where we used Eq. (3.35). This corresponds to the zero frequency noise of the power correlator as discussed in Chapter 3.4.

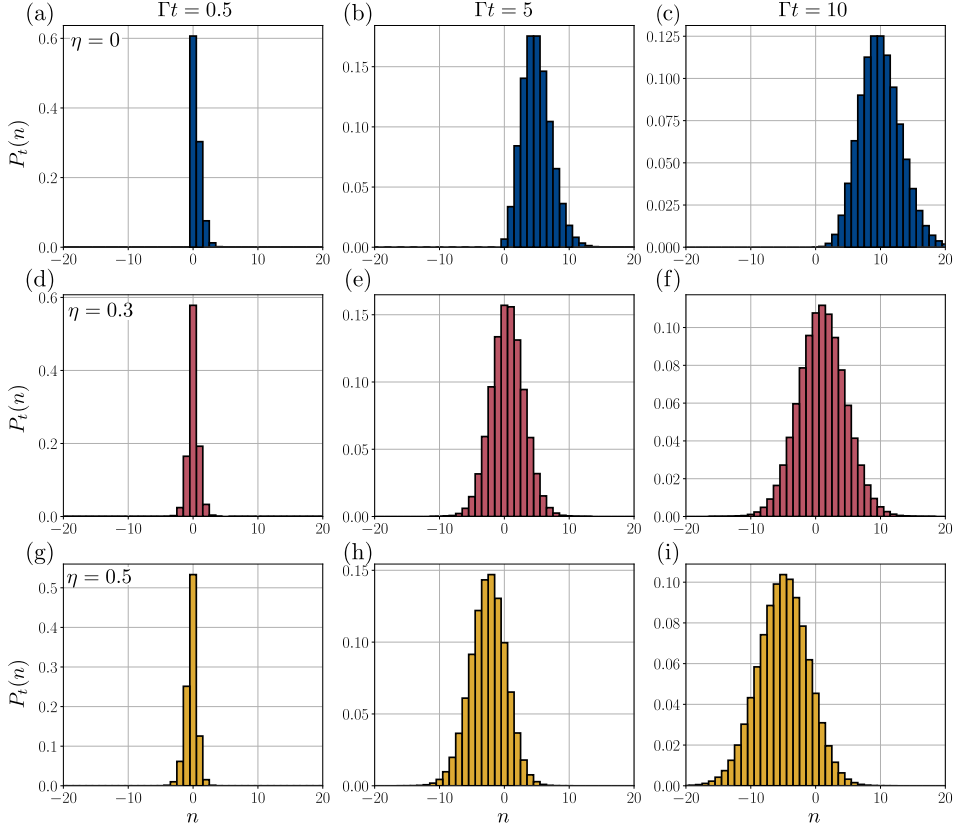**Figure 7.2:** Visualization of the distribution $P_t(n)$ of the number of extracted energy quanta n after time t in the classical toy model. Each column is evaluated at a specific value of Γt specified on the top of the figure. The rows are evaluated for different values of the error probability η. (a)-(c) $\eta = 0$. When no errors occur, the distribution is only non-zero for $n \geq 0$, and moves along the positive n-axis. (d)-(f) $\eta = 0.3$. The presence of feedback errors lead to dissipation of energy ($n < 0$). (g)-(i) $\eta = 0.5$. As the error probability is maximized, the distribution moves towards the negative n-axis as the asymmetry in excitation and de-excitation rates leads to dissipation. In these plots, we used $n_B = 1$.

For zero counting field, Eq. (7.8), can be written as

$$
\mathcal{L}_0 = \begin{pmatrix} -M_{10}^{(-)} - M_{10}^{(+)} & M_{01}^{(-)} + M_{01}^{(+)} \\ M_{10}^{(-)} + M_{10}^{(+)} & -M_{01}^{(-)} - M_{01}^{(+)} \end{pmatrix}. \tag{7.13}
$$

where $M_{ab}^{(\nu)}$ is the transition rate going from state b to a with level configuration $\nu = \pm$, with $(-)$ representing the configuration with $|0\rangle$ as ground state, and $(+)$ the configuration with $|1\rangle$ as ground state. The matrix elements read

$$
M_{01}^{(-)} = M_{10}^{(+)} = \eta\Gamma(n_B + 1), \qquad\qquad M_{10}^{(-)} = M_{01}^{(+)} = (1 - \eta)\Gamma n_B. \tag{7.14}
$$

We note that these rates satisfy the following modified local detailed balance relation,

$$\ln\left(\frac{M_{01}^{(\pm)}}{M_{10}^{(\pm)}}\right) = \mp\left[\frac{\Delta}{k_B T} - \ln\left(\frac{1-\eta}{\eta}\right)\right]. \tag{7.15}$$

The form of this relation is identical to Eq. (5.51), and the methods of Ref. [144] may be employed to derive a fluctuation theorem. The forward system trajectory can be defined as [similarly as in Eq. (5.10)]

$$X = (t_j, \nu_j, x_j)_{j=1}^n, \tag{7.16}$$

where the system makes the transition $x_{j-1} \to x_j$ at time t_j with level configuration ν_j. The time reversed trajectory X^{tr} can be defined similarly as in Eq. (5.28). As the average number of extracted energy quanta $\langle n \rangle$ grows linearly in time [see Eqs. (3.35) and (3.40)], the entropy change in the two-level system will be vanishingly small compared to the average steady state entropy production in the bath $\Delta s_{\mathrm{res}} = \langle n \rangle \Delta / T$. Therefore, we obtain the following detailed fluctuation theorem in the stationary limit,

$$\frac{P(X^{\mathrm{tr}})}{P(X)} = e^{N(X)\left[\frac{\Delta}{k_B T} - \ln\left(\frac{1-\eta}{\eta}\right)\right]}, \tag{7.17}$$

where $N(X)$ is the number of extracted energy quanta along trajectory X, Δ/T is the entropy change in the bath due to the exchange of a single energy quantum, and $\ln[(1-\eta)/\eta]$ is an information term due to the measurement and feedback process. This term is written on the form of the log odds of not making a feedback error, and corresponds to the difference in information content[1] between correctly and incorrectly applying feedback. Interestingly, most information obtained from the continuous measurement is discarded – it is only the information related to changes in $N(X)$ that plays an important role. In the error free limit, $\eta \to 0$, the information term diverges, and $P(X^{\mathrm{tr}})$ becomes vanishingly small compared to $P(X)$, illustrating absolute irreversibility. In this limit, all excitations are extracted. The fluctuation theorem may be rewritten on a more convenient form by introducing the probability $P(n) = \sum_{X:N(X)=n} P(X)$ of observing n extracted energy quanta. We now get

$$\frac{P(-n)}{P(n)} = e^{n\left[\frac{\Delta}{k_B T} - \ln\left(\frac{1-\eta}{\eta}\right)\right]}. \tag{7.18}$$

Note that $n > 0$ when extracting energy, and $n < 0$ when dissipating energy. This illustrates how the QFPME (1.1) may be used to highlight the connection between thermodynamics and information theory in conitnuously feedback controlled systems. Note that we can remove the 'tr' on the time reversed probability as the forward and backward experiments are identical, and as we consider the stationary limit where the distributions of the initial and final states can be neglected.

---

[1]The information content for a random event x is given by $I(x) = -\ln[p(x)]$, where $p(x)$ is the probability of observing x.

As the final part of this section, we study the first order correction to Eq. (7.8). Using Eqs. (6.67), (6.70) and (6.71), we find the counting field dependent correction

$$
\frac{\mathcal{L}_{\text{corr}}(\chi)}{\Gamma^2} = C_1 1 - \left[n_B e^{i\chi} - (n_B + 1)e^{-i\chi} \right] \left\{ n_B e^{i\chi}[C_2 + (1-\eta)C_0] - (n_B + 1)e^{-i\chi}[C_2 - \eta C_0] \right\} I
$$
$$
+ C_1 \left[n_B e^{i\chi} - (n_B + 1)e^{-i\chi} \right] \sigma_x - \left\{ n_B e^{i\chi}[C_2 + (1-\eta)C_0] - (n_B + 1)e^{-i\chi}[C_2 - \eta C_0] \right\} \sigma_x,
$$
$$(7.19)$$

where I is the two dimensional identity matrix, and σ_x is the Pauli-X matrix. The coefficients C_0, C_1, and C_2 are defined as

$$
C_0 = \frac{1}{2} \int_0^1 dy \frac{\text{erf}(2\sqrt{\alpha}) - \text{erf}[2\sqrt{\alpha}(1-2y)]}{y}, \qquad (7.20)
$$

$$
C_1 = \frac{\eta}{2} \int_0^1 dy \frac{\text{erf}(2\sqrt{\alpha}) - \text{erf}[2\sqrt{\alpha}(1-y)]}{y}
$$
$$
+ \frac{1}{2\pi} \int_0^1 dy \int_0^1 dz \left\{ \frac{e^{-4\alpha\left[1 + \frac{(1-y)^2}{1-y^2 z^2}\right]}}{\sqrt{1 - y^2 z^2}} - \sqrt{4\pi\alpha}\, e^{-4\alpha[1-y+yz]^2} \right. \qquad (7.21)
$$
$$
\left. \times \left[1 + \text{erf}\left(2\sqrt{\alpha} \frac{yz(1-y) + y^2 z^2 - 1}{\sqrt{1 - y^2 z^2}} \right) \right] \right\},
$$

$$
C_2 = \frac{\eta}{2} \int_0^1 dy \frac{\text{erf}[2\sqrt{\alpha}(1-y)] - \text{erf}[2\sqrt{\alpha}(1-2y)]}{y}
$$
$$
+ \frac{1}{2\pi} \int_0^1 dy \int_0^1 dz \left\{ \frac{e^{-4\alpha\left[1 + \frac{(1-y)^2}{1-y^2 z^2}\right]}}{\sqrt{1 - y^2 z^2}} - \sqrt{4\pi\alpha}\, e^{-4\alpha[1-y-yz]^2} \right. \qquad (7.22)
$$
$$
\left. \times \left[1 - \text{erf}\left(2\sqrt{\alpha} \frac{yz(1-y) - y^2 z^2 + 1}{\sqrt{1 - y^2 z^2}} \right) \right] \right\},
$$

where $\alpha = \lambda/\gamma$. At zero counting field, we get, to first order in γ^{-1}, the total feedback Liouvillian

$$
\mathcal{L}_{\text{fb}} = \mathcal{L}_0 + \gamma^{-1}\mathcal{L}_{\text{corr}} = \left\{ \Gamma \left[(1-\eta)n_B + \eta(n_B + 1) \right] \right.
$$
$$
\left. - \frac{\Gamma^2}{\gamma} \left[C_0(n_B + \eta) + C_1 - C_2 \right] \right\} \begin{pmatrix} -1 & 1 \\ 1 & -1 \end{pmatrix}. \qquad (7.23)
$$

Because of the symmetry of this matrix, the stationary system state is given by $\hat{\rho}_{\text{ss}} = 1/2$, with 1 being the identity matrix in two dimensions. With full counting statistics, we find the following correction to the average power production,

$$
P_{\text{corr}} = -i\Delta \,\text{tr}\{\mathcal{L}'_{\text{corr}}(\chi)|_{\chi=0}\hat{\rho}_{\text{ss}}\} = -\Gamma^2(2n_B + 1)[(n_B + \eta)C_0 - C_1 - C_2], \quad (7.24)
$$

where the prime denotes the derivative with respect to χ. The average power production to first order in γ^{-1} now reads

$$P = \Gamma\Delta\left[(1-\eta)n_B - \eta(n_B+1)\right] - \frac{\Gamma^2}{\gamma}(2n_B+1)\left[(n_B+\eta)C_0 - C_1 - C_2\right]. \quad (7.25)$$

This equation is plotted in Fig. 7.1(a) as colored, dashed lines. The solid lines in Fig. 7.1(a) were calculated numerically with Eq. (7.4) by solving the full QFPME (1.1) according to the method outlined in Appendix D, without any restrictions on the timescales. When the detector timescale is larger than the system timescale, there is a good agreement between Eq. (7.25) and the numerical solution. However, as the timescales become similar in size, the separation of timescales approximation breaks down [see blue lines in Fig. 7.1(a)]. We further note that the maximal extracted power decreases with the ratio γ/Γ. When the detector and system timescales become similar in size, the detector cannot resolve all excitation events in the system, missing opportunities to extract energy.

7.3 Quantum toy model

The quantum toy model is depicted in the inset of Fig. 7.1(b). It consists of a coherently driven qubit with energy splitting Δ. Similar to the classical toy model, we continuously measure $\hat{\sigma}_z = |1\rangle\langle 1| - |0\rangle\langle 0|$. Again, we assume that $D < 0$ when the system resides in $|0\rangle$, and $D \geq 0$ when the system resides in $|1\rangle$. Feedback is applied by flipping the levels [solid arrows in Fig. 7.1(b)] when an excitation [dashed arrow in Fig. 7.1(b)] is detected. Energy can thus be extracted from the driving field. This feedback protocol is represented by the Liouville superoperator $\mathcal{L}_t(D)\hat{\rho} = -i[\hat{H}_t(D), \hat{\rho}]$, where the Hamiltonian is given by

$$\hat{H}_t(D) = [1 - \theta(D)]\Delta\,|1\rangle\langle 1| + \theta(D)\Delta\,|0\rangle\langle 0| + g\cos(\Delta t)\hat{\sigma}_x, \quad (7.26)$$

where g is the strength of the drive, and $\hat{\sigma}_x$ is the Pauli-X operator.

With the separation of timescales technique (Chapter 6), Eqs. (6.63) and (6.64) provide the leading order system dynamics

$$\mathcal{L}_0\hat{\rho} = -ig\cos(\Delta t)[\hat{\sigma}_x, \hat{\rho}]. \quad (7.27)$$

We can further find the first order correction with Eqs. (6.67)-(6.71),

$$\mathcal{L}_{\text{corr}}\hat{\rho} = \frac{\Delta^2 \ln(2)}{2}\mathcal{D}[\hat{\sigma}_z]\hat{\rho} - 2\Delta g D_0 \cos(\Delta t)\hat{\sigma}_x, \quad (7.28)$$

where $D_0 = \sqrt{4\lambda/\pi}\gamma_2 F_2(1/2, 1/2; 3/2, 3/2; -4\lambda/\gamma)$, with $_2F_2(\cdot)$ being a generalized hypergeometric function. Note that the first term adds additional dephasing to the system

beyond the backaction due to the continuous measurement. The second term is a source for quantum coherence. Without this source term, the stationary state of the system is given by the maximally mixed state. Note that the source term can give rise to negative eigenvalues in the density matrix. This should not be an issue in the separation of timescales regime, where this term scales as $1/\gamma$. To first order in γ^{-1}, the system evolves according to

$$
\begin{aligned}
\mathcal{L}_{\mathrm{fb}}\hat{\rho} &= \left(\mathcal{L}_0 + \lambda\mathcal{D}[\hat{\sigma}_z] + \gamma^{-1}\mathcal{L}_{\mathrm{corr}}\right)\hat{\rho}_t \\
&= -ig\cos(\Delta t)[\hat{\sigma}_x, \hat{\rho}_t]\hat{\rho}_t + \tilde{\lambda}\mathcal{D}[\hat{\sigma}_z] - \frac{2\Delta g}{\gamma}D_0\cos(\Delta t)\hat{\sigma}_x,
\end{aligned} \tag{7.29}
$$

where we get the effective dephasing rate $\tilde{\lambda} = \lambda + \Delta^2\ln(2)/2\gamma$.

Because of the periodic driving, the system tends to a periodic stationary state. To this end, we use the following ansatz to solve the equation of motion,

$$
\hat{\rho}_t = \hat{\rho}^{(0)} + \hat{\rho}^{(s)}\sin(\Delta t) + \hat{\rho}^{(c)}\cos(\Delta t), \tag{7.30}
$$

where $\hat{\rho}^{(0)}$, $\hat{\rho}^{(s)}$, and $\hat{\rho}^{(c)}$ are coefficient operators. To avoid higher order harmonics in the solution, we require that $0 = [\hat{\sigma}_x, \hat{\rho}^{(s)}] = [\hat{\sigma}_x, \hat{\rho}^{(c)}]$. With these assumptions, we find the periodic steady state

$$
\hat{\rho}_t = \frac{1}{2} - \frac{2\Delta g}{\gamma}D_0\frac{2\tilde{\lambda}\cos(\Delta t) + \Delta\sin(\Delta t)}{\Delta^2 + 4\tilde{\lambda}^2}\hat{\sigma}_x. \tag{7.31}
$$

To leading order, i.e., in the limit $\gamma \to \infty$, this becomes the maximally mixed state as discussed above.

The power in the system is defined as

$$
P(t) = \int_{-\infty}^{\infty} dD\,\mathrm{tr}\{\partial_t H_t(D)\hat{\rho}_t(D)\}. \tag{7.32}
$$

Since $\partial_t\hat{H}_t(D) = -\Delta g\sin(\Delta t)\hat{\sigma}_x$, the stationary power can be calculated with Eq. (7.31),

$$
P(t) = \frac{4g^2\Delta^2}{\gamma}D_0\sin(\Delta t)\frac{2\tilde{\lambda}\cos(\Delta t) + \Delta\sin(\Delta t)}{\Delta^2 + 4\tilde{\lambda}^2}. \tag{7.33}
$$

Averaging this power over one driving period $\tau = 2\pi/\Delta$, we get

$$
\bar{P} = \frac{1}{\tau}\int_0^{\tau} dt\,P(t) = \frac{2g^2\Delta}{\gamma}D_0\frac{\Delta^2}{\Delta^2 + 4\tilde{\lambda}^2}. \tag{7.34}
$$

This equation is plotted in Fig. 7.1(b) as dashed lines. For strong measurements ($\lambda \gg \gamma$), the power goes to zero due to the quantum Zeno effect, see discussion in Chapter 4. For weak measurements ($\lambda \ll \gamma$), the feedback is applied randomly (see discussion in Sec. 7.2),

and due to the symmetric driving, no power can be extracted on average. To go beyond the separation of timescales approximation, we also calculated the power numerically under weak driving, i.e., we assume $g \ll \Delta$ – see the solid lines in Fig. 7.1(b). As for the classical model, we find that the separation of timescales approximation breaks down as γ becomes similar in size to the other system parameters.

Finally, we briefly outline how the power was calculated numerically by solving the full QFPME (1.1). As the system tends to a periodic stationary state, we can expand the system-detector density matrix as a Fourier series,

$$\hat{\rho}_t(D) = \sum_{q=-\infty}^{\infty} \hat{\rho}_q(D) e^{iq\Delta t}, \qquad (7.35)$$

where the expansion coefficients can be calculated via

$$\hat{\rho}_q(D) = \frac{1}{\tau} \int_0^\tau dt \hat{\rho}_t(D) e^{-iq\Delta t}. \qquad (7.36)$$

Inserting this in the QFPME (1.1) yields

$$0 = \left[\tilde{\mathcal{L}}(D) - iq\Delta \right] \hat{\rho}_q(D) + \hat{\mathcal{L}} \left[\hat{\rho}_{q-1}(D) + \hat{\rho}_{q+1}(D) \right], \qquad (7.37)$$

with

$$\tilde{\mathcal{L}}(D)\hat{\rho} = -i[\hat{h}(D), \hat{\rho}] + \lambda \mathcal{D}[\hat{\sigma}_z]\hat{\rho} - \gamma \partial_D \mathcal{A}(D)\hat{\rho} + \frac{\gamma^2}{8\lambda} \partial_D^2 \hat{\rho},$$

$$\hat{\mathcal{L}}\hat{\rho} = -\frac{ig}{2}[\hat{\sigma}_x, \hat{\rho}], \qquad (7.38)$$

where $\hat{h}(D) = [1 - \theta(D)]\Delta |1\rangle\langle 1| + \theta(D)\Delta |0\rangle\langle 0|$. To simplify calculations, we concentrate on the weak driving regime where $g \ll \Delta$. Under this assumption, we expand the expansion coefficients to first order in g/Δ as $\hat{\rho}_q(D) \approx \hat{\rho}_q^{(0)}(D) + \frac{g}{\Delta}\hat{\rho}_q^{(1)}(D)$. Together with Eq. (7.37), we get the following set of equations,

$$0 = [\Delta^{-1}\tilde{\mathcal{L}}(D) - iq]\hat{\rho}_q^{(0)}(D), \qquad (7.39a)$$

$$0 = [\Delta^{-1}\tilde{\mathcal{L}}(D) - iq]\hat{\rho}_q^{(1)}(D) + g^{-1}\hat{\mathcal{L}}[\hat{\rho}_{q-1}^{(0)}(D) + \hat{\rho}_{q+1}^{(0)}(D)]. \qquad (7.39b)$$

Equation (7.39a) yields complex solutions for the diagonal density matrix elements for $q \neq 0$. Therefore, these solutions must be neglected, and we can solely focus on the case $q = 0$. To zeroth order we get

$$\hat{\rho}_{q=0}^{(0)}(D) = \frac{1}{2}\sqrt{\frac{4\lambda}{\pi\gamma}} \left[e^{-\frac{4\lambda}{\gamma}(D+1)^2} |0\rangle\langle 0| + e^{-\frac{4\lambda}{\gamma}(D-1)^2} |1\rangle\langle 1| \right]. \qquad (7.40)$$

To find the first order solution $\hat{\rho}_q^{(1)}(D)$, we solve Eq. (7.39b) for $q = \pm 1$ with the numerical method outlined in Appendix D. With Eq. (7.32), we find the system power. The time averaged power is visualized as solid lines in Fig. 7.1(b). In Fig. 7.1(c), we plot the numerically calculated density matrix elements for $t = \tau = 2\pi/\Delta$.

Chapter 8

Summary and outlook

In this thesis, we derived and discussed the quantum Fokker-Planck master equation in Eq. (1.1). This equation describes the joint system-detector dynamics of a continuously feedback controlled quantum system. The novelty of this equation lies in its ability to describe feedback protocols that depend linearly as well as nonlinearly on the measured signal. Two derivations of this result were provided. One based on conventional calculus, and one based on stochastic calculus. We showed how the quantum Fokker-Planck master equation can be reduced to a Markovian master equation describing the system dynamics alone. In particular, we noted that this master equation generalizes the Wiseman-Milburn equation to nonlinear feedback protocols. To illustrate the usefulness of the developed formalism, two information engines based on nonlinear feedback were studied. First, we discussed a classical model where continuous measurement and feedback was used to extract energy from a heat bath. In particular, we derived a fluctuation theorem that provides insight into the thermodynamics of information. Second, we studied a quantum model, where we demonstrated that energy can be extracted from an external driving field, while simultaneously stabilizing quantum coherence in the long time limit.

With the classical model, we demonstrated that the quantum Fokker-Planck master equation can provide insights into the connection between thermodynamics and information theory. Building on this, future studies of the derived formalism could investigate the thermodynamics of continuous measurements and feedback. This could provide insights about the energetic costs of performing a continuous measurement. In addition, exploring the possibility of deriving general, system independent fluctuation theorems for the joint system-detector description could lead to an increased understanding of the thermodynamics of continuous information processing. Of fundamental interest is also to extend these fluctuation theorems to the quantum realm.

A number of possible extensions of the formalism are of interest. First, by including the description of multiple simultaneous measurements of different observables, the formalism could be used to describe more complex feedback protocols. Additionally, if these observables are non-commuting, the formalism could shine light on the fundamental limits of feedback control in quantum systems. Second, as the quantum Fokker-Planck equation is restricted to Markovian systems, it is of interest to extend it to include the description of non-Markovian dynamics. Another interesting extension would be to include state-estimation feedback [55, 153] and delays in the application of feedback.

In Chapter 4, we noted that linear feedback has been used to improve entanglement production in systems where entanglement can be generated autonumously. Inspired by this, future studies should investigate the possibility to improve the entanglement production with nonlinear feedback. The quantum Fokker-Planck master equation is a promising tool for deriving analytical results in this direction. A concrete candidate for investigating this is the system discussed in Ref. [154], where a quantum heat engine is used to produce entanglement in the long time limit.

References

[1] K. J. Åström and R. M. Murray. *Feedback systems - An Introduction for Scientists and Engineers*. Princton University Press, 2008.

[2] M. A. Nielsen and I. L. Chuang. *Quantum information and quantum computation*. Cambridge University Press, 2010.

[3] D. Risté, M. Dukalski, C. A. Watson, G. De Lange, M. J. Tiggelman, Y. M. Blanter, K. W. Lehnert, R. N. Schouten, and L. DiCarlo. Deterministic entanglement of superconducting qubits by parity measurement and feedback. *Nature*, 502(7471):350–354, 2013.

[4] W. P. Smith, J. E. Reiner, L. A. Orozco, S. Kuhr, and H. M. Wiseman. Capture and release of a conditional state of a cavity QED system by quantum feedback. *Phys. Rev. Lett.*, 89:133601, Sep 2002.

[5] C. Sayrin, I. Dotsenko, X. Zhou, B. Peaudecerf, T. Rybarczyk, S. Gleyzes, P. Rouchon, M. Mirrahimi, H. Amini, M. Brune, J.-M. Raimond, and S. Haroche. Real-time quantum feedback prepares and stabilizes photon number states. *Nature*, 477(7362):73–77, 2011.

[6] R. Vijay, C. Macklin, D. H. Slichter, S. J. Weber, K. W. Murch, R. Naik, A. N. Korotkov, and I. Siddiqi. Stabilizing Rabi oscillations in a superconducting qubit using quantum feedback. *Nature*, 490(7418):77–80, 2012.

[7] Z. K. Minev, S. O. Mundhada, S. Shankar, P. Reinhold, R. Gutiérrez-Jáuregui, R. J. Schoelkopf, M. Mirrahimi, H. J. Carmichael, and M. H. Devoret. To catch and reverse a quantum jump mid-flight. *Nature*, 570:200–204, 2019.

[8] S. Vinjanampathy and J. Anders. Quantum thermodynamics. *Contemp. Phys.*, 57(4):545–579, 2016.

[9] J. C. Maxwell. *Theory of heat*. Longmans, Green, and Co., 1871.

[10] H. S. Leff and A. F. Rex, editors. *Maxwell's Demon 2 Entropy, Classical and Quantum Information, Computing*. CRC Press, Boca Raton, 2002.

[11] K. Maruyama, F. Nori, and V. Vedral. Colloquium: The physics of Maxwell's demon and information. *Rev. Mod. Phys.*, 81:1, 2009.

[12] T. Sagawa and M. Ueda. Second law of thermodynamics with discrete quantum feedback control. *Phys. Rev. Lett.*, 100:080403, 2008.

[13] T. Sagawa and M. Ueda. Generalized Jarzynski equality under nonequilibrium feedback control. *Phys. Rev. Lett.*, 104:090602, 2010.

[14] M. Ponmurugan. Generalized detailed fluctuation theorem under nonequilibrium feedback control. *Phys. Rev. E*, 82:031129, 2010.

[15] J. M. Horowitz and S. Vaikuntanathan. Nonequilibrium detailed fluctuation theorem for repeated discrete feedback. *Phys. Rev. E*, 82:061120, Dec 2010.

[16] Y. Morikuni and H. Tasaki. Quantum Jarzynski-Sagawa-Ueda relations. *J. Stat. Phys.*, 143(1):1–10, 2011.

[17] T. Sagawa and M. Ueda. Fluctuation theorem with information exchange: Role of correlations in stochastic thermodynamics. *Phys. Rev. Lett.*, 109:180602, 2012.

[18] T. Sagawa and M. Ueda. Nonequilibrium thermodynamics of feedback control. *Phys. Rev. E*, 85:021104, 2012.

[19] D. Abreu and U. Seifert. Thermodynamics of genuine nonequilibrium states under feedback control. *Phys. Rev. Lett.*, 108:030601, 2012.

[20] K. Funo, Y. Watanabe, and M. Ueda. Integral quantum fluctuation theorems under measurement and feedback control. *Phys. Rev. E*, 88:052121, Nov 2013.

[21] C. W. Wächtler, P. Strasberg, and T. Brandes. Stochastic thermodynamics based on incomplete information: generalized Jarzynski equality with measurement errors with or without feedback. *New J. Phys.*, 18(11):113042, 2016.

[22] P. P. Potts and P. Samuelsson. Detailed fluctuation relation for arbitrary measurement and feedback schemes. *Phys. Rev. Lett.*, 121:210603, 2018.

[23] T. Sagawa. Thermodynamics of information processing in small systems. *Prog. Theor. Phys.*, 127:1, 2012.

[24] J. M. R. Parrondo, J. M. Horowitz, and T. Sagawa. Thermodynamics of information. *Nat. Phys.*, 11:131, 2015.

[25] J. Goold, M. Huber, A. Riera, L. del Rio, and P. Skrzypczyk. The role of quantum information in thermodynamics—a topical review. *J. Phys. A*, 49(14):143001, feb 2016.

[26] V. Serreli, C. F. Lee, E. R. Kay, and D. A. Leigh. A molecular information ratchet. *Nature*, 445:523, 2007.

[27] S. Toyabe, T. Sagawa, M. Ueda, E. Muneyuki, and M. Sano. Experimental demonstration of information-to-energy conversion and validation of the generalized Jarzynski equality. *Nat. Phys.*, 6:988, 2010.

[28] J. V. Koski, V. F. Maisi, J. P. Pekola, and D. V. Averin. Experimental realization of a Szilard engine with a single electron. *Proc. Natl. Acad. Sci. U.S.A.*, 111:13786, 2014.

[29] J. V. Koski, V. F. Maisi, T. Sagawa, and J. P. Pekola. Experimental observation of the role of mutual information in the nonequilibrium dynamics of a Maxwell demon. *Phys. Rev. Lett.*, 113:030601, 2014.

[30] K. Chida, S. Desai, K. Nishiguchi, and A. Fujiwara. Power generator driven by Maxwell's demon. *Nat. Commun.*, 8:15310, 2017.

[31] A. Kumar, T.-Y. Wu, F. Giraldo, and D. S. Weiss. Sorting ultracold atoms in a three-dimensional optical lattice in a realization of Maxwell's demon. *Nature*, 561:83, 2018.

[32] D. Barker, M. Scandi, S. Lehmann, C. Thelander, K. A. Dick, M. Perarnau-Llobet, and V. F. Maisi. Experimental verification of the work fluctuation-dissipation relation for information-to-work conversion. *Phys. Rev. Lett.*, 128:040602, Jan 2022.

[33] M. Ribezzi-Crivellari and F. Ritort. Large work extraction and the Landauer limit in a continuous Maxwell demon. *Nat. Phys.*, 15:660, 2019.

[34] M. D. Vidrighin, O. Dahlsten, M. Barbieri, M. S. Kim, V. Vedral, and I. A. Walmsley. Photonic Maxwell's demon. *Phys. Rev. Lett.*, 116:050401, 2016.

[35] N. Cottet, S. Jezouin, L. Bretheau, P. Campagne-Ibarcq, Q. Ficheux, J. Anders, A. Auffèves, R. Azouit, P. Rouchon, and B. Huard. Observing a quantum Maxwell demon at work. *Proc. Natl. Acad. Sci. U.S.A.*, 114:7561, 2017.

[36] Y. Masuyama, K. Funo, Y. Murashita, A. Noguchi, S. Kono, Y. Tabuchi, R. Yamazaki, M. Ueda, and Y. Nakamura. Information-to-work conversion by Maxwell's demon in a superconducting circuit quantum electrodynamical system. *Nat. Commun.*, 9:1291, 2018.

[37] M. Naghiloo, J. J. Alonso, A. Romito, E. Lutz, and K. W. Murch. Information gain and loss for a quantum Maxwell's demon. *Phys. Rev. Lett.*, 121:030604, 2018.

[38] J. P. Pekola. Towards quantum thermodynamics in electronic circuits. *Nat. Phys.*, 11:118, 2015.

[39] W. G. van der Wiel, S. De Franceschi, J. M. Elzerman, T. Fujisawa, S. Tarucha, and L. P. Kouwenhoven. Electron transport through double quantum dots. *Rev. Mod. Phys.*, 75:1–22, Dec 2002.

[40] M. Kjaergaard, M. E. Schwartz, J. Braumüller, P. Krantz, J. I.-J. Wang, S. Gustavsson, and W. D. Oliver. Superconducting qubits: Current state of play. *Annu. Rev. Condens. Matter Phys.*, 11:369–395, 2020.

[41] C. Fasth, A. Fuhrer, M. T. Björk, and L. Samuelson. Tunable double quantum dots in InAs nanowires defined by local gate electrodes. *Nano Letters*, 5(7):1487–1490, 2005.

[42] K. W. Murch, R. Vijay, and I. Siddiqi. *Weak Measurement and Feedback in Superconducting Quantum Circuits*, pages 163–185. Springer International Publishing, Cham, 2016.

[43] D. Barker, S. Lehmann, L. Namazi, M. Nilsson, C. Thelander, K. A. Dick, and V. F. Maisi. Individually addressable double quantum dots formed with nanowire polytypes and identified by epitaxial markers. *Appl. Phys. Lett.*, 114, 2019.

[44] B. Küng, C. Rössler, M. Beck, M. Marthaler, D. S. Golubev, Y. Utsumi, T. Ihn, and K. Ensslin. Irreversibility on the level of single-electron tunneling. *Phys. Rev. X*, 2:011001, 2012.

[45] A. Hofmann, V. F. Maisi, J. Basset, C. Reichl, W. Wegscheider, T. Ihn, K. Ensslin, and C. Jarzynski. Heat dissipation and fluctuations in a driven quantum dot. *Phys. Status Solidi B*, 254(3):1600546, 2017.

[46] D. Ristè, C. C. Bultink, K. W. Lehnert, and L. DiCarlo. Feedback control of a solid-state qubit using high-fidelity projective measurement. *Phys. Rev. Lett.*, 109:240502, Dec 2012.

[47] P. Campagne-Ibarcq, E. Flurin, N. Roch, D. Darson, P. Morfin, M. Mirrahimi, M. H. Devoret, F. Mallet, and B. Huard. Persistent control of a superconducting qubit by stroboscopic measurement feedback. *Phys. Rev. X*, 3:021008, May 2013.

[48] V. P. Belavkin. On the theory of controlling observable quantum systems. *Autom. Remote Control*, 44(2):178–188, 1983.

[49] V. P. Belavkin. Non-demolition measurement and control in quantum dynamical systems. In A. Blaquiere, S. Diner, and G. Lochak, editors, *Information Complexity and Control in Quantum Physics*, pages 311–329, Vienna, 1987. Springer Vienna.

[50] V. P. Belavkin. Quantum stochastic calculus and quantum nonlinear filtering. *J. Multivar. Anal.*, 42(2):171–201, 1992.

[51] V. P. Belavkin. Quantum continual measurements and a posteriori collapse on CCR. *Commun. Math. Phys.*, 146(3):611–635, 1992.

[52] H. M. Wiseman and G. J. Milburn. Quantum theory of optical feedback via homodyne detection. *Phys. Rev. Lett.*, 70:548–551, Feb 1993.

[53] H. M. Wiseman. Quantum theory of continuous feedback. *Phys. Rev. A*, 49:2133–2150, Mar 1994.

[54] M. Yanagisawa and H. Kimura. A control problem for Gaussian states. In *Learning, control and hybrid systems*, pages 294–313. Springer, 1999.

[55] A. C. Doherty and K. Jacobs. Feedback control of quantum systems using continuous state estimation. *Phys. Rev. A*, 60:2700–2711, Oct 1999.

[56] A. N. Korotkov. Selective quantum evolution of a qubit state due to continuous measurement. *Phys. Rev. B*, 63:115403, Feb 2001.

[57] H. M. Wiseman and G. J. Milburn. *Quantum measurement and control.* Cambridge Univeristy Press, 2010.

[58] K. Jacobs. *Quantum measurement theory and its applications.* Cambridge University Press, 2014.

[59] J. Zhang, Y.-X. Liu, R.-B. Wu, K. Jacobs, and F. Nori. Quantum feedback: Theory, experiments, and applications. *Phys. Rep.*, 679:1–60, 2017.

[60] D. E. Kirk. *Optimal control theory - an introduction.* Dover Publications, Inc., 2004.

[61] V. Cavina, A. Mari, A. Carlini, and V. Giovannetti. Optimal thermodynamic control in open quantum systems. *Phys. Rev. A*, 98:012139, Jul 2018.

[62] P. Warszawski and H. M. Wiseman. Quantum trajectories for realistic photodetection: I. General formalism. *J. Opt. B: Quantum and Semiclassical Optics*, 5(1):1–14, nov 2002.

[63] P. Warszawski and H. M. Wiseman. Quantum trajectories for realistic photodetection: II. Application and analysis. *J. Opt. B: Quantum and Semiclassical Optics*, 5(1):15–28, nov 2002.

[64] K. Jacobs. *Stochastic processes for physicists - understanding noisy nystems.* Cambridge University Press, 2010.

[65] J. B. Johnson. Thermal agitation of electricity in conductors. *Phys. Rev.*, 32:97–109, Jul 1928.

[66] H. Nyquist. Thermal agitation of electric charge in conductors. *Phys. Rev.*, 32:110–113, Jul 1928.

[67] Y. M. Blanter and M. Büttiker. Shot noise in mesoscopic conductors. *Phys. Rep.*, 336:1, 2000.

[68] H.P. Breuer and F. Petruccione. *The theory of open quantum systems*. Oxford Univeristy Press, 2002.

[69] C. W. Gardiner. *Handbook of stochastic methods*. Springer Berlin, 1985.

[70] O. Vasicek. An equilibrium characterization of the term structure. *J. Financ. Econ.*, 5(2):177–188, 1977.

[71] G. Grynberg, A. Aspect, and C. Fabre. *Introfuction to quantum optics - From a semiclassical approach to quantized light*. Cambridge University Press, 2010.

[72] Daniel F Walls and Gerard J Milburn. *Quantum optics*. Springer Science & Business Media, 2007.

[73] A. Rivas and S. F. Huelga. *Open quantum systems - an introduction*. Springer, 2012.

[74] G. Lindblad. On the generators of quantum dynamical semigroups. *Commun. Math. Phys.*, 48:119–130, 1976.

[75] V. Gorini, A. Kossakowski, and E. C. G. Sudarshan. Completely positive dynamical semigroups of N⊠level systems. *J. Math. Phys.*, 17:821, 1976.

[76] L. S. Levitov, H. Lee, and G. B. Lesovik. Electron counting statistics and coherent states of electric current. *J. Math. Phys.*, 37:4845, 1996.

[77] D. A. Bagrets and Yu. V. Nazarov. Full counting statistics of charge transfer in coulomb blockade systems. *Phys. Rev. B*, 67:085316, Feb 2003.

[78] G. Schaller. *Open quantum systems far from equilibrium*, volume 881. Springer, 2014.

[79] C. Matthiesen, M. J. Stanley, M. Hugues, E. Clarke, and M. Atatüre. Full counting statistics of quantum dot resonance fluorescence. *Sci. Rep.*, 4, 2014.

[80] J. D. Cohen, S. M. Meenehan, G. S. MacCabe, S. Gröblacher, A. H. Safavi-Naeini, F. Marsili, M. D. Shaw, and O Painter. Phonon counting and intensity interferometry of a nanomechanical resonator. *Nature*, 520:522–525, 2015.

[81] S. Gustavsson, R. Leturcq, B. Simovič, R. Schleser, T. Ihn, P. Studerus, K. Ensslin, D. C. Driscoll, and A. C. Gossard. Counting statistics of single electron transport in a quantum dot. *Phys. Rev. Lett.*, 96:076605, 2006.

[82] T. Fujisawa, T. Hayashi, R. Tomita, and Y. Hirayama. Bidirectional counting of single electrons. *Science*, 312:1634, 2006.

[83] C. Fricke, F. Hohls, W. Wegscheider, and R. J. Haug. Bimodal counting statistics in single-electron tunneling through a quantum dot. *Phys. Rev. B*, 76:155307, Oct 2007.

[84] C. Flindt, C. Fricke, F. Hohls, T. Novotny, K. Netočný, T. Brandes, and R. J. Haug. Universal oscillations in counting statistics. *Proc. Natl. Acad. Sci. U.S.A.*, 106(25):10116–10119, 2009.

[85] N. Ubbelohde, C. Fricke, C. Flindt, F. Hohls, and R. J. Haug. Measurement of finite-frequency current statistics in a single-electron transistor. *Nat. Commun.*, 3, 2012.

[86] Y. V. Nazarov. *Quantum noise in mesoscopic physics*, volume 97. Springer Science & Business Media, 2003.

[87] Y.V. Nazarov and M. Kindermann. Full counting statistics of a general quantum mechanical variable. *Eur. Phys. J. B*, 35:413–420, 2003.

[88] A. Gut. *An Intermediate Course in Probability*. Springer, 2009.

[89] H. E. Daniels. Saddlepoint approximations in statistics. *Ann. Math. Stat.*, 25(4):631–650, 1954.

[90] H. Touchette. The large deviation approach to statistical mechanics. *Phys. Rep.*, 478(1):1–69, 2009.

[91] F. Brange, P. Menczel, and C. Flindt. Photon counting statistics of a microwave cavity. *Phys. Rev. B*, 99:085418, Feb 2019.

[92] A. Hofmann, V.F. Maisi, J. Basset, C. Reichl, W. Wegscheider, T. Ihn, K. Ensslin, and C. Jarzynski. Heat dissipation and fluctuations in a driven quantum dot. *Phys. Status Solidi B*, 254:1600546, 2017.

[93] J. M. Elzerman, R. Hanson, L. H. Willems van Beveren, B. Witkamp, L. M. K. Vandersypen, and L. P. Kouwenhoven. Single-shot read-out of an individual electron spin in a quantum dot. *Nature*, 430:431–435, 2004.

[94] L. Rippe, B. Julsgaard, A. Walther, Yan Ying, and S. Kröll. Experimental quantum-state tomography of a solid-state qubit. *Phys. Rev. A*, 77:022307, Feb 2008.

[95] M. Sarovar, C. Ahn, K. Jacobs, and G. J. Milburn. Practical scheme for error control using feedback. *Phys. Rev. A*, 69:052324, May 2004.

[96] K. Jacobs and D. A. Steck. A straightforward introduction to continuous quantum measurement. *Contemp. Phys.*, 47(5):279–303, 2006.

[97] A. Bednorz, W. Belzig, and A. Nitzan. Nonclassical time correlation functions in continuous quantum measurement. *New J. Phys.*, 14, 2012.

[98] B. Misra and E. C. G. Sudarshan. The zeno's paradox in quantum theory. *J. Math. Phys.*, 18:756–763, Dec 1977.

[99] M. B. Mensky. *Quantum measurements and decoherence - models and phenomenology*. Springer Science & Business Media, 2000.

[100] M. Sarovar, H.-S. Goan, T. P. Spiller, and G. J. Milburn. High-fidelity measurement and quantum feedback control in circuit QED. *Phys. Rev. A*, 72:062327, Dec 2005.

[101] Z. Liu, L. Kuang, K. Hu, L. Xu, S. Wei, L. Guo, and X.-Q. Li. Deterministic creation and stabilization of entanglement in circuit QED by homodyne-mediated feedback control. *Phys. Rev. A*, 82:032335, Sep 2010.

[102] T. A. Wheatley, D. W. Berry, H. Yonezawa, D. Nakane, H. Arao, D. T. Pope, T. C. Ralph, H. M. Wiseman, A. Furusawa, and E. H. Huntington. Adaptive optical phase estimation using time-symmetric quantum smoothing. *Phys. Rev. Lett.*, 104:093601, Mar 2010.

[103] W. Feng, P. Wang, X. Ding, L. Xu, and X.-Q. Li. Generating and stabilizing the Greenberger-Horne-Zeilinger state in circuit QED: Joint measurement, Zeno effect, and feedback. *Phys. Rev. A*, 83:042313, Apr 2011.

[104] J. Wang and H. M. Wiseman. Feedback-stabilization of an arbitrary pure state of a two-level atom. *Phys. Rev. A*, 64:063810, Nov 2001.

[105] J. Wang, H. M. Wiseman, and G. J. Milburn. Dynamical creation of entanglement by homodyne-mediated feedback. *Phys. Rev. A*, 71:042309, Apr 2005.

[106] N. Yamamoto. Parametrization of the feedback Hamiltonian realizing a pure steady state. *Phys. Rev. A*, 72:024104, Aug 2005.

[107] S. Mancini and J. Wang. Towards feedback control of entanglement. *Eur. Phys. J. D*, 32:257–260, 2005.

[108] J.-G. Li, J. Zou, B. Shao, and J.-F. Cai. Steady atomic entanglement with different quantum feedbacks. *Phys. Rev. A*, 77:012339, Jan 2008.

[109] A. R. R. Carvalho, A. J. S. Reid, and J. J. Hope. Controlling entanglement by direct quantum feedback. *Phys. Rev. A*, 78:012334, Jul 2008.

[110] Y. Li, B. Luo, and H. Guo. Entanglement and quantum discord dynamics of two atoms under practical feedback control. *Phys. Rev. A*, 84:012316, Jul 2011.

[111] P. Tombesi and D. Vitali. Macroscopic coherence via quantum feedback. *Phys. Rev. A*, 51:4913–4917, Jun 1995.

[112] P. Goetsch, P. Tombesi, and D. Vitali. Effect of feedback on the decoherence of a Schrödinger-cat state: A quantum trajectory description. *Phys. Rev. A*, 54:4519–4527, Nov 1996.

[113] H. M. Wiseman and G. J. Milburn. Squeezing via feedback. *Phys. Rev. A*, 49:1350–1366, Feb 1994.

[114] P. Tombesi and D. Vitali. Physical realization of an environment with squeezed quantum fluctuations via quantum-nondemolition-mediated feedback. *Phys. Rev. A*, 50:4253–4257, Nov 1994.

[115] H. M. Wiseman. In-loop squeezing is like real squeezing to an in-loop atom. *Phys. Rev. Lett.*, 81:3840–3843, Nov 1998.

[116] L. K. Thomsen, S. Mancini, and H. M. Wiseman. Spin squeezing via quantum feedback. *Phys. Rev. A*, 65:061801, Jun 2002.

[117] M. T. Mitchison, J. Goold, and J. Prior. Charging a quantum battery with linear feedback control. *Quantum*, 5:500, July 2021.

[118] M. Campisi, P. Hänggi, and P. Talkner. Colloquium: Quantum fluctuation relations: Foundations and applications. *Rev. Mod. Phys.*, 83:771, 2011.

[119] C. Jarzynski. Equalities and inequalities: Irreversibility and the second law of thermodynamics at the nanoscale. *Annu. Rev. Condens. Matter Phys.*, 2:329, 2011.

[120] C. Bustamante, J. Liphardt, and F. Ritort. The nonequilibrium thermodynamics of small systems. *Phys. Today*, 8:43, 2005.

[121] U. Seifert. Stochastic thermodynamics, fluctuation theorems and molecular machines. *Rep. Prog. Phys.*, 75:126001, 2012.

[122] R. J. Harris and G. M. Schütz. Fluctuation theorems for stochastic dynamics. *J. Stat. Mech.: Theory Exp.*, 2007:P07020, 2007.

[123] M. Esposito. Stochastic thermodynamics under coarse graining. *Phys. Rev. E*, 85:041125, 2012.

[124] M. Esposito, U. Harbola, and S. Mukamel. Nonequilibrium fluctuations, fluctuation theorems, and counting statistics in quantum systems. *Rev. Mod. Phys.*, 81:1665–1702, Dec 2009.

[125] U. Seifert. Stochastic thermodynamics: principles and perspectives. *Eur. Phys. J. B*, 64:423, 2008.

[126] C. Van den Broeck and M. Esposito. Ensemble and trajectory thermodynamics: A brief introduction. *Physica A: Statistical Mechanics and its Applications*, 418:6–16, 2015. Proceedings of the 13th International Summer School on Fundamental Problems in Statistical Physics.

[127] L. Peliti and S. Pigolotti. *Stochastic thermodynamics - an introduction*. Princton University Press, 2021.

[128] C. Jarzynski. Nonequilibrium equality for free energy differences. *Phys. Rev. Lett.*, 78:2690, 1997.

[129] C. Jarzynski. Equilibrium free-energy differences from nonequilibrium measurements: A master-equation approach. *Phys. Rev. E*, 56:5018–5035, Nov 1997.

[130] G. E. Crooks. Entropy production fluctuation theorem and the nonequilibrium work relation for free energy differences. *Phys. Rev. E*, 60:2721, 1999.

[131] G. E. Crooks. Path-ensemble averages in systems driven far from equilibrium. *Phys. Rev. E*, 61:2361–2366, Mar 2000.

[132] J. R. Gomez-Solano, A. Petrosyan, S. Ciliberto, R. Chetrite, and K. Gawedzki. Experimental verification of a modified fluctuation-dissipation relation for a micronsized particle in a nonequilibrium steady state. *Phys. Rev. Lett.*, 103:040601, Jul 2009.

[133] A. Mossa, M. Manosas, N. Forns, J. M. Huguet, and F. Ritort. Dynamic force spectroscopy of DNA hairpins: I. Force kinetics and free energy landscapes. *J. Stat. Mech.: Theory Exp.*, 2009(02):P02060, feb 2009.

[134] K. Hayashi, H. Ueno, R. Iino, and H. Noji. Fluctuation theorem applied to F1-ATPase. *Phys. Rev. Lett.*, 104:218103, May 2010.

[135] J. V. Koski, T. Sagawa, O-P. Saira, Y. Yoon, A. Kutvonen, P. Solinas, M. Möttönen, T. Ala-Nissila, and J. P. Pekola. Distribution of entropy production in a single-electron box. *Nat. Phys.*, 9:644–648, 2013.

[136] A. Hofmann, V.F. Maisi, J. Basset, C. Reichl, W. Wegscheider, T. Ihn, K. Ensslin, and C. Jarzynski. Heat dissipation and fluctuations in a driven quantum dot. *Phys. Status Solidi B*, 254, 2013.

[137] S. Ciliberto. Experiments in stochastic thermodynamics: Short history and perspectives. *Phys. Rev. X*, 7:021051, 2017.

[138] H. B. Callen. *Thermodynamics and an introduction to thermostatistics*. John Wiley and Sons, 1985.

[139] M. Esposito and C. Van den Broeck. Three faces of the second law. I. Master equation formulation. *Phys. Rev. E*, 82:011143, 2010.

[140] U. Seifert. Entropy production along a stochastic trajectory and an integral fluctuation theorem. *Phys. Rev. Lett.*, 95:040602, Jul 2005.

[141] C. H. Bennett. The thermodynamics of computation-A review. *Int. J. Theor. Phys.*, 21:905, 1982.

[142] R. Landauer. Irreversibility and heat generation in the computing process. *IBM J. Res. Dev.*, 5:183, 1961.

[143] T. Sagawa and M. Ueda. Minimal energy cost for thermodynamic information processing: Measurement and information erasure. *Phys. Rev. Lett.*, 102:250602, Jun 2009.

[144] M. Esposito and G. Schaller. Stochastic thermodynamics for "Maxwell demon" feedbacks. *EPL*, 99(3):30003, 2012.

[145] G. Schaller, C. Emary, G. Kiesslich, and T. Brandes. Probing the power of an electronic Maxwell's demon: single-electron transistor monitored by a quantum point contact. *Phys. Rev. B*, 84:085418, 2011.

[146] S. H. Strogatz. *Nonlinear Dynamics and Chaos: With Applications to Physics, Biology, Chemistry, and Engineering*. CRC Press, 2018.

[147] C. W. Wächtler, P. Strasberg, S. H. L. Klapp, G. Schaller, and C. Jarzynski. Stochastic thermodynamics of self-oscillations: the electron shuttle. *New J. Phys.*, 21(7):073009, jul 2019.

[148] D. Mandal and C. Jarzynski. Analysis of slow transitions between nonequilibrium steady states. *J. Stat. Mech: Theory Exp.*, 2016(6):063204, 2016.

[149] M. Scandi and M. Perarnau-Llobet. Thermodynamic length in open quantum systems. *Quantum*, 3:197, October 2019.

[150] S. Nakajima. On quantum theory of transport phenomena: Steady diffusion. *Prog. Theor. Phys.*, 20(6):948, 12 1958.

[151] R. Zwanzig. Ensemble method in the theory of irreversibility. *J. Chem. Phys.*, 33(5):1338–1341, 1960.

[152] J. A. Gyamfi. Fundamentals of quantum mechanics in Liouville space. *Eur. J. Phys.*, 41(6):063002, oct 2020.

[153] M. Yanagisawa. Non-Gaussian state generation from linear elements via feedback. *Phys. Rev. Lett.*, 103:203601, Nov 2009.

[154] J. Bohr Brask, G. Haack, N. Brunner, and M. Huber. Autonomous quantum thermal machine for generating steady-state entanglement. *New J. Phys.*, 17(11):113029, nov 2015.

Scientific publications

Author contributions

Co-authors are abbreviated as follows:
Faraj Bakhshinezhad (FB), Debankur Bhattacharyya (DB), Guilherme De Sousa (GDS), Christopher Jarzynski (CJ), Peter Samuelsson (PS), Patrick P. Potts (PPP)

Paper I: Quantum Fokker-Planck Master Equation for Continuous Feedback Control

I and PPP derived the quantum Fokker-Planck master equation, and the leading order contribution in the separation of timescales expansion. PPP, DB, GDS, and CJ developed two separate techniques for finding the correction term in the separation of timescales expansion. All authors derived results for the classical toy model. I and PPP derived the results for the quantum toy model. I wrote the bulk of the manuscript. All authors contributed to the analysis of the results and took part in revising the manuscript.

Paper I

Quantum Fokker-Planck Master Equation for Continuous Feedback Control

Björn Annby-Andersson[1,*], Faraj Bakhshinezhad[1], Debankur Bhattacharyya[2], Guilherme De Sousa[3],
Christopher Jarzynski[2], Peter Samuelsson[1], and Patrick P. Potts[1,4]

[1]*Physics Department and NanoLund, Lund University, Box 118, 22100 Lund, Sweden*
[2]*Institute for Physical Science and Technology, University of Maryland, College Park, Maryland 20742, USA*
[3]*Department of Physics, University of Maryland, College Park, Maryland 20742, USA*
[4]*Department of Physics, University of Basel, Klingelbergstrasse 82, 4056 Basel, Switzerland*

Measurement and feedback control are essential features of quantum science, with applications ranging from quantum technology protocols to information-to-work conversion in quantum thermodynamics. Theoretical descriptions of feedback control are typically given in terms of stochastic equations requiring numerical solutions, or are limited to linear feedback protocols. Here we present a formalism for continuous quantum measurement and feedback, both linear and nonlinear. Our main result is a quantum Fokker-Planck master equation describing the joint dynamics of a quantum system and a detector with finite bandwidth. For fast measurements, we derive a Markovian master equation for the system alone, amenable to analytical treatment. We illustrate our formalism by investigating two basic information engines, one quantum and one classical.

Introduction.—Quantum measurement and feedback control are key elements for emerging quantum technologies, enabling a wide range of applications, including quantum error correction [1], deterministic entanglement generation [2], atomic clocks [3], and quantum state stabilization [4–6]. The past two decades have also witnessed a large number of fundamental experiments on feedback control of quantum systems [7–18]. Of special interest are experiments in quantum thermodynamics [19] —by using measurement and feedback, processes that are otherwise forbidden by the second law of thermodynamics may be realized, compellingly illustrated by Maxwell's demon [20–22]. Over the past ten years, the demon has been realized in a wide range of experimental settings, both in classical [23–29] and, recently, quantum systems [30–34]. This activity has inspired further work investigating the connection between thermodynamics and information theory [35–37], and has resulted in generalizations of the second law for feedback controlled systems [38–48]. A promising platform for exploring feedback control within quantum thermodynamics is solid-state electronic systems [49], ranging from semiconductor quantum dots [50] to superconducting qubits [51]. Key features in these systems are large and fast tunability of system properties [52–54]

and time resolved measurements [55,56]. Moreover, both discrete [29,57,58] and continuous [6,27] feedback protocols have been demonstrated experimentally.

The theoretical description of feedback control in quantum systems is typically based on stochastic differential equations [59–70]—powerful tools that can describe discrete as well as continuous feedback protocols. In general, these equations must be solved numerically, providing limited qualitative insight. An important exception, amenable to analytical treatment, is the Wiseman-Milburn equation [63], a Markovian master equation for continuous feedback protocols that depend linearly on the measured signal. However, optimal control often requires nonlinear protocols, for instance, bang-bang control [71,72] which has promising thermodynamic applications in solid-state architectures [27,73–75]. For such continuous, nonlinear feedback protocols, no master equation description exists, emphasizing a need for further analytical tools. We stress that the word "nonlinear" here refers to the protocol's dependence on the measured signal, not to the system's dynamics.

In this Letter, we satisfy this need by developing a general framework for continuous measurement and feedback control in quantum systems, able to provide analytical insight into nonlinear feedback protocols. Our main result, Eq. (1) below, is a quantum Fokker-Planck master equation describing the joint dynamics of a quantum system and a detector with finite bandwidth (see Fig. 1). This equation is applicable to any quantum or classical system undergoing continuous feedback control. For fast measurements, Eq. (1) reduces to a Markovian master equation for the
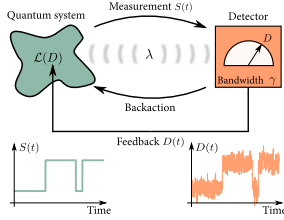
FIG. 1. Illustration of a generic measurement and feedback setup, consisting of an open quantum system and a detector with finite bandwidth γ. The detector continuously measures an arbitrary system observable. The measurement strength λ determines measurement backaction. Continuous feedback is applied using the measurement outcome D to control the Liouville superoperator $\mathcal{L}(D)$ of the system. The time traces visualize trajectories for the system state $S(t)$ and the measurement record $D(t)$.

system alone, generalizing the Wiseman-Milburn equation to nonlinear feedback protocols. The broad scope of Eq. (1) suggests that our results will impact a wide variety of topics where nonlinear, continuous feedback control can be applied, such as quantum error correction [1], entanglement generation [2], quantum state stabilization [6], Maxwell's demon [74,75], and machine learning [76].

To illustrate our formalism, we investigate two toy models, a classical and a quantum two-level system, operated via nonlinear feedback protocols. For the classical model, we also derive a fluctuation theorem, highlighting the role of continuous measurement and feedback in information thermodynamics.

Fokker-Planck master equation.—A general setup for continuous measurement and feedback is depicted in Fig. 1. We consider an open quantum system whose dynamics, in the absence of measurement and feedback, are described by a Liouville superoperator $\mathcal{L}$. A detector continuously measures a system observable $\hat{A}$. The measurement strength λ determines the magnitude of the measurement backaction, the limit $\lambda \to 0$ ($\lambda \to \infty$) corresponds to a weak, nonintrusive (strong, projective) measurement preserving (destroying) the quantum coherence of the system. Weak measurements thus reduce backaction, but increase measurement uncertainty. To provide a realistic detector description, we consider a finite bandwidth γ, acting as a low-pass frequency filter, eliminating high frequency measurement noise at the cost of introducing a time delay scaling as $1/\gamma$. Feedback control is incorporated by continuously feeding back the measurement outcome D into the system, controlling the system Liouville superoperator via $\mathcal{L}(D)$.

Our main result is the following deterministic Fokker-Planck master equation (derivation outlined below),

$$\partial_t \hat{\rho}_t(D) = \mathcal{L}(D)\hat{\rho}_t(D) + \lambda \mathcal{D}[\hat{A}]\hat{\rho}_t(D)$$
$$- \gamma \partial_D \mathcal{A}(D)\hat{\rho}_t(D) + \frac{\gamma^2}{8\lambda}\partial_D^2\hat{\rho}_t(D), \quad (1)$$

describing the joint system-detector dynamics under continuous measurement and feedback control. The density operator $\hat{\rho}_t(D)$ represents the joint state of system and detector, where $\hat{\rho}_t \equiv \int dD\, \hat{\rho}_t(D)$ is the system state for an unknown measurement outcome D, and $P_t(D) \equiv \text{tr}\{\hat{\rho}_t(D)\}$ defines the probability distribution of the measurement outcome D. Note that $\int dD\, P_t(D) = 1$ and $\text{tr}\{\hat{\rho}_t\} = 1$; see Supplemental Material (SM) [77]. The first term on the rhs of Eq. (1) describes the feedback-controlled evolution of the system. This term allows for feedback protocols that are nonlinear in D. The second term, where $\mathcal{D}[\hat{A}]\hat{\rho} = \hat{A}\hat{\rho}\hat{A} - \frac{1}{2}\{\hat{A}^2, \hat{\rho}\}$ (note $\hat{A}^\dagger = \hat{A}$), describes how the system is dephased in the eigenbasis of $\hat{A}$ at a rate proportional to λ due to measurement backaction. The last two terms constitute a Fokker-Planck equation describing the detector time evolution. These terms define an Ornstein-Uhlenbeck process [87] with a system dependent superoperator drift coefficient $\mathcal{A}(D)\hat{\rho} \equiv \frac{1}{2}\{\hat{A} - D, \hat{\rho}\}$ and diffusion constant $\gamma/8\lambda$. This describes a noisy relaxation of the measurement outcome toward a value determined by the system state. The derivation of Eq. (1) is rather involved; see details in SM [77]. The main text instead aims to highlight its implications and applications. However, we sketch the derivation at the end of the Letter.

Equation (1) is, like most formalisms for continuous measurement and feedback, typically restricted to numerical solutions. However, when there exists a wide separation between the system and detector timescales, Eq. (1) simplifies to a Markovian master equation for the system state $\hat{\rho}_t$, allowing for analytical treatment. The detector timescale $1/\gamma$ appears in the last two terms in Eq. (1), and the system timescale $1/\Gamma$ is determined by $\mathcal{L}(D) + \lambda \mathcal{D}[\hat{A}]$. The role of λ, the measurement strength, is subtle; see below. When $\gamma \gg \Gamma$, $\hat{\rho}_t$ evolves, to first order in $1/\gamma$, according to

$$\partial_t \hat{\rho}_t = [\mathcal{L}_0 + \lambda \mathcal{D}[\hat{A}] + \gamma^{-1}\mathcal{L}_{\text{corr}}]\hat{\rho}_t, \quad (2)$$

with zeroth order Liouville superoperator $\mathcal{L}_0$ and first order correction $\mathcal{L}_{\text{corr}}$. $\mathcal{L}_0$ is obtained by approximating the system-detector density operator as $\hat{\rho}_t(D) = [\sum_{aa'} \pi_{aa'}(D)\mathcal{V}_{aa'}]\hat{\rho}_t$, with

$$\pi_{aa'}(D) = \sqrt{4\lambda/\pi\gamma}\, e^{-(4\lambda/\gamma)[D-(\xi_a+\xi_{a'})/2]^2}, \quad (3)$$

and superoperators $\mathcal{V}_{aa'}\hat{\rho} \equiv \langle a|\hat{\rho}|a'\rangle|a\rangle\langle a'|$, where we used the eigenvalues and eigenvectors of the measured operator $\hat{A} = \sum_a \xi_a |a\rangle\langle a|$. In this approximation, the detector is
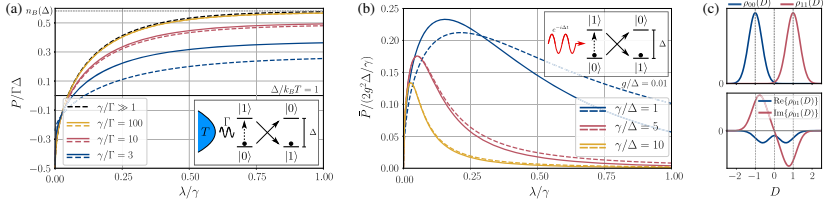
FIG. 2. Steady state power for classical (a) and quantum (b) toy models, varying the measurement strength λ. Solid lines obtained by numerically solving Eq. (1), dashed lines obtained analytically using the separation of timescales technique. The separation of timescales assumption breaks down when system and detector timescales are comparable. (a) The inset illustrates a feedback protocol of a classical two-level system coupled to a thermal reservoir. When excited (dashed arrow), the levels are flipped (solid arrows), extracting energy. For strong measurements ($\lambda \gg \gamma$), the average occupation of the bath $[n_B(\Delta)]$ sets an upper limit on extracted power, see dashed grey line, and is only reached for fast detectors ($\gamma/\Gamma \gg 1$) [cf. Eq. (6)]. For weak measurements ($\lambda \ll \gamma$), feedback is applied randomly and energy is dissipated into the reservoir. (b) The inset depicts a feedback protocol for a qubit, coherently driven by an external driving field. The protocol is identical to (a). For strong measurements, the power vanishes because of the quantum Zeno effect. For weak measurements, no power can be extracted as feedback is applied randomly. (c) Visualization of $\hat{\rho}_t(D)$ for the quantum toy model, with stationary matrix elements $\rho_{ab}(D) = \langle a|\hat{\rho}_t(D)|b\rangle$. Here we use $g/\Delta = 0.01$ and $\gamma = \Delta = \lambda$. Top panel: diagonal elements of $\hat{\rho}_t(D)$. Bottom panel: real and imaginary part of $\rho_{01}(D)$.

always in a system dependent stationary distribution $\pi_{aa'}(D)$. This is justified for $\gamma \gg \Gamma$, where changes of the system occur with a rate much smaller than the inverse detector relaxation time. Inserting this approximation in Eq. (1) results in $\mathcal{L}_0 = \int dD\,\mathcal{L}(D)[\sum_{aa'} \pi_{aa'}(D)\mathcal{V}_{aa'}]$, describing the system dynamics for a detector with zero delay time. The first order correction $\gamma^{-1}\mathcal{L}_{\text{corr}}$ accounts for the lag of the detector due to its finite response time γ^{-1}. As usual in linear response theory, this correction can be written in terms of time-integrated correlation functions; see SM [77]. Note that λ plays a special role in the separation of timescales since it appears in both the first and second line of Eq. (1). In general, Eq. (2) is thus only justified for $\lambda \ll \gamma$. Here we keep λ/γ arbitrary as there are scenarios where Eq. (2) also holds for strong measurements; see below.

We emphasize that Eq. (2) describes arbitrary feedback protocols, both linear and nonlinear in D. As a consistency check, we recover the Wiseman-Milburn equation [63] from Eq. (1) by employing the separation of timescales approximation to first order in $1/\gamma$, using a linear feedback Liouville superoperator $\mathcal{L}(D)\hat{\rho} = \mathcal{L}\hat{\rho} - iD[\hat{F}, \hat{\rho}]$, with feedback Hamiltonian $\hat{F}$, and taking the infinite bandwidth limit (see SM [77]). Our formalism thus generalizes the important earlier work of Ref. [63] to nonlinear feedback protocols.

In the following, we highlight the usefulness of Eq. (1) by studying protocols for power production in two toy models.

Classical toy model.—By classical system, we refer to a situation with discrete energy levels, but where the density matrix remains diagonal in the energy basis at all times.

This can be achieved either by suppressing quantum coherence by environmental noise or by decoupling the diagonal and off-diagonal elements of $\hat{\rho}_t$ (see SM for details [77]). Under these conditions, $[\hat{\rho}_t(D), \hat{A}] = 0$ and the backaction term in Eq. (1) has no influence on the dynamics. To facilitate a comparison between the classical and quantum models, we use the same notation. We consider a classical two-level system, with states $|0\rangle$ and $|1\rangle$, coupled to a thermal reservoir at temperature T; see inset of Fig. 2(a). The system and reservoir exchange energy quanta with energy Δ at rate Γ. The state of the system is continuously monitored by measuring the observable $\hat{A} = \hat{\sigma}_z$, with Pauli-Z operator $\hat{\sigma}_z = |1\rangle\langle 1| - |0\rangle\langle 0|$, such that whenever the measurement outcome $D < 0$ ($D \geq 0$) for an ideal detector (low noise and delay), the system resides in $|0\rangle$ ($|1\rangle$). Feedback is incorporated by flipping the levels according to the solid arrows in Fig. 2(a) when an excitation is detected, i.e., when D changes sign, thereby extracting energy from the reservoir. The Hamiltonian is given by $\hat{H}(D) = [1 - \theta(D)]\Delta|1\rangle\langle 1| + \theta(D)\Delta|0\rangle\langle 0|$, where $\theta(D)$ is the Heaviside step function. Note that $[\hat{H}(D), \hat{A}] = 0$, ensuring that $\hat{\rho}_t(D)$ remains diagonal in the energy basis. The feedback protocol is represented by the Liouville superoperator,

$$\mathcal{L}(D) = [1 - \theta(D)]\mathcal{L}_- + \theta(D)\mathcal{L}_+, \quad (4)$$

where $\mathcal{L}_-\hat{\rho} = \Gamma n_B(\Delta)\mathcal{D}[\hat{\sigma}^\dagger]\hat{\rho} + \Gamma[n_B(\Delta) + 1]\mathcal{D}[\hat{\sigma}]\hat{\rho}$ is the protocol applied for $D < 0$, and $\mathcal{L}_+\hat{\rho} = \Gamma[n_B(\Delta) + 1]\mathcal{D}[\hat{\sigma}^\dagger]\hat{\rho} + \Gamma n_B(\Delta)\mathcal{D}[\hat{\sigma}]\hat{\rho}$ is the protocol applied for $D \geq 0$, with system ladder operator $\hat{\sigma} = |0\rangle\langle 1|$, and

Bose-Einstein distribution $n_B(x) = [\exp(x/k_BT) - 1]^{-1}$, with x denoting energy and k_B the Boltzmann constant.

Employing the separation of timescales technique, using $\gamma \gg \Gamma$ with Eqs. (2) and (3), the system evolves, to zeroth order in $1/\gamma$, according to the feedback Liouville superoperator,

$$\mathcal{L}_0 = [(1-\eta)\mathcal{L}_- + \eta\mathcal{L}_+]\mathcal{V}_{00} + [\eta\mathcal{L}_- + (1-\eta)\mathcal{L}_+]\mathcal{V}_{11}, \quad (5)$$

where we introduced the feedback error probability $\eta = [1 - \text{erf}(2\sqrt{\lambda/\gamma})]/2$ for a single feedback event, where $\text{erf}(\cdot)$ is the error function and $0 \leq \eta \leq 1/2$. Feedback is applied incorrectly when the measurement outcome does not reflect the true system state. Note that weak (strong) measurements yield high (low) detector noise and increase (decrease) the error probability.

To zeroth order in $1/\gamma$, the average power production reads

$$P = \Gamma\Delta[(1-\eta)n_B(\Delta) - \eta[n_B(\Delta) + 1]], \quad (6)$$

where $P > 0$ corresponds to extracting energy from the bath. For strong measurements ($\eta \to 0$), feedback is consistently applied correctly and energy is only extracted from the reservoir. The maximum extraction rate $P = \Gamma\Delta n_B(\Delta)$ is limited by the coupling Γ and the average occupation $n_B(\Delta)$ of the bath. For weak measurements, feedback errors together with the asymmetry between excitation and deexcitation rates lead to a net dissipation of energy. Interestingly, the maximum dissipation rate $P = -\Gamma\Delta/2$ is independent of $n_B(\Delta)$. Equation (6) is plotted with a black, dashed line in Fig. 2, illustrating the behavior for weak and strong measurements. Additionally, we computed the power by (i) numerically solving Eq. (1) (solid colored lines) and (ii) using the separation of timescales technique to first order in $1/\gamma$ (dashed colored lines) (see SM for details [77]). As γ decreases, the extracted power decreases because the detector can no longer resolve fast changes in the system, missing opportunities to extract energy. The separation of timescales approximation gradually breaks down as γ and Γ become comparable.

Following Ref. [88], in the longtime limit, Eq. (5) implies the detailed fluctuation theorem,

$$\frac{P(-m)}{P(m)} = e^{m(\Delta/k_BT - \ln[(1-\eta)/\eta])}, \quad (7)$$

for the number of extracted energy quanta m, where $m > 0$ ($m < 0$) corresponds to extracting (dissipating) energy from the bath. The term Δ/T is the entropy change in the bath related to the exchange of a single quantum. The information term $\ln[(1-\eta)/\eta]$ is given by the log-odds of not making an error and can be interpreted as the difference in information content between correctly and incorrectly applying feedback. Note that most information from the

continuous measurement is discarded—it is only the information during a change in the system state that matters. In the error-free limit, $\eta \to 0$, the information term diverges, illustrating absolute irreversibility; i.e., all excitations are extracted. See SM for a derivation of Eq. (7) [77].

Quantum toy model.—We consider a qubit coherently driven by an external driving field; see inset of Fig. 2(b). Measurement and feedback are identical to the classical toy model, now extracting energy from the driving field. The feedback protocol is described by $\mathcal{L}_t(D)\hat{\rho} = -i[\hat{H}_t(D), \hat{\rho}]$ with Hamiltonian

$$\hat{H}_t(D) = [1 - \theta(D)]\Delta|1\rangle\langle1| + \theta(D)\Delta|0\rangle\langle0| + g\cos(\Delta t)\hat{\sigma}_x, \quad (8)$$

where Δ is the qubit level spacing, g the strength of the qubit-driving field coupling, and $\hat{\sigma}_x$ the Pauli-X operator.

Separating system and detector timescales to first order in $1/\gamma$ results in system Liouville superoperator (details in SM [77]),

$$[\mathcal{L}_0 + \lambda\mathcal{D}[\hat{\sigma}_z] + \gamma^{-1}\mathcal{L}_{\text{corr}}]\hat{\rho} = -ig\cos(\Delta t)[\hat{\sigma}_x, \hat{\rho}] + \tilde{\lambda}\mathcal{D}[\hat{\sigma}_z]\hat{\rho}$$
$$- \frac{2\Delta g}{\gamma}D_0\cos(\Delta t)\hat{\sigma}_x, \quad (9)$$

with effective dephasing rate $\tilde{\lambda} = \lambda + \Delta^2 \ln(2)/2\gamma$, and coefficient $D_0 = 2\sqrt{\lambda/\pi\gamma} {}_2F_2(1/2, 1/2; 3/2, 3/2; -4\lambda/\gamma)$, where ${}_2F_2(\cdot)$ is a generalized hypergeometric function. The first term on the rhs of Eq. (9) represents the coherent drive, while the second term describes dephasing due to measurement and feedback. The third term is a source for quantum coherence, stabilizing the coherence in the long-time limit. We emphasize that the first order correction is essential to compute the power as the steady state coherence vanishes to leading order, and hence, no power can be extracted. Note that the third term, which goes beyond leading order, can lead to negativities in $\hat{\rho}_t$, which is of no concern in the separation of timescales regime where the term is small. We stress that this term is trace preserving as $\hat{\sigma}_x$ is traceless.

The average power of the system is given by $P(t) = \text{tr}\{[\partial_t\hat{H}(D)]\hat{\rho}_t\}$, where power is extracted [dissipated] when $P(t) > 0$ [$P(t) < 0$]. Over one driving period $\tau = 2\pi/\Delta$, the time averaged power reads

$$\bar{P} = \frac{2g^2\Delta}{\gamma}D_0\frac{\Delta^2}{\Delta^2 + 4\tilde{\lambda}^2}. \quad (10)$$

For strong measurements $\lambda \gg \gamma$, the power vanishes because of the quantum Zeno effect. For weak measurements $\lambda \ll \gamma$, large detector noise leads to completely random feedback, and the power goes to zero because of the symmetric driving. This is highlighted in Fig. 2(b),

where we plot Eq. (10) as dashed lines. The solid lines were computed numerically by solving the full Eq. (1). The corresponding steady state matrix elements of $\hat{\rho}_t(D)$ are visualized in Fig. 2(c) (details in SM [77]). Similar to the classical toy model, the separation of timescales assumption breaks down when system and detector timescales are comparable.

Outline derivation main result.—To outline the main steps in the derivation of Eq. (1), we start by describing the continuous measurement. For a single instantaneous measurement, the system state $\hat{\rho}_t$ transforms as

$$\hat{\rho}_t(z) = \hat{K}(z)\hat{\rho}_t\hat{K}^\dagger(z), \tag{11}$$

where $\hat{K}(z)$ is the measurement operator for obtaining outcome z, obeying the completeness relation $\int dz\,\hat{K}^\dagger(z)\hat{K}(z) = \mathbb{1}$, $\mathrm{tr}\{\hat{\rho}_t(z)\}$ is the probability of obtaining z, and $\int dz\,\hat{\rho}_t(z)$ is the system state for an unknown measurement outcome. Stressing that temporal coarse graining results in Gaussian noise for any measurement operator [89], we consider Gaussian measurement operators [89,90],

$$\hat{K}(z) = \left(\frac{2\lambda\delta t}{\pi}\right)^{1/4} e^{-\lambda\delta t(z-\hat{A})^2}, \tag{12}$$

where δt is the time between measurements. A weak continuous measurement is obtained by repeatedly measuring the system, taking the limit $\lambda\delta t \to 0$ for a fixed measurement strength λ. In this limit, the sequence of outcomes becomes a continuous signal $z(t)$.

The detector bandwidth γ is introduced through a low-pass frequency filter [1,12,91–95],

$$D(t) = \int_{-\infty}^{t} ds\,\gamma e^{-\gamma(t-s)} z(s), \tag{13}$$

such that the measurement outcome $D(t)$ is a smoothened version of the signal $z(t)$. The filter reduces the high frequency measurement noise and introduces a detector delay. This provides a realistic detector model, but the filter is also necessary for nonlinear feedback protocols because higher orders of $z(t)$ are ill defined due to its white noise spectrum which includes diverging frequencies [1,12,93].

Feedback is incorporated by controlling the system time evolution in between measurements, i.e., making the Liouville superoperator $\mathcal{L}(D)$ dependent on the frequency filtered measurement outcome D. Combining time evolution due to measurements and due to the Liouvillian, we find Eq. (1) in the continuous limit $\delta t \to 0$. The derivation can be carried out either in the framework of stochastic calculus following the methods outlined in Refs. [68,89] or under the rules of conventional calculus. See details in SM [77].

Conclusions.—We have derived a Fokker-Planck master equation for continuous feedback control, describing the joint system-detector dynamics for detectors with finite bandwidth. By separating system and detector timescales, we obtain a Markovian master equation for the system alone, opening a new avenue for analytical modeling of nonlinear feedback protocols. The Markovian description further implies fluctuation theorems, providing insight into the connection between thermodynamics and information theory. With two simple toy models, we highlighted the usefulness of our formalism, showing that it can be applied to a large variety of systems in both the classical and quantum regimes. Future endeavors include extensions of the formalism to include non-Markovian effects and state-estimation feedback [61,96].

[*]bjorn.annby-andersson@teorfys.lu.se

[1] M. Sarovar, C. Ahn, K. Jacobs, and G. J. Milburn, Practical scheme for error control using feedback, Phys. Rev. A **69**, 052324 (2004).

[2] D. Risté, M. Dukalski, C. A. Watson, G. De Lange, M. J. Tiggelman, Y. M. Blanter, K. W. Lehnert, R. N. Schouten, and L. DiCarlo, Deterministic entanglement of superconducting qubits by parity measurement and feedback, Nature (London) **502**, 350 (2013).

[3] A. D. Ludlow, M. M. Boyd, J. Ye, E. Peik, and P. O. Schmidt, Optical atomic clocks, Rev. Mod. Phys. **87**, 637 (2015).

[4] W. P. Smith, J. E. Reiner, L. A. Orozco, S. Kuhr, and H. M. Wiseman, Capture and Release of a Conditional State of a Cavity QED System by Quantum Feedback, Phys. Rev. Lett. **89**, 133601 (2002).

[5] C. Sayrin, I. Dotsenko, X. Zhou, B. Peaudecerf, T. Rybarczyk, S. Gleyzes, P. Rouchon, M. Mirrahimi, H. Amini, M. Brune, J.-M. Raimond, and S. Haroche, Real-time quantum feedback prepares and stabilizes photon number states, Nature (London) **477**, 73 (2011).

[6] R. Vijay, C. Macklin, D. H. Slichter, S. J. Weber, K. W. Murch, R. Naik, A. N. Korotkov, and I. Siddiqi, Stabilizing Rabi oscillations in a superconducting qubit using quantum feedback, Nature (London) **490**, 77 (2012).

[7] M. A. Armen, J. K. Au, J. K. Stockton, A. C. Doherty, and H. Mabuchi, Adaptive Homodyne Measurement of Optical Phase, Phys. Rev. Lett. **89,** 133602 (2002).

[8] B. D'Urso, B. Odom, and G. Gabrielse, Feedback Cooling of a One-Electron Oscillator, Phys. Rev. Lett. **90,** 043001 (2003).

[9] P. Bushev, D. Rotter, A. Wilson, F. Dubin, C. Becher, J. Eschner, R. Blatt, V. Steixner, P. Rabl, and P. Zoller, Feedback Cooling of a Single Trapped Ion, Phys. Rev. Lett. **96,** 043003 (2006).

[10] B. L. Higgins, D. W. Berry, S. D. Bartlett, H. M. Wiseman, and G. J. Pryde, Entanglement-free Heisenberg-limited phase estimation, Nature (London) **450,** 393 (2007).

[11] G. G. Gillett, R. B. Dalton, B. P. Lanyon, M. P. Almeida, M. Barbieri, G. J. Pryde, J. L. O'Brien, K. J. Resch, S. D. Bartlett, and A. G. White, Experimental Feedback Control of Quantum Systems Using Weak Measurements, Phys. Rev. Lett. **104,** 080503 (2010).

[12] T. A. Wheatley, D. W. Berry, H. Yonezawa, D. Nakane, H. Arao, D. T. Pope, T. C. Ralph, H. M. Wiseman, A. Furusawa, and E. H. Huntington, Adaptive Optical Phase Estimation Using Time-Symmetric Quantum Smoothing, Phys. Rev. Lett. **104,** 093601 (2010).

[13] G.-Y. Xiang, B. L. Higgins, D. W. Berry, H. M. Wiseman, and G. J. Pryde, Entanglement-enhanced measurement of a completely unknown optical phase, Nat. Photonics **5,** 43 (2011).

[14] X. Zhou, I. Dotsenko, B. Peaudecerf, T. Rybarczyk, C. Sayrin, S. Gleyzes, J. M. Raimond, M. Brune, and S. Haroche, Field Locked to a Fock State by Quantum Feedback with Single Photon Corrections, Phys. Rev. Lett. **108,** 243602 (2012).

[15] R. Okamoto, M. Iefuji, S. Oyama, K. Yamagata, H. Imai, A. Fujiwara, and S. Takeuchi, Experimental Demonstration of Adaptive Quantum State Estimation, Phys. Rev. Lett. **109,** 130404 (2012).

[16] D. Ristè, C. C. Bultink, K. W. Lehnert, and L. DiCarlo, Feedback Control of a Solid-State Qubit Using High-Fidelity Projective Measurement, Phys. Rev. Lett. **109,** 240502 (2012).

[17] H. Yonezawa, D. Nakane, T. A. Wheatley, K. Iwasawa, S. Takeda, H. Arao, K. Ohki, K. Tsumura, D. W. Berry, T. C. Ralph, H. M. Wiseman, E. H. Huntington, and A. Furusawa, Quantum-enhanced optical-phase tracking, Science **337,** 1514 (2012).

[18] Z. K. Minev, S. O. Mundhada, S. Shankar, P. Reinhold, R. Gutierrez-Jauregui, R. J. Schoelkopf, M. Mirrahimi, H. J. Carmichael, and M. H. Devoret, To catch and reverse a quantum jump mid-flight, Nature (London) **570,** 200 (2019).

[19] S. Vinjanampathy and J. Anders, Quantum thermodynamics, Contemp. Phys. **57,** 545 (2016).

[20] J. C. Maxwell, *Theory of Heat* (Longmans, Green, and Co., London, 1871).

[21] *Maxwell's Demon 2 Entropy, Classical and Quantum Information, Computing*, edited by H. S. Leff and A. F. Rex (CRC Press, Boca Raton, FL, 2002).

[22] K. Maruyama, F. Nori, and V. Vedral, Colloquium: The physics of Maxwell's demon and information, Rev. Mod. Phys. **81,** 1 (2009).

[23] V. Serreli, C. F. Lee, E. R. Kay, and D. A. Leigh, A molecular information ratchet, Nature (London) **445,** 523 (2007).

[24] S. Toyabe, T. Sagawa, M. Ueda, E. Muneyuki, and M. Sano, Experimental demonstration of information-to-energy conversion and validation of the generalized Jarzynski equality, Nat. Phys. **6,** 988 (2010).

[25] J. V. Koski, V. F. Maisi, J. P. Pekola, and D. V. Averin, Experimental realization of a Szilard engine with a single electron, Proc. Natl. Acad. Sci. U.S.A. **111,** 13786 (2014).

[26] J. V. Koski, V. F. Maisi, T. Sagawa, and J. P. Pekola, Experimental Observation of the Role of Mutual Information in the Nonequilibrium Dynamics of a Maxwell Demon, Phys. Rev. Lett. **113,** 030601 (2014).

[27] K. Chida, S. Desai, K. Nishiguchi, and A. Fujiwara, Power generator driven by Maxwell's demon, Nat. Commun. **8,** 15310 (2017).

[28] A. Kumar, T.-Y. Wu, F. Giraldo, and D. S. Weiss, Sorting ultracold atoms in a three-dimensional optical lattice in a realization of Maxwell's demon, Nature (London) **561,** 83 (2018).

[29] D. Barker, M. Scandi, S. Lehmann, C. Thelander, K. A. Dick, M. Perarnau-Llobet, and V. F. Maisi, Experimental Verification of the Work Fluctuation-Dissipation Relation for Information-to-Work Conversion, Phys. Rev. Lett. **128,** 040602 (2022).

[30] M. D. Vidrighin, O. Dahlsten, M. Barbieri, M. S. Kim, V. Vedral, and I. A. Walmsley, Photonic Maxwell's Demon, Phys. Rev. Lett. **116,** 050401 (2016).

[31] N. Cottet, S. Jezouin, L. Bretheau, P. Campagne-Ibarcq, Q. Ficheux, J. Anders, A. Auffèves, R. Azouit, P. Rouchon, and B. Huard, Observing a quantum Maxwell demon at work, Proc. Natl. Acad. Sci. U.S.A. **114,** 7561 (2017).

[32] Y. Masuyama, K. Funo, Y. Murashita, A. Noguchi, S. Kono, Y. Tabuchi, R. Yamazaki, M. Ueda, and Y. Nakamura, Information-to-work conversion by Maxwell's demon in a superconducting circuit quantum electrodynamical system, Nat. Commun. **9,** 1291 (2018).

[33] M. Naghiloo, J. J. Alonso, A. Romito, E. Lutz, and K. W. Murch, Information Gain and Loss for a Quantum Maxwell's Demon, Phys. Rev. Lett. **121,** 030604 (2018).

[34] M. Ribezzi-Crivellari and F. Ritort, Large work extraction and the Landauer limit in a continuous Maxwell demon, Nat. Phys. **15,** 660 (2019).

[35] T. Sagawa, Thermodynamics of information processing in small systems, Prog. Theor. Phys. **127,** 1 (2012).

[36] J. M. R. Parrondo, J. M. Horowitz, and T. Sagawa, Thermodynamics of information, Nat. Phys. **11,** 131 (2015).

[37] J. Goold, M. Huber, A. Riera, L. del Rio, and P. Skrzypczyk, The role of quantum information in thermodynamics—a topical review, J. Phys. A **49,** 143001 (2016).

[38] T. Sagawa and M. Ueda, Second Law of Thermodynamics with Discrete Quantum Feedback Control, Phys. Rev. Lett. **100,** 080403 (2008).

[39] T. Sagawa and M. Ueda, Generalized Jarzynski Equality Under Nonequilibrium Feedback Control, Phys. Rev. Lett. **104,** 090602 (2010).

[40] M. Ponmurugan, Generalized detailed fluctuation theorem under nonequilibrium feedback control, Phys. Rev. E **82,** 031129 (2010).

[41] J. M. Horowitz and S. Vaikuntanathan, Nonequilibrium detailed fluctuation theorem for repeated discrete feedback, Phys. Rev. E **82,** 061120 (2010).

[42] Y. Morikuni and H. Tasaki, Quantum Jarzynski-Sagawa-Ueda relations, J. Stat. Phys. **143,** 1 (2011).

[43] T. Sagawa and M. Ueda, Fluctuation Theorem with Information Exchange: Role of Correlations in Stochastic Thermodynamics, Phys. Rev. Lett. **109,** 180602 (2012).

[44] T. Sagawa and M. Ueda, Nonequilibrium thermodynamics of feedback control, Phys. Rev. E **85,** 021104 (2012).

[45] D. Abreu and U. Seifert, Thermodynamics of Genuine Nonequilibrium States Under Feedback Control, Phys. Rev. Lett. **108,** 030601 (2012).

[46] K. Funo, Y. Watanabe, and M. Ueda, Integral quantum fluctuation theorems under measurement and feedback control, Phys. Rev. E **88,** 052121 (2013).

[47] C. W. Wächtler, P. Strasberg, and T. Brandes, Stochastic thermodynamics based on incomplete information: Generalized Jarzynski equality with measurement errors with or without feedback, New J. Phys. **18,** 113042 (2016).

[48] P. P. Potts and P. Samuelsson, Detailed Fluctuation Relation for Arbitrary Measurement and Feedback Schemes, Phys. Rev. Lett. **121,** 210603 (2018).

[49] J. P. Pekola, Towards quantum thermodynamics in electronic circuits, Nat. Phys. **11,** 118 (2015).

[50] W. G. van der Wiel, S. De Franceschi, J. M. Elzerman, T. Fujisawa, S. Tarucha, and L. P. Kouwenhoven, Electron transport through double quantum dots, Rev. Mod. Phys. **75,** 1 (2002).

[51] M. Kjaergaard, M. E. Schwartz, J. Braumller, P. Krantz, J. I.-J. Wang, S. Gustavsson, and W. D. Oliver, Superconducting qubits: Current state of play, Annu. Rev. Condens. Matter Phys. **11,** 369 (2020).

[52] C. Fasth, A. Fuhrer, M. T. Björk, and L. Samuelson, Tunable double quantum dots in InAs nanowires defined by local gate electrodes, Nano Lett. **5,** 1487 (2005).

[53] K. W. Murch, R. Vijay, and I. Siddiqi, Weak measurement and feedback in superconducting quantum circuits, in *Superconducting Devices in Quantum Optics,* edited by R. H. Hadfield and G. Johansson (Springer International Publishing, Cham, 2016), pp. 163–185.

[54] D. Barker, S. Lehmann, L. Namazi, M. Nilsson, C. Thelander, K. A. Dick, and V. F. Maisi, Individually addressable double quantum dots formed with nanowire polytypes and identified by epitaxial markers, Appl. Phys. Lett. **114** (2019).

[55] B. Küng, C. Rössler, M. Beck, M. Marthaler, D. S. Golubev, Y. Utsumi, T. Ihn, and K. Ensslin, Irreversibility on the Level of Single-Electron Tunneling, Phys. Rev. X **2,** 011001 (2012).

[56] A. Hofmann, V. F. Maisi, J. Basset, C. Reichl, W. Wegscheider, T. Ihn, K. Ensslin, and C. Jarzynski, Heat dissipation and fluctuations in a driven quantum dot, Phys. Status Solidi B **254,** 1600546 (2017).

[57] D. Ristè, C. C. Bultink, K. W. Lehnert, and L. DiCarlo, Feedback Control of a Solid-State Qubit Using High-Fidelity Projective Measurement, Phys. Rev. Lett. **109,** 240502 (2012).

[58] P. Campagne-Ibarcq, E. Flurin, N. Roch, D. Darson, P. Morfin, M. Mirrahimi, M. H. Devoret, F. Mallet, and B. Huard, Persistent Control of a Superconducting Qubit by Stroboscopic Measurement Feedback, Phys. Rev. X **3,** 021008 (2013).

[59] V. P. Belavkin, On the theory of controlling observable quantum systems, Autom. Remote Control (Engl. Transl.) **44,** 178 (1983).

[60] V. P. Belavkin, Non-demolition measurement and control in quantum dynamical systems, in *Information Complexity and Control in Quantum Physics,* edited by A. Blaquiere, S. Diner, and G. Lochak (Springer, Vienna, 1987), pp. 311–329.

[61] V. P. Belavkin, Quantum stochastic calculus and quantum nonlinear filtering, J. Multivariate Anal. **42,** 171 (1992).

[62] V. P. Belavkin, Quantum continual measurements and a posteriori collapse on CCR, Commun. Math. Phys. **146,** 611 (1992).

[63] H. M. Wiseman and G. J. Milburn, Quantum Theory of Optical Feedback via Homodyne Detection, Phys. Rev. Lett. **70,** 548 (1993).

[64] H. M. Wiseman, Quantum theory of continuous feedback, Phys. Rev. A **49,** 2133 (1994).

[65] M. Yanagisawa and H. Kimura, A control problem for Gaussian states, in *Learning, Control and Hybrid Systems* (Springer, New York, 1999), pp. 294–313.

[66] A. C. Doherty and K. Jacobs, Feedback control of quantum systems using continuous state estimation, Phys. Rev. A **60,** 2700 (1999).

[67] A. N. Korotkov, Selective quantum evolution of a qubit state due to continuous measurement, Phys. Rev. B **63,** 115403 (2001).

[68] H. M. Wiseman and G. J. Milburn, *Quantum Measurement and Control* (Cambridge Univeristy Press, Cambridge, England, 2010).

[69] K. Jacobs, *Quantum Measurement Theory and its Applications* (Cambridge University Press, Cambridge, England, 2014).

[70] J. Zhang, Y.-X. Liu, R.-B. Wu, K. Jacobs, and F. Nori, Quantum feedback: Theory, experiments, and applications, Phys. Rep. **679,** 1 (2017).

[71] D. E. Kirk, *Optimal Control Theory—An Introduction* (Dover Publications, Inc., New York, 2004).

[72] V. Cavina, A. Mari, A. Carlini, and V. Giovannetti, Optimal thermodynamic control in open quantum systems, Phys. Rev. A **98,** 012139 (2018).

[73] G. Schaller, C. Emary, G. Kiesslich, and T. Brandes, Probing the power of an electronic Maxwell's demon: Single-electron transistor monitored by a quantum point contact, Phys. Rev. B **84,** 085418 (2011).

[74] D. V. Averin, M. Möttönen, and J. P. Pekola, Maxwell's demon based on a single-electron pump, Phys. Rev. B **84,** 245448 (2011).

[75] B. Annby-Andersson, P. Samuelsson, V. F. Maisi, and P. P. Potts, Maxwell's demon in a double quantum dot with continuous charge detection, Phys. Rev. B **101,** 165404 (2020).

[76] R. Porotti, A. Essig, B. Huard, and F. Marquardt, Deep reinforcement learning for quantum state preparation with weak nonlinear measurements, Quantum **6,** 747 (2022).

[77] See Supplemental Material at http://link.aps.org/supplemental/10.1103/PhysRevLett.129.050401 for detailed derivations of the results in this Letter, which includes Refs. [79–87].

[78] V. P. Belavkin, Nondemolition measurements, nonlinear filtering and dynamic programming of quantum stochastic processes, in *Modeling and Control of Systems*, edited by A. Blaquiére (Springer, Berlin, 1989), p. 245.

[79] S. Nakajima, On quantum theory of transport phenomena: Steady diffusion, Prog. Theor. Phys. **20**, 948 (1958).

[80] R. Zwanzig, Ensemble method in the theory of irreversibility, J. Chem. Phys. **33**, 1338 (1960).

[81] D. Mandal and C. Jarzynski, Analysis of slow transitions between nonequilibrium steady states, J. Stat. Mech. (2016) 063204.

[82] M. Scandi and M. Perarnau-Llobet, Thermodynamic length in open quantum systems, Quantum **3**, 197 (2019).

[83] S. H. Strogatz, *Nonlinear Dynamics and Chaos: With Applications to Physics, Biology, Chemistry, and Engineering* (CRC Press, Boca Raton, FL, 2018).

[84] J. A. Gyamfi, Fundamentals of quantum mechanics in Liouville space, Eur. J. Phys. **41**, 063002 (2020).

[85] D. Manzano, A short introduction to the Lindblad master equation, AIP Adv. **10**, 025106 (2020).

[86] G. Schaller, *Open Quantum Systems Far from Equilibrium* (Springer, New York, 2014), Vol. 881.

[87] C. W. Gardiner, *Handbook of Stochastic Methods* (Springer, Berlin, 1985).

[88] M. Esposito and G. Schaller, Stochastic thermodynamics for Maxwell demon feedbacks, Europhys. Lett. **99**, 30003 (2012).

[89] K. Jacobs and D. A. Steck, A straightforward introduction to continuous quantum measurement, Contemp. Phys. **47**, 279 (2006).

[90] A. Bednorz, W. Belzig, and A. Nitzan, Nonclassical time correlation functions in continuous quantum measurement, New J. Phys. **14** (2012).

[91] P. Warszawski and H. M. Wiseman, Quantum trajectories for realistic photodetection: I. General formalism, J. Opt. B **5**, 1 (2003).

[92] P. Warszawski and H. M. Wiseman, Quantum trajectories for realistic photodetection: II. Application and analysis, J. Opt. B **5**, 15 (2003).

[93] M. Sarovar, H.-S. Goan, T. P. Spiller, and G. J. Milburn, High-fidelity measurement and quantum feedback control in circuit QED, Phys. Rev. A **72**, 062327 (2005).

[94] Z. Liu, L. Kuang, K. Hu, L. Xu, S. Wei, L. Guo, and X.-Q. Li, Deterministic creation and stabilization of entanglement in circuit QED by homodyne-mediated feedback control, Phys. Rev. A **82**, 032335 (2010).

[95] W. Feng, P. Wang, X. Ding, L. Xu, and X.-Q. Li, Generating and stabilizing the Greenberger-Horne-Zeilinger state in circuit QED: Joint measurement, Zeno effect, and feedback, Phys. Rev. A **83**, 042313 (2011).

[96] M. Yanagisawa, Non-Gaussian State Generation from Linear Elements via Feedback, Phys. Rev. Lett. **103**, 203601 (2009).

Appendix
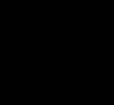
Appendix A

Averaging using path integrals

In Chapter 2, we introduced the Itô stochastic differential equation

$$dX(t) = a[X(t)]dt + b[X(t)]dW(t), \tag{A.1}$$

where the stochastic process $X(t)$ and the Wiener increment $dW(t)$ at time t are statistically independent. Due to this independence, we argued that averages $\langle f[X(t)]dW(t)\rangle$ should vanish as $\langle dW(t)\rangle = 0$. Here, we prove that this is true. We evaluate

$$\langle f[X(t)]dW(t)\rangle = \int \mathcal{D}[\boldsymbol{X}]f[X(t)]dW(t)P[\boldsymbol{X}] = \int dx_j dx_{j+1}f(x_j)dW_j P[x_j, x_{j+1}], \tag{A.2}$$

where we used that $t = t_0 + jdt$, with $0 < j < n - 1$, can be any time in between t_0 and $t_0 + (n-1)dt$. Note that we need to integrate over both x_j and x_{j+1} under the integral in the last equality as x_{j+1} is dependent on dW_j. To proceed, we make use of Bayes rule to rewrite $P[x_j, x_{j+1}] = P[x_{j+1}|x_j]P[x_j]$, and get

$$\int dx_j dx_{j+1}f(x_j)dW_j P[x_j, x_{j+1}] = \int dx_j f(x_j)P[x_j] \int dx_{j+1}dW_j P[x_{j+1}|x_j]. \tag{A.3}$$

The conditional probability $P[x_{j+1}|x_j]$ may be found since we know that the probability distribution of dW_j is (see Chapter 2.3)

$$P[dW_j] = \frac{e^{-dW_j^2/2dt}}{\sqrt{2\pi dt}}, \tag{A.4}$$

and that $x_{j+1} = x_j + a(x_j)dt + b(x_j)dW_j$ from the Itô equation. The conditional probability is obtained via

$$P[x_{j+1}|x_j] = \int d[dW_j]\delta\left(x_{j+1} - [x_j + a(x_j)dt + b(x_j)dW_j]\right)P[dW_j] = \frac{e^{-\frac{\left(x_{j+1} - [x_j + a(x_j)dt]\right)^2}{2b^2(x_j)dt}}}{\sqrt{2\pi b^2(x_j)dt}}, \tag{A.5}$$

where we used that the delta function is an even function, and that $\delta(\alpha x) = \delta(x)/|\alpha|$ for a constant α. We understand that once x_j is known, x_{j+1} is a Gaussian random variable with mean $x_j + a(x_j)dt$ and variance $b^2(x_j)dt$. This mean and variance agrees with what we find from the Itô equation assuming $X(t) = x_j$ at time t. The rightmost integral in Eq. (A.3) can now be evaluated using $dW_j = [x_{j+1} - x_j - a(x_j)dt]/b(x_j)$,

$$\int dx_{j+1} dW_j P[x_{j+1}|x_j] = \int dx_{j+1} \frac{x_{j+1} - x_j - a(x_j)dt}{b(x_j)} P[x_{j+1}|x_j] = 0, \qquad \text{(A.6)}$$

and we get $\langle f[X(t)]dW(t)\rangle = 0$.

A.1 Details Chapter 6.2

Evaluating the RHS of Eq. (6.15) gives three terms,

$$\mathrm{E}\Big[d\big(\delta[D(t)-D]\hat{\rho}_c(t)\big)\Big] = \mathrm{E}\Big[\big(d\delta[D(t)-D]\big)\hat{\rho}_c(t)\Big] + \mathrm{E}\Big[\delta[D(t)-D]d\hat{\rho}_c(t)\Big] + \mathrm{E}\Big[d\delta[D(t)-D]d\hat{\rho}_c(t)\Big].$$
(A.7)

By using the path integral formulations from Chapter 2, the first term becomes

$$\mathrm{E}\Big[\big(d\delta[D(t)-D]\big)\hat{\rho}_c(t)\Big] = \gamma dt \mathrm{E}\Big[\delta'[D(t)-D]\langle\hat{A}\rangle_c\hat{\rho}_c(t)\Big] + \gamma dt \partial_D[D\hat{\rho}_t(D)] + \frac{\gamma^2 dt}{8\lambda}\partial_D^2\hat{\rho}_t(D),$$
(A.8)

where the prime denotes differentiation with respect to $D(t)$. The second term reads

$$\mathrm{E}\Big[\delta[D(t) - D]d\hat{\rho}_c(t)\Big] = dt\mathcal{L}(D)\hat{\rho}_t(D) + \lambda dt \mathcal{D}[\hat{A}]\hat{\rho}_t(D), \qquad \text{(A.9)}$$

and for the third term, we get

$$\mathrm{E}\Big[d\delta[D(t) - D]d\hat{\rho}_c(t)\Big] = -\frac{\gamma dt}{2}\partial_D\{\hat{A}, \hat{\rho}_t(D)\} - \gamma dt \mathrm{E}\Big[\delta'[D(t) - D]\langle\hat{A}\rangle_c\hat{\rho}_c(t)\Big]. \quad \text{(A.10)}$$

Adding the three terms of Eq. (A.7) gives Eq. (6.17).

Appendix B

Derivations Chapter 6

B.1 Exponential superoperator

We begin to note that for an integer j,

$$\tilde{\mathcal{F}}^j(D) = \sum_{aa'} \tilde{\mathcal{F}}^j_{aa'}(D) \mathcal{V}_{aa',aa'} \tag{B.1}$$

as $\mathcal{V}_{bb',aa'} \mathcal{V}_{dd',cc'} = \delta_{ad}\delta_{a'd'} \mathcal{V}_{bb',cc'}$. The exponentiated Fokker-Planck superoperator acting on an arbitrary state $\hat{\rho}(D)$ may be evaluated as

$$
\begin{aligned}
e^{\Gamma \tau_2 \tilde{\mathcal{F}}(D)} \hat{\rho}(D) &= \sum_{aa'} \sum_{j=0}^{\infty} \frac{(\Gamma \tau_2)^j}{j!} \tilde{\mathcal{F}}^j_{aa'}(D) \mathcal{V}_{aa',aa'} \sum_{bb'} \sum_{n=0}^{\infty} c_{bb',n} \lambda^{(R)}_{bb',n}(D) \ket{b}\bra{b'} = \\
&= \sum_{aa'} \sum_{j=0}^{\infty} \sum_{n=0}^{\infty} \frac{(-n\Gamma \tau_2)^j}{j!} c_{aa',n} \lambda^{(R)}_{aa',n}(D) \ket{a}\bra{a'} = \\
&= \sum_{aa'} \sum_{n=0}^{\infty} e^{-n\Gamma \tau_2} c_{aa',n} \lambda^{(R)}_{aa',n}(D) \ket{a}\bra{a'} = \\
&= \sum_{aa'} c_{aa',0} \pi_{aa'}(D) \ket{a}\bra{a'} + \sum_{aa'} \sum_{n=1}^{\infty} e^{-n\Gamma \tau_2} c_{aa',n} \lambda^{(R)}_{aa',n}(D) \ket{a}\bra{a'},
\end{aligned}
\tag{B.2}
$$

where we in the last double sum of the first line expanded the density matrix $\hat{\rho}(D)$ in terms of the right eigenfunctions $\lambda^{(R)}_{aa',n}(D)$ of $\tilde{\mathcal{F}}(D)$ given by Eq. (6.26). In the last equality we separated the $n = 0$ term from the sum over n such that the first term corresponds to the projection onto $\mathcal{P}$-space and the second term corresponds to the projection onto $\mathcal{Q}$-space.

When τ_2 is very large, the second term becomes vanishingly small, and we get

$$e^{\Gamma\tau_2\tilde{\mathcal{F}}(D)}\hat{\rho}(D) \approx \mathcal{P}\hat{\rho}(D) = \mathcal{G}(D)\hat{\rho}, \tag{B.3}$$

where $\hat{\rho} = \int_{-\infty}^{\infty} dD\hat{\rho}(D)$. That is, when τ_2 is large, the state $\hat{\rho}(D)$ quickly becomes the steady state with respect to $\tilde{\mathcal{F}}(D)$.

B.2 Superoperator identities

For an arbitrary state $\hat{\rho}(D)$, for which $\hat{\rho} = \int_{-\infty}^{\infty} dD\hat{\rho}(D)$, the following equalities,

$$\mathcal{Q}\mathcal{G}(D)\hat{\rho} = \mathcal{Q}\sum_{aa'} \pi_{aa'}(D)\mathcal{V}_{aa',aa'}\hat{\rho} = \mathcal{Q}\mathcal{P}\hat{\rho}(D) = 0 \tag{B.4}$$

show that $\mathcal{Q}\mathcal{G}(D) = 0$, as $\mathcal{Q}\mathcal{P} = 0$. Note that we used that $\hat{\rho} = \int dD\hat{\rho}(D)$.

The following equalities prove why $\mathcal{P}\tilde{\mathcal{F}}^{-1}(D)\mathcal{Q} = 0$,

$$\mathcal{P}\tilde{\mathcal{F}}^{-1}(D)\mathcal{Q} = -\mathcal{P}\int_0^{\infty} dz e^{z\tilde{\mathcal{F}}(D)}\mathcal{Q} = -\mathcal{P}\int_0^{\infty} dz \sum_{j=0}^{\infty} \frac{z^j}{j!}\tilde{\mathcal{F}}^j(D)\mathcal{Q} = -\int_0^{\infty} dz\mathcal{P}\mathcal{Q} = 0, \tag{B.5}$$

where we in the first equality used the definition of $\tilde{\mathcal{F}}^{-1}(D)$ in Eq. (6.39), that $\mathcal{Q}^2 = \mathcal{Q}$, and that $\mathcal{P}\tilde{\mathcal{F}}^j(D) = 0$ for all $j \neq 0$ in the third equality.

B.3 Equivalence of Eqs. (6.39) and (6.52)

Starting from the inverse in Eq. (6.39), we have

$$\mathcal{F}^{-1}(D) = -\int_0^{\infty} dz e^{z\mathcal{F}(D)}\mathcal{Q} = -\int_0^{\infty} dz e^{z\mathcal{Q}\mathcal{F}(D)\mathcal{Q}}\mathcal{Q}, \tag{B.6}$$

where we in the second equality inserted $1 = \mathcal{P} + \mathcal{Q}$ on both sides of $\mathcal{F}(D)$ in the exponential.

We further show that $\mathcal{L}_{\text{corr}}$ in Eqs. (6.45) and (6.54) are equivalent by demonstrating that

the leftmost $\mathcal{Q}$ in Eq. (6.54) can be absorbed into the inverse $\mathcal{F}^{-1}(D)$. We have

$$\mathcal{Q}\mathcal{F}^{-1}(D) = -\mathcal{Q}\int_0^\infty dz e^{z\mathcal{Q}\mathcal{F}(D)\mathcal{Q}}\mathcal{Q} = -\mathcal{Q}\int_0^\infty dz \sum_{j=0}^\infty \frac{z^j}{j!}[\mathcal{Q}\mathcal{F}(D)\mathcal{Q}]^j\mathcal{Q} =$$

$$= -\int_0^\infty dz \left[\mathcal{Q} + \sum_{j=1}^\infty \frac{z^j}{j!}[\mathcal{Q}\mathcal{F}(D)\mathcal{Q}]^j\mathcal{Q}\right] = \tag{B.7}$$

$$= -\int_0^\infty dz \sum_{j=0}^\infty \frac{z^j}{j!}[\mathcal{Q}\mathcal{F}(D)\mathcal{Q}]^j\mathcal{Q} = \mathcal{F}^{-1}(D),$$

where we used Eq. (6.52) in the first equality, expanded the exponential superoperator in the second equality, isolated the $j = 0$ term and used the property $\mathcal{Q}^2 = \mathcal{Q}$ in the third equality.

B.4 Derivation Eq. (6.71)

To convert the double sum in Eq. (6.71) into the integral representation, we begin to note that the factors $1/(n+1)$ and $1/(k+1)$ can be rewritten as

$$\frac{1}{n+1} = \int_0^1 dz z^n. \tag{B.8}$$

Secondly, we can remove the sum over k by using the following property,

$$H_n(x+y) = \sum_{k=0}^n \binom{n}{k}(2y)^{n-k}H_k(x). \tag{B.9}$$

With the identity

$$H_n(x) = \frac{2^n}{\sqrt{\pi}}\int_{-\infty}^\infty dy(x+iy)^n e^{-y^2}, \tag{B.10}$$

we may rewrite the double sum as

$$\sum_{n=0}^\infty \sum_{k=0}^n \binom{n}{k}\frac{[\sqrt{\alpha}(b-a)]^{n-k}}{2^{k+1}(k+1)(n+1)!\pi}e^{-\alpha(a^2+b^2)}H_k\left[\sqrt{\alpha}a\right]H_n\left[\sqrt{\alpha}b\right] =$$

$$= \frac{e^{-\alpha(a^2+b^2)}}{2\pi^2}\int_{-\infty}^\infty dw \int_{-\infty}^\infty dx \int_0^1 dy \int_0^1 dz e^{2z(\sqrt{\alpha}b+ix)[\sqrt{\alpha}(b-a[1-y])+iyw]-x^2-w^2}. \tag{B.11}$$

Performing the integral over x followed by the one over y results in

$$\frac{e^{-\alpha a^2}}{4\pi}\int_{-\infty}^\infty dw \int_0^1 dz \frac{e^{-w^2}\left\{\text{erf}\left[\sqrt{\alpha}(az+b[1-z])\right] - \text{erf}\left[\sqrt{\alpha}b(1-z) - iwz\right]\right\}}{z(\sqrt{\alpha}a+iw)}. \tag{B.12}$$

Finally, we use that

$$\mathrm{erf}(x+iy) = \mathrm{erf}(x) + \frac{2iy}{\sqrt{\pi}}e^{-x^2}\int_0^1 dz e^{y^2z^2-2ixyz},$$ (B.13)

and perform the integration over w to get Eq. (6.71).

Appendix C

n-resolved density matrix

To derive the n-resolved master equation (3.29), we begin by introducing the Laplace transform of the density matrix,

$$\tilde{\rho}_z = \int_0^\infty dt e^{-zt} \hat{\rho}_t, \qquad \text{(C.1)}$$

where the hat and tilde indicate whether the density matrix belongs to the time domain or the Laplace domain. In Laplace space, master equation (3.28) reads

$$\tilde{\rho}_z = \Omega(z)\hat{\rho}_0, \qquad\qquad \Omega(z) = \frac{1}{z - \mathcal{L}_0 - \mathcal{J}_+ - \mathcal{J}_-}, \qquad \text{(C.2)}$$

where $\Omega(z)$ is the Laplace space propagator. Making use of the Neumann series, we can write the Laplace space propagator as an expansion in $\mathcal{J}_+ + \mathcal{J}_-$ as

$$\Omega(z) = \sum_{n=0}^\infty \Omega_0(z)[(\mathcal{J}_+ + \mathcal{J}_-)\Omega_0(z)]^n, \qquad \text{(C.3)}$$

where $\Omega_0(z) = 1/(z - \mathcal{L}_0)$. Investigating the sum term by term, we identify

$$
\begin{aligned}
n = 0: \quad & \Omega_0(z), \\
n = 1: \quad & \Omega_0(z)\mathcal{J}_+\Omega_0(z) + \Omega_0(z)\mathcal{J}_-\Omega_0(z), \\
n = 2: \quad & \Omega_0(z)\mathcal{J}_+\Omega_0(z)\mathcal{J}_+\Omega_0(z) + \Omega_0(z)\mathcal{J}_-\Omega_0(z)\mathcal{J}_-\Omega_0(z) \\
& + \Omega_0(z)\mathcal{J}_+\Omega_0(z)\mathcal{J}_-\Omega_0(z) + \Omega_0(z)\mathcal{J}_-\Omega_0(z)\mathcal{J}_+\Omega_0(z), \\
\vdots \quad &
\end{aligned}
\qquad \text{(C.4)}
$$

We see that the first term ($n = 0$) leaves the number of particles in the reservoir unchanged. The second term ($n = 1$) contains one part increasing the number of particles

in the reservoir by one, and one term decreasing the number of particles by one. The third term ($n = 2$) contains two parts where the reservoir particle number is either increased or decreased by two, and two terms where the net particle number is left unchanged. By using Eqs. (C.2) and (C.3), we note that different combinations of the terms in the sum can be interpreted as number resolved states $\tilde{\rho}_z(\pm n)$. We write $\tilde{\rho}_z(0) = \Omega_0(z)\hat{\rho}_0$, and $\tilde{\rho}_z(\pm 1) = [\Omega_0(z)\mathcal{J}_\pm \Omega_0(z) + \ldots]\hat{\rho}_0$, where '...' denotes all possible combinations of Ω_0 and $\mathcal{J}_\pm$ that results in ± 1 particles in the reservoir. By using this recursively, we may write down similar expressions for a general $\tilde{\rho}_z(\pm n)$, and we obtain the following Laplace space relation for the number resolved density matrix,

$$\tilde{\rho}_z(n) = \Omega_0(z)\mathcal{J}_+\tilde{\rho}_z(n-1) + \Omega_0(z)\mathcal{J}_-\tilde{\rho}_z(n+1). \tag{C.5}$$

Transforming this back to the time domain, using the initial condition $\hat{\rho}_0(n) = \delta_{n,0}\hat{\rho}_0$, we get Eq. (3.29).

Appendix D

Numerical method

In this appendix, we briefly describe the numerical method used to solve the full QFPME (1.1). Here we are only interested in finding the steady state solution for two-level systems, but the method can be generalized to include time dependence and larger systems. We begin by expanding the system-detector density matrix in terms of the generalized Hermite polynomials (6.21) as

$$\hat{\rho}_t(D) = \sum_{n=0}^{N-1} M_n \frac{He_n^{[\sigma]}(D)}{\sqrt{n!\sigma^n}} \frac{e^{-D^2/2\sigma}}{\sqrt{2\pi\sigma}}, \qquad M_n = \begin{pmatrix} a_n & c_n \\ c_n^* & b_n \end{pmatrix}, \qquad \text{(D.1)}$$

where we truncate the sum at N terms. The matrix M_n is written in the basis $\{\lvert 0\rangle, \lvert 1\rangle\}$, and a_n, b_n, and c_n are expansion coefficients for the density matrix elements. Inserting this in the QFPME, multiplying with $He_m^{[\sigma]}(D)/\sqrt{m!\sigma^m}$, and integrating over all D, results in a relation

$$0 = \boldsymbol{f}_m(\{a_n, b_n, c_n\}_{n=0}^{N-1}), \qquad \text{(D.2)}$$

where $\boldsymbol{f}_m$ is a vector valued function of the expansion coefficients. Equation (D.2) can be rewritten as a matrix equation that can be solved numerically to find the expansion coefficients a_n, b_n, and c_n. With the normalization condition $1 = \int_{-\infty}^{\infty} dD \operatorname{tr}\{\hat{\rho}_t(D)\} = a_0 + b_0$, we find the normalized density matrix $\hat{\rho}_t(D)$. For threshold feedback, we use the following integral to find $\boldsymbol{f}_m$,

$$\int_0^{\infty} \frac{He_m^{[\sigma]}(x)}{\sqrt{\sigma^m m!}} \frac{He_n^{[\sigma]}(x)}{\sqrt{\sigma^n n!}} \frac{e^{-x^2/2\sigma}}{\sqrt{2\pi\sigma}} dx = \begin{cases} 1/2, & n = m, \\ 0, & n + m \text{ even}, \\ C_{nm}, & n + m \text{ odd}, \end{cases} \qquad \text{(D.3)}$$

with

$$C_{nm} = \frac{(-1)^{(n+m-1)/2} m!! (n-1)!!}{\sqrt{2\pi n! m!}(m-n)}, \qquad \text{(D.4)}$$

which is given for even n and odd m, and we note that $(-1)!! = 1$.